June 2006
Draft Research Report: UCPRC-RR-2004-07

Full-Depth Pavement Reclamation with Foamed Asphalt: First-Level Analysis Report on HVS Testing on State Route 89

Authors:
H Theyse, F Long, D Jones, and J Harvey

Partnered Pavement Research Program (PPRC) Strategic Plan Element 4.12: Development of Improved Mix and Structural Design and Construction Guidelines for Full-Depth Reclamation with Foamed Asphalt

PREPARED FOR:

California Department of Transportation
Division of Research and Innovation
Office of Roadway Research

PREPARED BY:

University of California
Pavement Research Center
UC Davis, UC Berkeley

DOCUMENT RETRIEVAL PAGE			**Research Report: UCPRC-RR-2004-07**
Title: Full-Depth Pavement Reclamation with Foamed Asphalt: First-Level Analysis Report on HVS Testing on State Route 89			
Authors: Hechter Theyse, Fenella Long, David Jones, and John Harvey			
Prepared for: Caltrans	**FHWA No.:** CA101069B	**Work Submitted Date:** June 30, 2006	**Date**: June, 2006
Strategic Plan Element No: 4.12	**Status:** Final		**Version No:** 03/31/10

Abstract:

This report focuses on the HVS testing of a foamed asphalt treated, reclaimed asphalt pavement (RAP) on State Route 89 near Sierraville. The report discusses the expected behavior of the HVS test sections, presents the results from field surveys done during June 2003, October 2003 and May 2004 as well as the 1st level analysis of HVS results from the test site. Results from field surveys done prior to, during and after HVS testing show that the pavement structure of the HVS test sections on SR89 is not representative of the mainline and foamed asphalt treated, reclaimed asphalt concrete in general.

The mode of distress of the test sections differs between the favorable conditions in summer and fall and unfavorable conditions in winter. The mode of distress before the onset of winter consisted of gradual deformation of the pavement resulting in a terminal surface rut with limited fatigue cracking. After the winter, the mode changed to a more rapid rate of rutting and on Sections 595FD and 596FD tested during spring, shear failure of the base layer occurred in certain locations. These sections also showed extensive fatigue cracking

The pavement structure of the HVS test section showed sensitivity to high moisture contents in terms of elastic and plastic response. The resilient modulus of the base layer decreased during the winter and spring and the rut rate increased. Although not to the same extent, a reduction in base layer resilient modulus on the mainline was also observed from FWD results. It is recommended that FWD surveys should be done in each of the four seasons of the year to track changes in pavement condition. If the reduction in base layer resilient modulus is permanent, it may lead to early fatigue of the asphalt surfacing layer.

The pavement bearing capacity only exceeded the design value under favorable conditions in the fall and early winter. The pavement structure of the HVS test sections is, however, not representative of the mainline pavement structure and therefore not representative of the bearing capacity of foamed asphalt treated, reclaimed asphalt pavements. The bearing capacity of the pavement is subject to seasonal effects and cannot be estimated from a single HVS test result. It is recommended that a seasonal simulation should be done using the results from the HVS tests in each season and seasonal traffic data in a second level analysis of the HVS data.

Keywords:
Full-depth reclamation, Full-depth recycling, FDR, Deep in situ recycling, DISR, foamed asphalt, HVS testing.

Proposals for implementation:

Related documents:

Signatures:

D. Jones 1st Author	J Harvey Technical Review	D. Spinner Editor	J. Harvey Principal Investigator	T.J. Holland Caltrans Contract Manager

DISCLAIMER

The contents of this report reflect the views of the authors who are responsible for the facts and accuracy of the data presented herein. The contents do not necessarily reflect the official views or policies of the State of California or the Federal Highway Administration. This report does not constitute a standard, specification, or regulation.

PROJECT OBJECTIVES

The objective of this project is to develop improved mix and structural design and construction guidelines for full-depth reclamation (FDR) of cracked asphalt concrete with foamed asphalt.

This objective will be met after completion of six tasks:

1. Undertake literature survey, and technology and research scan.
2. Perform mechanistic sensitivity analysis.
3. Undertake assessment of Caltrans projects built to date based on available data.
4. Measure properties on Caltrans full-depth reclamation with foamed asphalt projects to be built in the future.
5. Carry out laboratory testing to identify specimen preparation and test methods, and develop information for mix design, structural design and construction guidelines.
6. Prepare interim guidelines for project selection, mix design, structural design, and construction.

This document covers part of Task 3.

ANALYSIS LEVELS IN HVS REPORTS

The primary purpose of a first-level HVS report is to present a complete and validated set of HVS data without detailed analysis and interpretation of the data. The scope of a first-level report is confined to the HVS data and associated test results from a single HVS site. The conclusions of the first-level report are therefore site specific with little interpretation and should not be generalized. The primary aim of the second-level analysis report is to interpret and explain the observed behavior contained in the first-level report. By combining the results from a number of test sites or combining the HVS and associated test results with data from other case studies on the same material and pavement type, it is possible to determine whether the observed response and behavior are representative of the response and behavior of the material and pavement type in general. However, if any pavement behavior or design models are developed during the second-level analysis, their scope is limited to the particular HVS site under investigation. The content of the third-level analysis is similar to that of the second-level analysis, but the data that were generated from HVS and associated testing on a number of sites are combined to develop general behavior and design models for the material or pavement type under investigation.

This document is a first-level report only. The preparation of a second-level report will be considered at a later date once laboratory and other field studies have been completed.

EXECUTIVE SUMMARY

This report describes the results of HVS testing on a full-scale experiment carried out on a turnout adjacent to State Route 89 near Calpine in northern California. Approximately 16 km (10 miles) of the road was rehabilitated using a full-depth reclamation process. Foamed asphalt (2.5 percent) and portland cement (1.0 percent) were incorporated into the mix as part of the recycling process. Four HVS tests, designated 593RF through 596RF, were completed. The testing forms part of Partnered Pavement Research Center Strategic Plan Item 4.12: "Development of Improved Mix and Structural Design and Construction Guidelines for Full-Depth Reclamation (FDR) of Cracked Asphalt Concrete with Foamed Asphalt."

The objective of this project is to develop improved mix and structural design and construction guidelines for full-depth reclamation (FDR) of cracked asphalt concrete with foamed asphalt. This objective will be met after completion of nine tasks:

1. Undertake literature survey and technology and research scan.
2. Perform mechanistic sensitivity analysis.
3. Undertake assessment of Caltrans projects built to date based on available data.
4. Measure properties on Caltrans full-depth reclamation with foamed asphalt projects to be built in the future.
5. Carry out laboratory testing to identify specimen preparation and test methods, and develop information for mix design, structural design and construction guidelines.
6. Prepare project selection recommendations.
7. Prepare mix design recommendations.
8. Prepare structural design recommendations.
9. Prepare construction recommendations

This report addresses part of Task 3. It consists of three main chapters. Chapter 2 provides information on similar HVS tests carried out in South Africa, together with expected results of the SR 89 study based on this experience. Chapter 3 summarizes the experiment layout, pavement design, test duration, pavement instrumentation and monitoring methods, loading program, and the test section failure criteria. Chapter 4 summarizes the FWD testing and test pit investigations. Although the test pits were excavated after HVS testing, the Chapter is ahead of the HVS data summary (Chapter 5) to add clarity to the interpretation of the results. Chapter 5 includes a summary of environmental data, surface and depth response data, and visual observations. Chapter 6 provides a summary and lists key findings.

Prior to recycling, the road consisted of multiple layers of asphalt concrete on in situ weathered granite subgrade (R-value of 78). The road had extensive thermal and fatigue cracking. The nominal existing asphalt concrete thickness for the FDR design was 150 mm (6.0 in), although actual thickness varied as a result of repairs during the life of the road. Indirect Tensile Strength (ITS) tests on foamed asphalt mixes were performed by Caltrans to determine the mix design. A foamed asphalt content of 2.5 percent and portland cement content of 1.0 percent was adopted, which resulted in average unsoaked ITS values of 300 kPa (43.5 psi) to 390 kPa (56.5 psi), depending on the location of the test materials. Construction took place in the summer of 2002 with a nominal reclamation depth of 200 mm (8 in). The road was surfaced with 45 mm (1.8 in) of dense-graded asphalt concrete. An HVS test lane was specially constructed adjacent to the roadway at post-mile 27 in Sierra County. Material was imported to provide the support layers and was later found to be different to that of the main roadway. The base layer was reclaimed asphalt concrete treated with foamed asphalt and cement and was constructed with the excess material from the main roadway and not as a full-depth reclaimed layer per se. The reclaimed material had an R-value of 82. This material was stockpiled for less than a week before construction of the HVS test lane. The test section base layer was primed with an SS-1 emulsion before being surfaced with 50 mm (2.0 in) of asphalt concrete.

HVS trafficking on the sections commenced in August 2003 and was completed in May 2004. During this period a total of 1,863,595 load repetitions were applied across the four sections. One test was carried out with controlled water flow across the surface. A temperature chamber was used to maintain the pavement temperature at 20°C±4°C (68°F±7°F) for two of the tests, and at 5°±4°C (41°F±7°F) for one test. The last test (wet) was carried out at ambient temperatures. A dual tire (690 kPa [100 psi] pressure) and bidirectional loading with lateral wander was used in all tests.

Findings and observations based on the data collected during this HVS study include:

- Results from field surveys done prior to, during, and after HVS testing showed that the pavement structure of the HVS test sections was not representative of the mainline, and foamed bitumen treated, reclaimed asphalt concrete in general. The base layer thickness on the HVS test sections varied between 74 mm and 100 mm, compared to the design thickness of 200 mm. The base layer was supported by a weak clay-like layer and decomposed granite subgrade. A very weak support layer was identified in the vicinity of one of the test sections and test-pit results showed that the moisture content in the subgrade of this section exceeded 20 percent.
- The mode of distress of the test sections differed between favorable conditions in summer and fall and unfavorable conditions in winter and spring. The mode of distress before the onset of winter consisted of gradual deformation of the pavement resulting in a terminal surface rut with limited

fatigue cracking. After the winter, the mode changed to a more rapid rate of rutting and on the two sections tested during spring, shear failure of the base layer occurred in certain locations. These sections also showed extensive fatigue cracking, but this was probably caused by the weak soft base layer (low resilient modulus), with large plastic strains generating high tensile strains in the asphalt surfacing layer.

- The pavement structure of the HVS test track showed sensitivity to high moisture contents in terms of elastic and plastic response. The resilient modulus of the base layer decreased during the winter and spring and the rut rate increased. Although not to the same extent, a reduction in base layer resilient modulus on the mainline was also observed from Falling Weight Deflectometer (FWD) results. It is not clear whether the reduction in base layer resilient modulus was permanent. If it is, early fatigue of the asphalt surfacing layer is likely.
- The pavement bearing capacity only exceeded the design value under favorable conditions in the fall and early winter. The pavement structure of the HVS test sections was, however, not representative of the mainline pavement structure or of typical foamed bitumen treated, reclaimed asphalt pavement projects that will be constructed in California, and therefore not representative of the bearing capacity of these types of pavements. The bearing capacity of the pavement is subject to seasonal effects and cannot be estimated from a single HVS test result.

Based on the above findings and the limitations associated with testing on an unrepresentative section, no recommendations as to the use of full-depth reclamation with foamed asphalt in rehabilitation strategies are made at this time. These recommendations will be included in a later report when additional data from field monitoring at other projects and laboratory testing has been collected and analyzed.

TABLE OF CONTENTS

LIST OF TABLES

LIST OF FIGURES

CONVERSION FACTORS

SI* (MODERN METRIC) CONVERSION FACTORS				
Symbol	**Convert From**	**Convert To**	**Symbol**	**Conversion**
LENGTH				
mm	millimeters	inches	in	mm x 0.039
m	meters	feet	ft	m x 3.28
km	kilometers	mile	mile	km x 1.609
micron	micron	mil	mil	micron / 25
AREA				
mm^2	square millimeters	square inches	in^2	mm^2 x 0.0016
m^2	square meters	square feet	ft^2	m^2 x 10.764
VOLUME				
m^3	cubic meters	cubic feet	ft^3	m^3 x 35.314
MASS				
kg	kilograms	pounds	lb	kg x 2.202
TEMPERATURE (exact degrees)				
C	Celsius	Fahrenheit	F	°C x 1.8 + 32
FORCE and PRESSURE or STRESS				
N	newtons	poundforce	lbf	N x 0.225
kPa	kilopascals	poundforce/square inch	lbf/in^2	kPa x 0.145

*SI is the symbol for the International System of Units. Appropriate rounding should be made to comply with Section 4 of ASTM E380. (Revised March 2003)

1. INTRODUCTION

1.1 Objectives

The objective of this project is to evaluate the performance of the full-depth reclamation (FDR) with foamed asphalt of a pavement under HVS trafficking. The 2003-04 Strategic Plan for the Partnered Pavement Research Center (PPRC) listed FDR as a current experimental strategy under evaluation by the California Department of Transportation (Caltrans) with the aim of it becoming standard practice. This evaluation process started as a special forensic investigation but has since been identified as a full research goal (HVS Goal 10) in the Strategic Plan. Although the evaluation process will ultimately address aspects including selection criteria, pre-design investigation procedures, design methods and construction practices, this report focuses on the Heavy Vehicle Simulator (HVS) testing of a full-depth reclaimed asphalt pavement treated with foamed asphalt (FDR-FA) on SR89 near Sierraville, California (03-SIE-89, PM20.0/29.6). The report discusses the expected behavior of the HVS test sections, presents the results from field surveys done during June 2003, October 2003 and May 2004 as well as the 1st level HVS results from the test site, located on a specially constructed turnout adjacent to the travelled way.

1.2 Structure of the Report

This report presents the field, laboratory and validated HVS test results as well as 1st level analysis of the HVS data for the foamed asphalt treated, reclaimed asphalt pavement on State Route 89. A background to the expected characteristics of foamed asphalt treated material is provided in Chapter 2 based on previous experience with the material. This includes aspects such as:

- General material behavior;
- Ranges of resilient modulus values;
- Resilient modulus reduction under traffic loading.

Chapter 3 provides details on the test and includes:

- Experiment Location
- Materials and Pavement Structure of SR89
- Mix Design
- HVS Sections
- Test Section Detail

Chapter 4 provides results from a number of field surveys carried prior to HVS testing (June to August 2003), after completion of the first HVS test 593FD (October 2003) and after completion of all the HVS tests (May 2004). The information collected during the field surveys consists of:

- Falling Weight Deflectometer (FWD) data;
- Core and test pit information;
- Dynamic Cone Penetrometer (DCP) data;
- Nuclear density gauge data.

This information contributes to the interpretation of the 1st Level HVS data provided in Chapter 5 under the following categories:

- Rainfall and temperature data;
- Visual observations;
- Surface deflection measurements;
- Surface rutting measurements;
- In depth elastic deflection measurements;
- Backcalculated resilient modulus results;

Chapter 6 presents a discussion of the HVS test results. The aspects of material and pavement behavior investigated include:

- The resilient response of the base layer material based on backcalculated resilient modulus values;
- The distress mechanisms and mode of failure observed during the HVS tests;
- An estimate of the structural bearing capacity of the test pavement.

Chapter 7 provides conclusions and recommendations.

1.3 Terminology

A variety of terms are used for describing the recycling of pavements, including but not limited to full-depth recycling or reclamation, partial-depth recycling or reclamation, deep in-situ recycling, cold in-place recycling (cold foam recycling/reclamation), and hot in-place recycling. In this document, the terms "full-depth reclamation," abbreviated as FDR, and "full-depth reclamation with foamed asphalt," abbreviated as FDR-foamed asphalt or FDR-FA are used throughout.

1.4 Measurement Units

Use of metric units was Caltrans practice when this project was begun, and during much of its execution. Metric units have always been used by the UCPRC in the design and layout of HVS test tracks, and for laboratory and field measurements and data storage. Caltrans has recently returned to the use of U.S. standard units. In this report, metric and English units (provided in parentheses after the metric units) are provided in general discussion. In keeping with convention, only metric units are used in laboratory and field data analyses. A conversion table is provided on Page xix at the beginning of this report.

2. EXPECTED BEHAVIOR OF TREATED MATERIALS

2.1 General Material Behavior

The matrix shown in Figure 2.1 sets out the basic characteristics of common road-building materials and the interaction of these characteristics when combined into foamed asphalt or emulsified asphalt treated material.

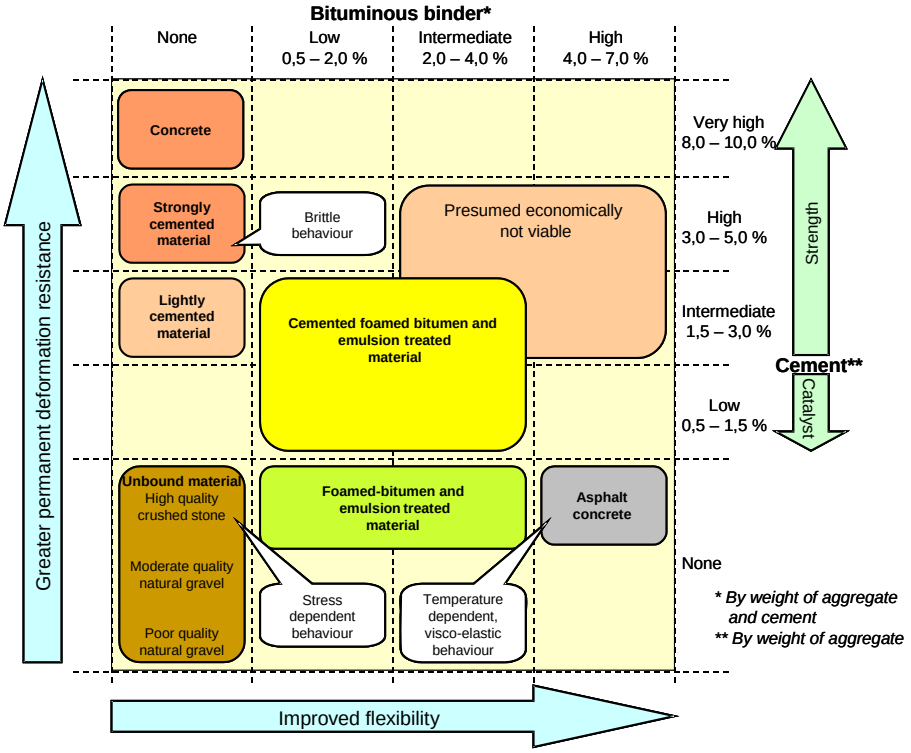

Figure 2.1: Matrix of the basic characteristics of road-building materials.

The unbound materials shown in the bottom left-hand corner of the matrix form the bulk of all road-building material. In the untreated form, these materials exhibit stress dependent behavior with an increase in resilient modulus under increasing confining stress, and a reduction in resilient modulus under increasing shear stress conditions. The permanent deformation resistance of these materials increases with an increase in the material quality from poor quality natural gravels to high quality, highly compacted crushed stone products. In addition to a lack of permanent deformation resistance, especially under wet conditions, certain natural materials may exhibit durability problems. Materials containing clays are unsuitable for road construction, having extremely low permanent deformation resistance under wet conditions.

The undesirable properties of certain marginal natural materials may be modified and their permanent deformation resistance increased with the addition of moderate to high quantities of pozzolanic stabilization agents such as lime and cement. This pozzolanic treatment is represented by a vertical movement on the diagram from the unbound materials in the lower left-hand corner to the cemented materials and concrete at the top of the vertical axis on the matrix in Figure 2.1. The addition of pozzolanic stabilization agents results in the modification of the clay and the formation of crystalline pozzolanic bonds in the material, resulting in a higher cohesion and increased permanent deformation resistance. Because of the crystalline nature of the pozzolanic bonds, lightly cemented materials tend to be brittle, while strongly cemented materials may be prone to shrinkage cracking and pumping of the underlying layers. In general, however, the addition of pozzolanic agents increases the resilient modulus, shear strength and permanent deformation resistance, and decreases the moisture sensitivity of the material, but, also reduces the ability of the material to sustain flexural bending without cracking. This reasoning may be taken to the extreme by adding a high percentage of cement to a good quality crushed stone and sand mixture to produce concrete, with a high permanent deformation resistance, but little tensile strength and flexibility.

On the other hand, bituminous binder may be added to the unbound material in increasing quantities. Such treatment with asphalt is represented by a horizontal movement from the unbound materials in the lower left-hand corner to asphalt concrete at the right-hand extreme of the horizontal axis on the matrix in Figure 2.1. The addition of bituminous stabilization agents results in the formation of pliable bituminous bonds in the material, resulting in a higher cohesion and increased permanent deformation resistance. However, because of the visco-elastic, temperature dependent behavior of these bituminous bonds, asphalt concrete may be prone to rutting under high temperatures and slow moving loads. In general, however, the addition of asphalt increases the resilient modulus, tensile strength, the ability of the material to sustain flexural bending and the resistance to moisture damage of the material.

Foamed asphalt and emulsified asphalt treated mixes may be produced by adding only bituminous stabilizer to the material or by adding bituminous stabilizer in combination with an inert filler. Pozzolanic filler is, however, often added to not only improve the permanent deformation resistance of the mix under high temperatures but also to assist in the early breaking of the emulsified-asphalt or to provide sufficient fines for foamed asphalt treatment. Foamed asphalt and emulsified asphalt mixes therefore often exhibit a combination of the stress dependent characteristics of the unbound aggregates; the brittle but permanent deformation resisting characteristics of pozzolanic stabilized materials; and the flexible characteristics of bituminous stabilized materials. The extent to which any of these characteristics will dominate in the mix depends on the proportions in which the basic constituents are

mixed and the properties of the individual constituents. If the unbound aggregate that forms the bulk of the volume of the mix had poor shear strength and permanent deformation characteristics, such as a sandy material, the shear strength and permanent deformation behavior of the mix will be dominated by either the pozzolanic or bituminous stabilizer depending on the relative quantities of these two stabilizers. If the pozzolanic stabilizer dominates in the mix, the mix will exhibit higher permanent deformation resistance but lower flexibility and if the bituminous stabilizer dominates in the mix, the mix will exhibit higher flexibility but less permanent deformation resistance. The ratio in which the pozzolanic and bituminous stabilizers are combined in the mix therefore largely determines the characteristics of the foamed asphalt or emulsified asphalt treated mix. This ratio and the balance between flexibility and permanent deformation resistance of the treated material should be reflected in the experimental design for all research investigations and should be carried through to the mix and structural design of these bituminous treated materials.

2.2 South African Experience

2.2.1 Resilient Modulus of Foamed Asphalt Treated Materials

Foamed asphalt treatment has been used in South Africa on a variety of material types, including reclaimed asphalt pavement (RAP). In this section, data from two such projects are shown, to provide evidence for the increase in resilient modulus when materials are treated with foamed asphalt. This resilient modulus is high initially and reduces under the action of traffic. This is demonstrated in the next section.

The first project was on Road P504 near Shongweni in Kwazulu-Natal, South Africa. The project used stockpiled RAP, which was treated with foamed asphalt and then placed on the road. The subgrade material is decomposed granite, which is very similar to that of State Route 89 (SR89). The section was in a mountainous environment, which is also similar to SR89. Some laboratory and field results from this project are shown in Table 2.1, and resilient moduli backcalculated from FWD deflections are shown in Table 2.2. The resilient modulus of the foamed asphalt treated RAP is fairly high, as expected.

The second project involved foamed asphalt treatment of a crushed stone base on the N7 freeway in the Western Cape, South Africa. The pavement was constructed using full-depth reclamation. A wealth of data are available for this project, as it has been used for HVS testing in combination with an extensive laboratory testing program (*1,2*). Histograms, and cumulative frequency plots of the resilient modulus, backcalculated from FWD deflections, for both the treated and untreated crushed stone materials are shown in Figure 2.2.

Table 2.1: Laboratory and Field Test Results for Road P504

Type of test		Test parameter	Reclaimed Asphalt Section		
			N	Average	CoV (%)
Laboratory tests	Density and voids	MTD (kg/m^3)	2	2,461.5	0.32
		BD (kg/m^3)	6	2,200.7	1.93
		GD (kg/m^3)	6	2,192.8	2.03
		Void content (%)	2	10.7	20.47
	Binder content	Binder content (%)	4	5.9	5.31
	Indirect Tensile Strength Test (ITS)	ITS (kPa)	2	421.5	9.29
		Strain at break (%)	2	4.4	63.30
		Stiffness modulus, E (MPa)	2	1,356.0	4.45
	Dynamic Creep	Creep modulus, E_c	2	33.6	51.41
		Slope (mm/ million cycles)	2	15.0	18.86
	Unconfined Compressive Strength test (UCS)	UCS (kPa)	2	938.5	5.35
Field tests	Surface Gauge	Bulk density (kg/m^3)	2	2,182.1	3.80
	Strata Gauge	Bulk density (kg/m^3)	1	2,071.3	-
	Dynamic Cone Penetrometer (DCP) test	DCP DN (mm/blow)	5	0.9	30.59
		DCP UCS (kPa)	5	2,649.3	17.00
		DCP resilient modulus, M_r (kPa)	5	1,325.8	27.91
		DCP DSN_{800} (blows)	5	348.0	14.85
	Rapid Compaction Control Device (RCCD) test	RCCD DN (mm/blow)	5	2.6	10.73
	Straight-edge rut depth	Inner wheel path rut (mm)	6	4.5	18.59
		Outer wheel rut (mm)	6	6.7	57.45

Table 2.2: Summary of Backcalculated Resilient Modulus Results for Road P504

Pavement layer		Subsection	Mean M_r (MPa)	CoV (%)
Base	175 mm foamed asphalt treated reclaimed base	km 3,00 to 3,20	1771	49,8
M_r - Resilient modulus		CoV - Coefficient of Variation		

The variation in the resilient modulus results for the foamed asphalt treated material is high. This is expected given the high resilient modulus of the material, which results in variations in the results obtained from the back-calculation process. The resilient modulus of the foamed asphalt treated material is significantly higher than that of the crushed stone material, even though the density of the crushed stone was slightly higher. It is also high compared to values normally obtained for foamed asphalt treated materials (i.e. around 1,000 MPa [145,000 psi]), probably because the parent material is of a high quality, and the grading of the material is continuous.

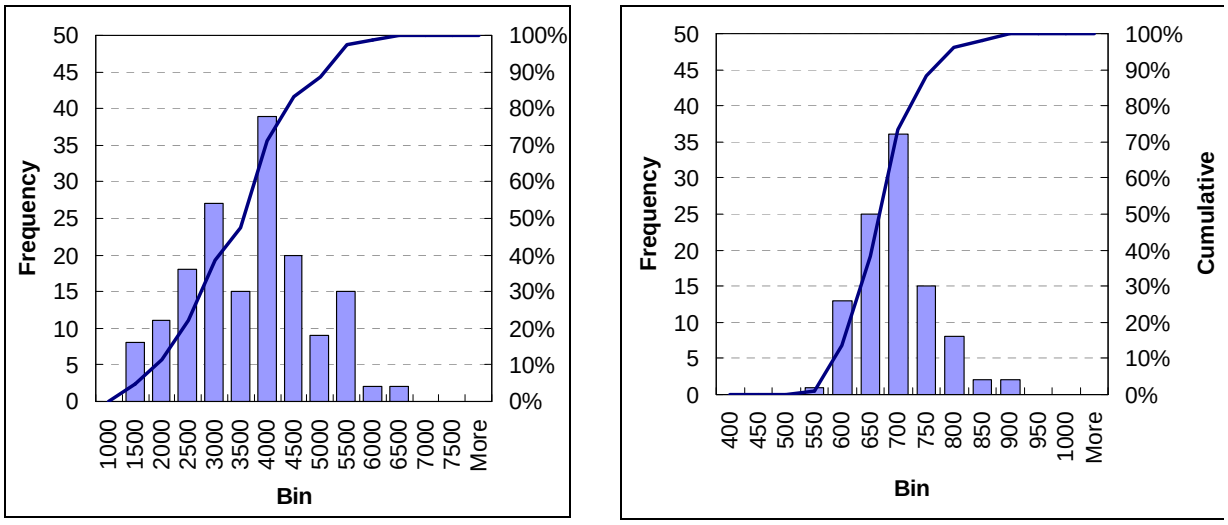

(a) Foamed asphalt treated (b) Crushed stone

Figure 2.2: Resilient modulus histograms for the southbound carriageway of the N7.

2.2.2 Resilient Modulus Reduction of Treated Materials Under Traffic Loading

On the N7 experiment, the depth deflection data for each Multi-Depth Deflectometer (MDD) stack were used in a linear-elastic routine to backcalculate the resilient moduli for the pavement layers of the foamed asphalt treated test section. Figure 2.3 shows the resilient modulus for the reclaimed, foamed asphalt treated base layer backcalculated from the 40 kN (9,000 lb) deflection data during the 40 kN (9,000 lb) and 80 kN (18,000 lb) phases of the HVS test, for Section 415A5 and for the 40 kN loading on Section 416A5. Only two MDDs are shown for Section 416A5, the data from MDD12 was inconsistent, and was therefore ignored. A function was fitted to the backcalculated base layer resilient modulus data for each of the MDD stacks, as shown in Figure 2.3.

The resilient modulus of the base layer of Section 415A5 (Figure 2.3a) initially varied between 900 MPa (130,533 psi) and 1,500 MPa (217,556 psi) but reduced rapidly under trafficking and leveled off between 300 MPa and 400 MPa towards the end of the test. The resilient modulus of the base layer on Section 416A5 (Figure 2.3b) initially varied between 1,500 MPa (217,556 psi) and 2,600 MPa (337,098 psi), but then also reduced under trafficking. The base layer resilient modulus for test 416A5 did not reach levels between 300 MPa (43,511 psi) and 400 MPa (58,015 psi) as happened during test 415A5 because of the much lower trafficking load. Had the trafficking continued, it is thought that the resilient modulus would eventually have reduced to those levels. Reasons for the differences between the stiffnesses of the two sections are discussed in Theyse, 2003 *(1)*.

2.3 Summary of Expected Behavior

The preceding selected results indicate that the initial resilient modulus of foamed asphalt treated material is expected to be at least above 1,000 MPa (145,000 psi) and even higher depending on the quality of the parent material. This initial high value of the resilient modulus is, however, reduced under trafficking, the rate of which is dependent on a range of factors including environment, traffic loading, and flexibility of the material. It has also been found that there is an interaction between the pozzolanic and bituminous binder in a foamed asphalt treated mix, giving the mix a combination of the permanent deformation resistance of cement treated material and the flexibility of bituminous materials.

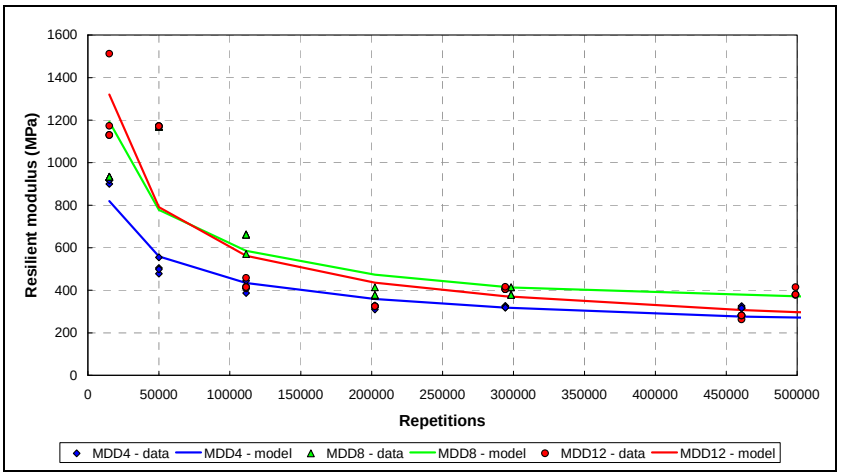

(a) Section 415A5, tested at 80 kN

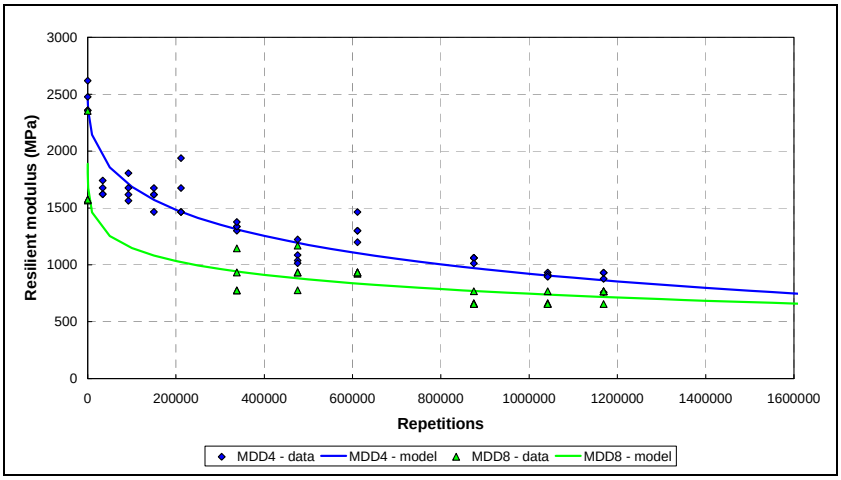

(b) Section 415A5, tested at 40 kN

Figure 2.3: Resilient modulus of the foamed asphalt treated base layer.

3. TEST DETAILS

3.1 Experiment Location

The HVS experiment was located on SR89 between Calpine and Graeagle. Figure 3.1 shows the location of State Route 89 and the approximate location of the HVS test site.

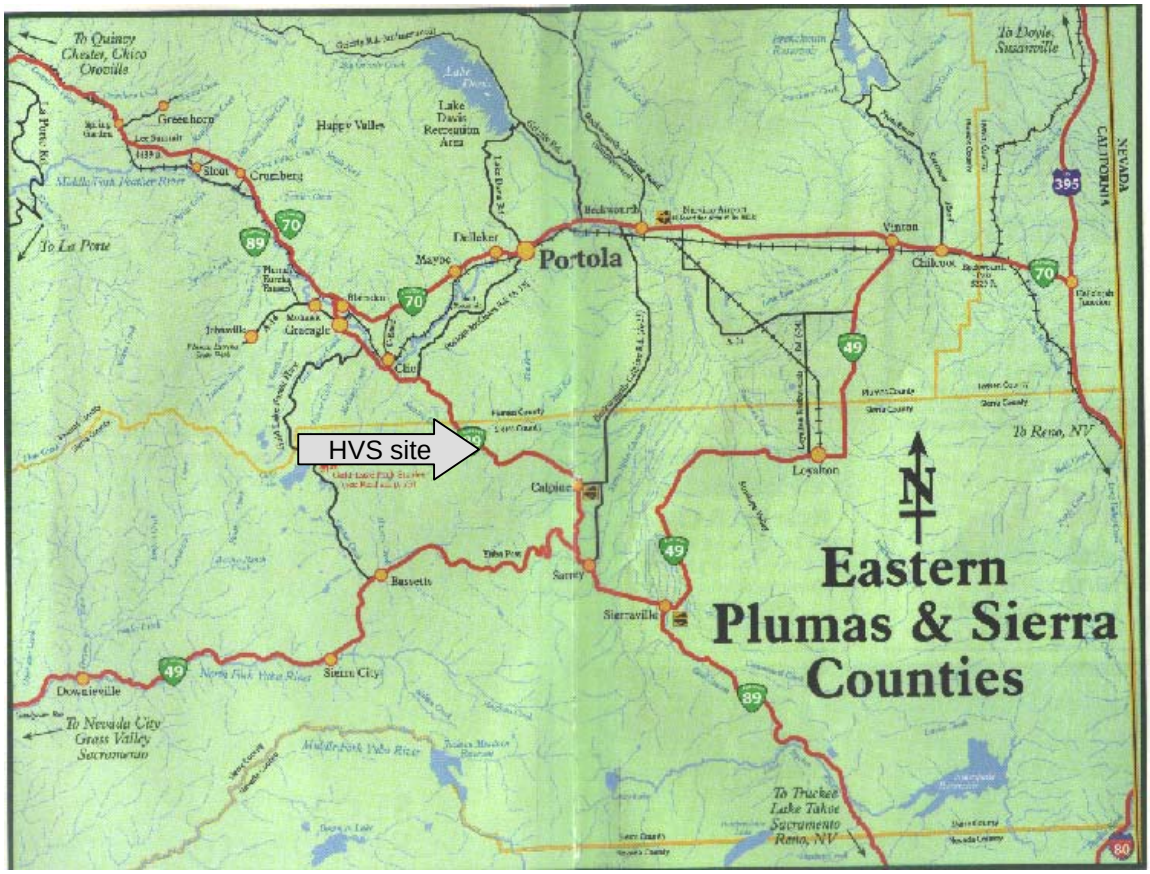

Figure 3.1: Location of State Route 89.

3.2 Materials, Pavement Structure and Construction

The original pavement structure of State Route 89 evolved from a gravel road and consisted of approximately 150 mm of dense graded asphalt concrete (DGAC) on in situ decomposed granite. The in situ material had originally been oiled prior to paving with asphalt concrete. Figure 3.2 shows the nominal pavement structure before and after rehabilitation. All values were obtained from the District 3 District Materials Engineer's (DME) office.

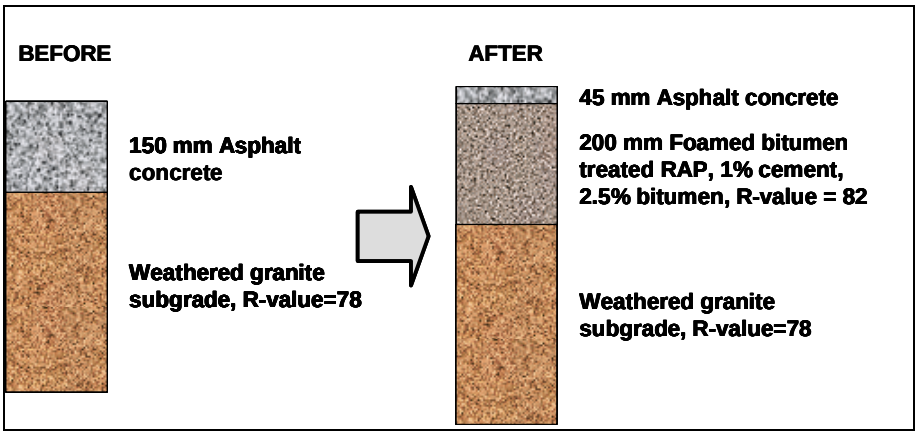

Figure 3.2: Nominal pavement structure of SR89 before and after recycling.

The original pavement structure was rehabilitated and upgraded using a Wirtgen WR2500 machine in July 2002. The reclaimed pavement was designed for a Traffic Index (TI) of 8.5 to 9.0, which is 800,000 to 1,000,000 equivalent standard axle loads (ESALs). The subbase layer of the main roadway is a decomposed granite material with an R-value of 78. During recycling, the pavement was milled to a nominal depth of 200 mm (8.0 in). The milled, untreated RAP has an R-value of 82.

A detailed cut plan of the mainline reconstruction was not available. However, the northbound lane was completed first and the cuts overlapped by 150 mm (6.0 in). According to the District Materials Engineer (DME), the northern end of the northbound lane in the area of the field testing may show different DCP and density readings, attributed to a change in the rolling pattern in that area. The vibratory pad-foot roller broke down, and, as a result, the initial compaction was accomplished with a steel drum roller in vibratory mode. This created minor delaminations of the foamed asphalt treated material that had to be removed prior to paving. The thickest delamination was approximately 25 mm to 30 mm *(3)*.

The HVS test lane was specially constructed adjacent to the roadway at post-mile 27 in Sierra County. Material was brought in to provide the support layers and was different to that of the main roadway. The condition of the support layers is discussed in Chapter 4. The base layer is reclaimed asphalt concrete treated with foamed asphalt and cement and was constructed with excess material from construction of the main roadway. This treated material was stockpiled for a week before construction of the HVS test lane. The reclaimed base layer was primed with an SS-1 emulsion before being surfaced with 50 mm of asphalt concrete.

3.3 Mix Design

Limited data on the mix design were received from the District 3 DME's office. It is thought that the specimens were manufactured from materials taken from the test pits excavated during the rehabilitation investigation. The RAP was crushed in the laboratory and treated with foamed asphalt. Specimens 100 mm (4.0 in) in diameter were prepared with California kneading compaction and then cured for 72 hours at 40°C.

The Indirect Tensile Strength (ITS) test data are shown in Figure 3.3. A wide range of ITS results was obtained for each binder content and do not show a clear optimum. A binder content of 2.5 percent and cement content of 1.0 percent were selected for the mix design.

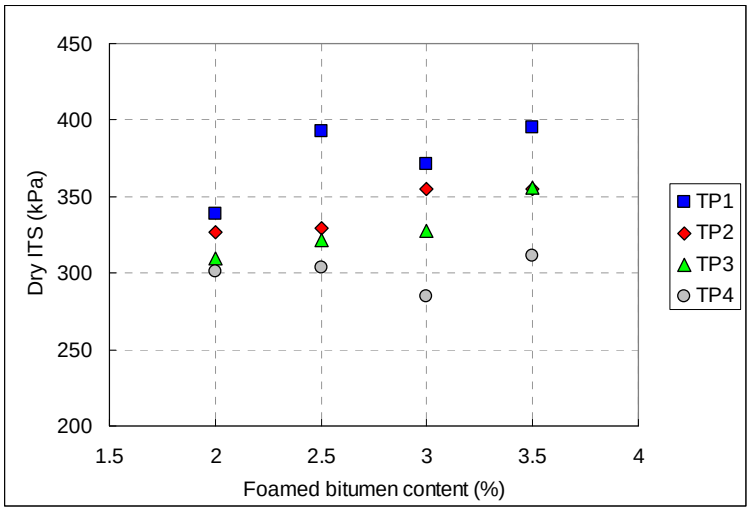

Figure 3.3: Indirect tensile strength test results.

3.4 HVS Test Section Layout

Four sections were subjected to HVS testing. The relative positions of the test sections are shown in Figure 3.4.

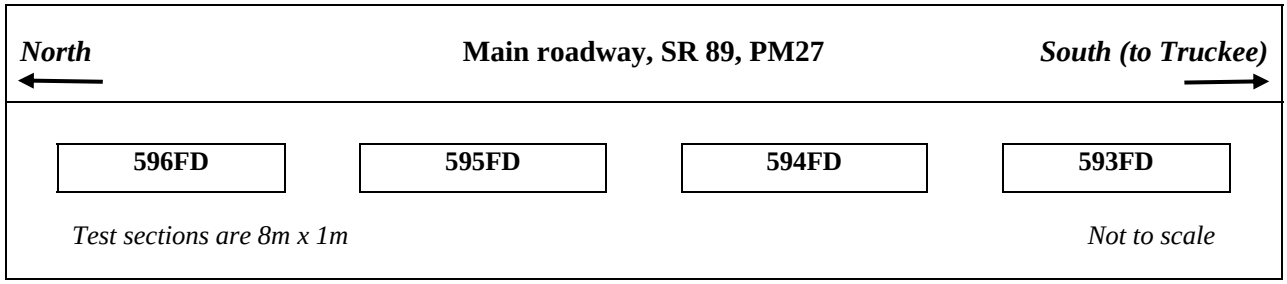

Figure 3.4: Location of HVS test sections adjacent to southbound SR89 at PM27.

3.5 HVS Testing Program

The testing periods were as follows:

- Section 593FD - August 2003 to mid-September 2003
- Section 594FD - early October 2003 to late February 2004
- Section 595FD - mid-March to early May 2004
- Section 596FD - early May to mid-May 2004

The test conditions are summarized in Table 3.1

Table 3.1: Summary of the Load History for the HVS Test Sections

Number of Load Repetitions	Wheel load (kN)		Temp (°C)	Wheel	Tire Pressure (kPa)	Direction	Wet*/dry
	Planned	Actual					
Section 593FD							
0 - 30,000	40	60	20	Dual	690	Bi	Dry
30,000 - 60,000	60	90	20	Dual	690	Bi	Dry
60,000 - 300,000	90	80	20	Dual	690	Bi	Dry
Section 594FD							
0 - 1,042,101	40	60	20	Dual	690	Bi	Dry
Section 595FD							
0 - 487,452	40	60	5	Dual	690	Bi	Dry
Section 596FD							
0 - 34,042	40	60	Ambient	Dual	690	Bi	Wet
* Water sprayed onto test section							

The loading program differs from the original test plan due to an incorrect hydraulic control system setup on loads less than 65 kN (14,625 lb) at the start of the experiment. The loading patterns were thus retained to facilitate comparisons of performance between all tests in the study. Testing was undertaken with a dual-wheel configuration, using radial truck tires (Goodyear G159 - 11R22.5- steel belt radial) inflated to a pressure of 690 kPa (100 psi), in a bidirectional loading mode. Lateral wander over the one-meter width (3.3 ft) of the test section was programmed to simulate traffic wander on a typical highway lane.

3.6 Test Section Detail

The layout of a test section is shown in Figure 3.5. The summary sheets presented in through Figure 3.9 show the MDD instrumentation detail and material properties for the HVS test sections on SR89. The material properties shown in these figures are based on the available site investigation and construction results discussed below.

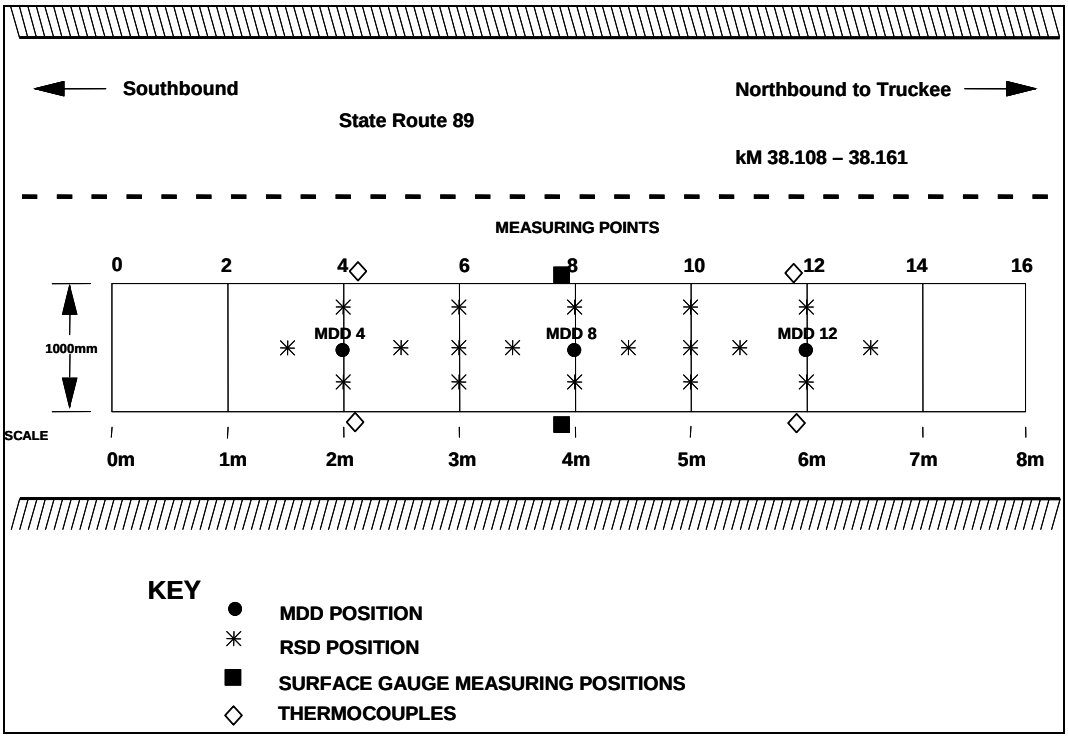

Figure 3.5: Layout of individual HVS test sections.

The levels at which the MDD modules were installed on Section 593FD, were selected to coincide with the layer interfaces to simplify analysis of the MDD data in the assessment of the performance of the individual pavement layers. The layer thicknesses were determined from the nominal design pavement structure. Subsequent to determining the actual layer thicknesses in the test pit on Section 593FD, the MDD module depths on Sections 594FD and 595FD were adjusted to coincide with the actual layer interfaces. The topcap of the MDD actually measures the deflection and permanent deformation 25 mm (1.0 in) below the surface of the layer, therefore some of the asphalt concrete is included in the layer thickness between the topcap and the next MDD module. This small amount will not significantly influence the backcalculated stiffnesses of the MDD modules. The load sequence data, which consists of the approximate number of load repetitions at which test conditions were changed, are also shown on the figures.

HVS-section Nr: 593FD	Region: Sierraville, CA	Road Nr: SR89	Year of test: 2003

Pavement structure

Instrumentation detail

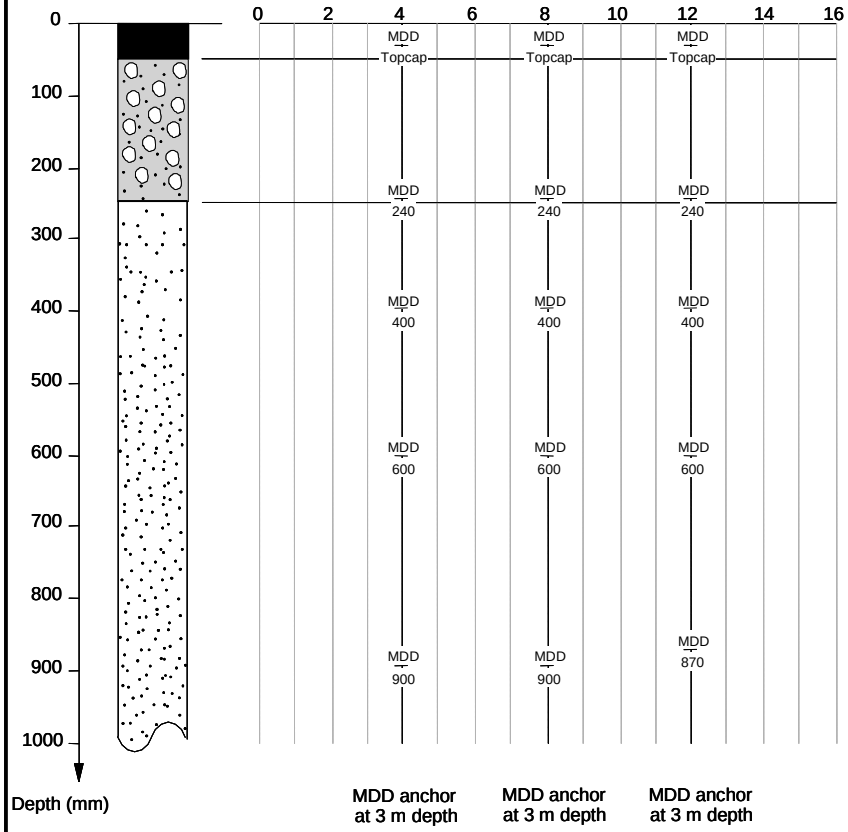

Pavement material information

Layer (mm)	Type	Material properties (UCS, CBR, mDD, OMC,etc)	Field: Density (kg/cub m)	Field: MC (%)	Material class
0 - 50	Asphalt				
50 - 250	Foamed bitumen treated base	Foamed bitumen treated recyceld asphalt pavement R-value: 82			
250 +	Crushed stone subbase	Weathered granite subgrade R-value: 78			

Note: mDD = maximum Dry Density

Load sequence detail:

Repetitions		Test information		
From	To	Wheel load	Tire pressure	Water added
0	15 000	60 kN	690 kPa	No
15 000	50 000	90 kN	690 kPa	No
50 000	700 000	80 kN	690 kPa	No

Related reports:

Figure 3.6: Section 593FD detail.

HVS-section Nr: 594FD	Region: Sierraville, CA	Road Nr: SR89	Year of test: 2003

Pavement structure

Instrumentation detail

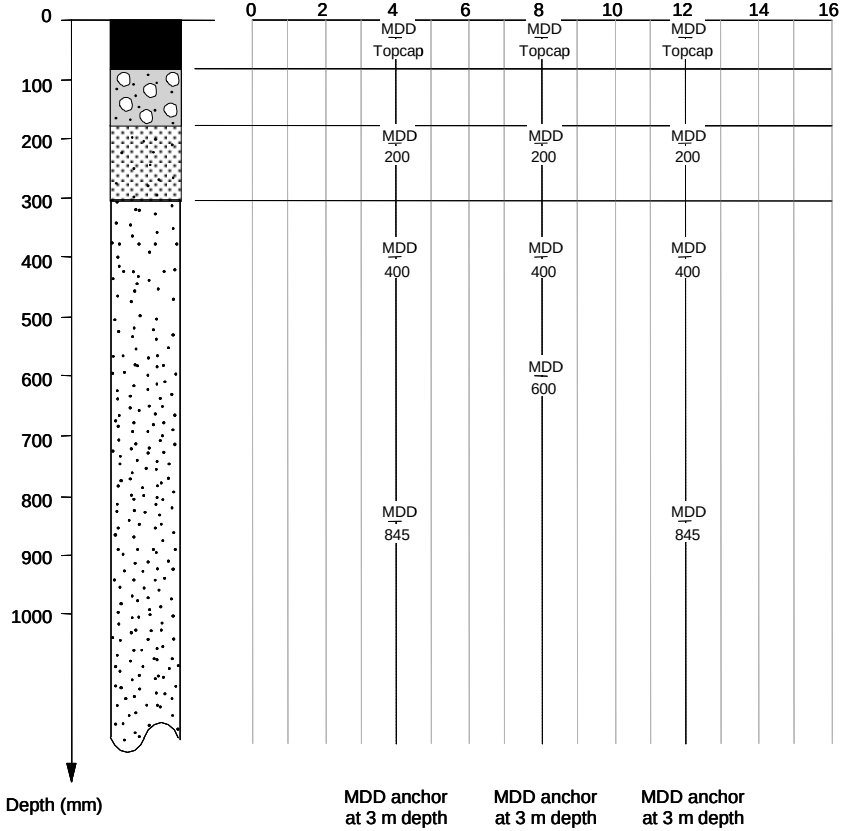

Pavement material information

Layer (mm)	Type	Material properties (UCS, CBR, mDD, OMC,etc)	Field: Density (kg/cub m)	Field: MC (%)	Material class
0 - 81	Asphalt				
81 - 178	Foamed bitumen treated base	Foamed bitumen treated recyceld asphalt pavement R-value: 82			
178 - 301	Grey, clay-like material	Grey, clay material			
301 +	D/granite	Decomposed granite subgrade R-value: 78			

Note: mDD = maximum Dry Density

Load sequence detail:

Repetitions		Test information		
From	To	Wheel load	Tyre pressure	Water added
0	1 042 100	60 kN	690 kPa	No

Related reports:

Figure 3.7: Section 594FD detail.

HVS-section Nr: 595FD	Region: Sierraville, CA	Road Nr: SR89	Year of test: 2004

Pavement structure

Instrumentation detail

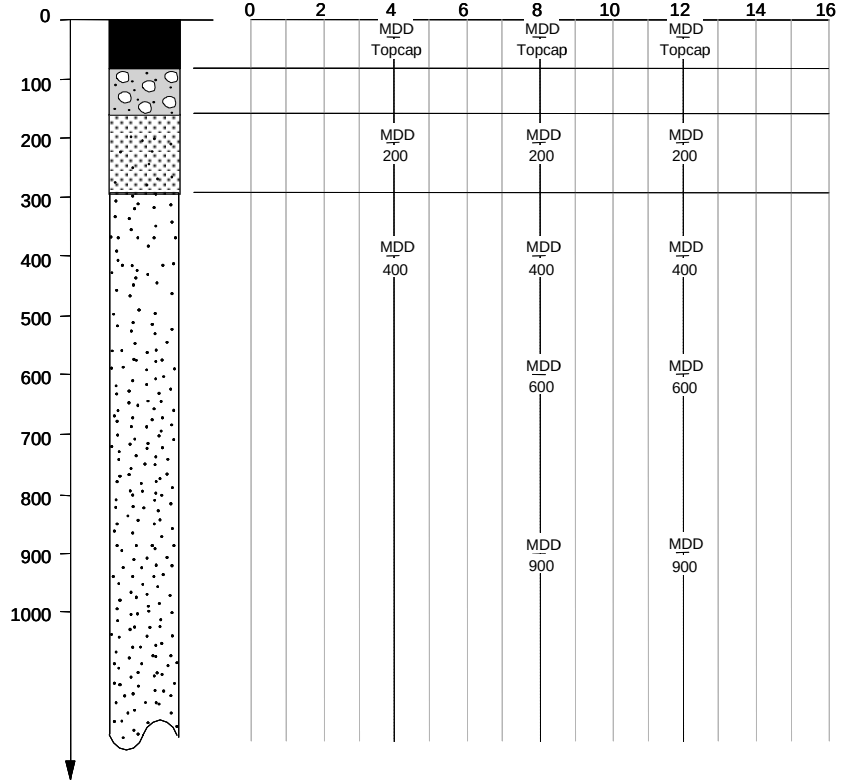

Pavement material information

Layer (mm)	Type	Material properties (UCS, CBR, mDD, OMC,etc)	Field		Material class
			Density (kg/cub m)	MC (%)	
0 - 81	Asphalt				
81 - 159	Foamed bitumen treated base	Foamed bitumen treated recyceld asphalt pavement R-value: 82			
159 - 292	Grey, clay-like material	Grey, clay material			
292 +	D/granite	Decomposed granite subgrade R-value: 78			

Note: mDD = maximum Dry Density

Load sequence detail:

Repetitions		Test information		
From	To	Wheel load	Tyre pressure	Water added
0	487 452	60 kN	690 kPa	No

Related reports:

Figure 3.8: Section 595FD detail.

HVS-section Nr: 596FD	Region: Sierraville, CA	Road Nr: SR89	Year of test: 2004

Pavement structure

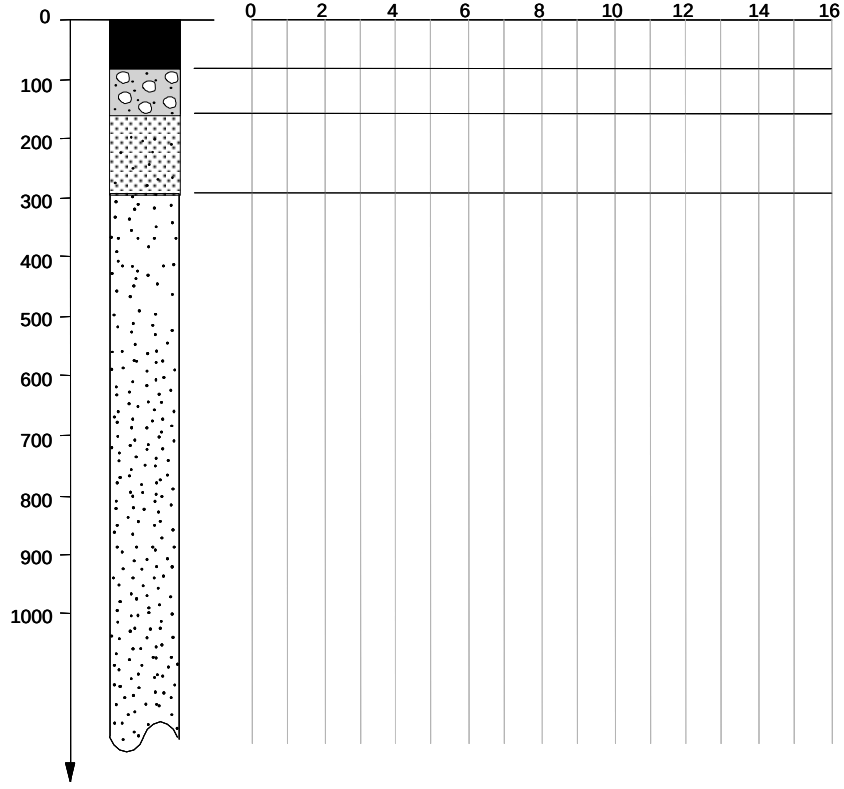

Instrumentation detail

Pavement material information

Layer (mm)	Type	Material properties (UCS, CBR, mDD, OMC,etc)	Field: Density (kg/cub m)	Field: MC (%)	Material class
0 - 81	Asphalt				
81 - 159	Foamed bitumen treated base	Foamed bitumen treated recyceld asphalt pavement R-value: 82			
159 - 292	Grey, clay-like material	Grey, clay material			
292 +	D/granite	Decomposed granite subgrade R-value: 78			

Note: mDD = maximum Dry Density

Load sequence detail:

Repetitions		Test information		
From	To	Wheel load	Tyre pressure	Water added
0	34 042	60 kN	690 kPa	Yes

Related reports:

Figure 3.9: Section 596FD detail.

4. SITE INVESTIGATIONS

Preliminary field test results were collected on the mainline and the constructed turnout sections on SR89 between Calpine and Graeagle during June, July and August 2003. Testing consisted of Falling Weight Deflectometer (FWD) deflection measurements on the mainline between PM20 and PM30 and FWD deflections and Dynamic Cone Penetrometer (DCP) tests on the HVS test area. The results from these tests as well as preliminary HVS results showed:

- A difference in the resilient modulus of the upper pavement layers between the mainline and HVS lane with the foamed asphalt treated base of the mainline having higher resilient modulus values;
- The resilient modulus of the foamed asphalt treated base of the HVS lane to be well below what would normally be expected for this type of pavement; and
- The initial HVS Multi-depth Deflectometer (MDD) deflection to be well in excess of what would normally be expected from a newly constructed pavement of this type.

A second round of field testing was therefore motivated to investigate the differences between the mainline and HVS lane in the vicinity of HVS Section 593FD. Caltrans provided a lane closure on October 29 2003 during which nuclear density, DCP and FWD tests were carried out, cores were cut from the base layer and a test pit was excavated on the mainline. Additional DCP and nuclear density tests were carried out on the HVS lane and a partial test pit was excavated on Section 593FD. HVS testing on Section 593FD had been completed by the time of the October 2003 field testing. Figure 4.1 shows the layout of the test locations on the mainline and HVS lane. DCP tests D1 to D9 were done during August 2003 and the remainder of the DCP tests during October 2003. DCP tests D22 to D25 were done close to the locations of selected DCP tests done during August to confirm that no changes occurred in the pavement from August to October. FWD tests were done on the mainline in the vicinity of the HVS site at 1.0 m intervals at 40 kN and 80 kN deflection loads during the October lane closure.

4.1 Falling Weight Deflectometer Survey

Falling Weight Deflectometer (FWD) surveys were performed one year after construction on 10 and 11 June 2003, again during the road closure on 29 October 2003 and after completion of HVS testing on 25 May 2004.

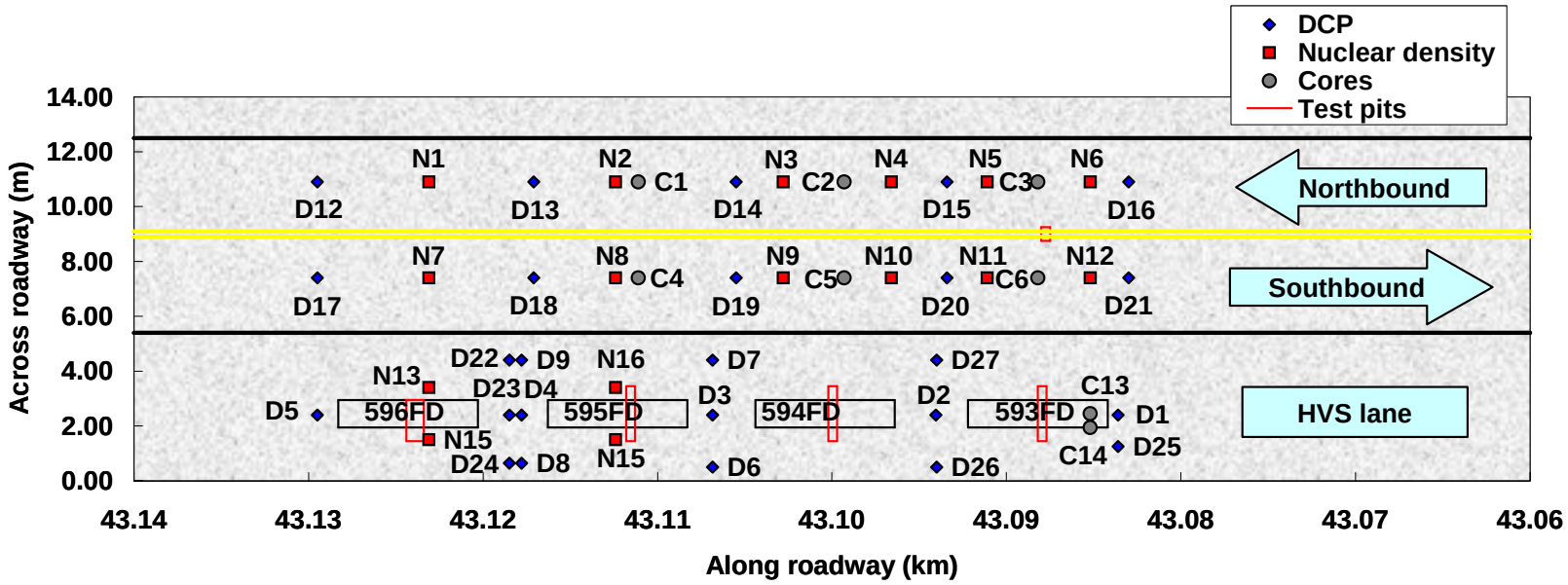

Figure 4.1: Layout of the field test locations on the mainline and HVS lane.

4.1.1 June 2003 FWD Survey

In the first FWD survey, deflections were measured on 10 and 11 June 2003 on the outer wheel paths of both carriageways on the main roadway, and on both turnouts available for HVS testing. Two rows of data were collected on the HVS test sections. A third row was attempted right on the edge (away from the roadway) of the section eventually selected for HVS testing (Section 1), but the pavement structure was so weak it was not possible to measure deflections.

The peak deflection histograms for the main roadway and the HVS test lane are shown in Figure 4.2 and Figure 4.3. The most frequently occurring values (mode) of the deflections are between 450 micron and 550 micron for the main roadway, 950 micron to 1,050 micron for Row 1 and 1,150 micron to 1,450 micron for Row 2 on the HVS test lane. The deflection on the main roadway was significantly smaller than on the specially built HVS test lane. The deflection also increased away from the mainline and Row 2, with the highest deflection coinciding with the centerline of the HVS test sections on the HVS lane.

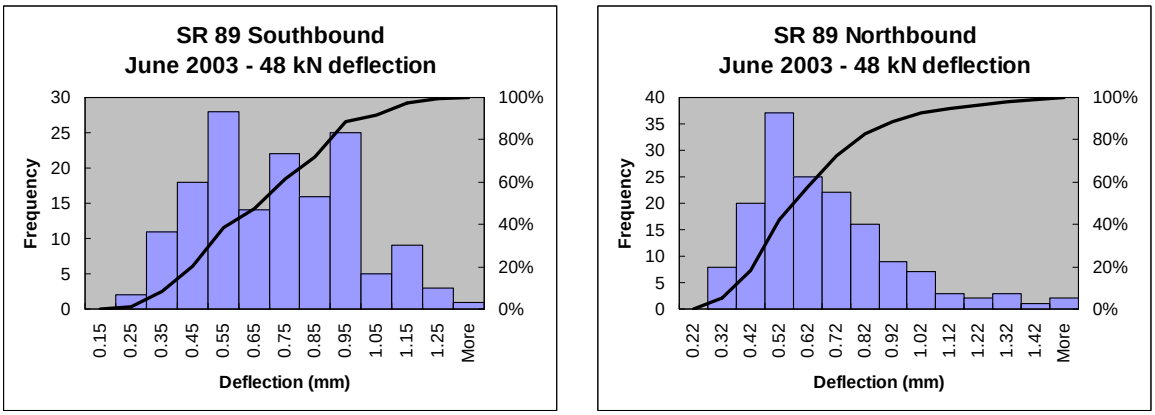

Figure 4.2: Peak FWD deflections for the main roadway during June 2003.

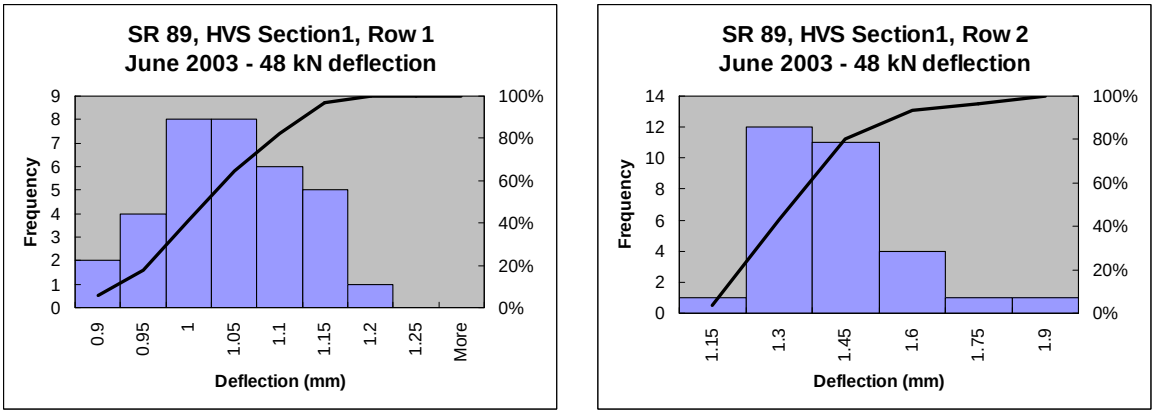

Figure 4.3: Peak FWD deflections on HVS test lane during June 2003.

The deflection histogram for the southbound lane appeared to have a secondary peak of higher deflection in the order of 750 micron to 950 micron (30 to 38 mils).

International experience indicates that deflections in the order of 500 micron (20 mils) are expected for newly constructed pavements with a granular base, and between 250 micron and 400 micron (10 and 16 mils) for pavements with a stabilized base. Although the deflections of the main roadway were slightly higher than these typical values, the deflections on the HVS test lane were significantly higher. The HVS test lane was therefore not representative of the main roadway, and was probably not representative of other full-depth reclaimed foamed asphalt pavements. It is recommended that data from newly constructed pavements treated with foamed asphalt be sought, for comparison with SR89.

Resilient moduli for the foamed asphalt treated RAP and subgrade layers were backcalculated from the FWD data using the *back-PADS*™ software. The best estimate of the layer thicknesses based on the test pit and coring results (see Section 4.2) were used in the back-calculation procedure.

The backcalculated resilient moduli for the foamed asphalt treated RAP layer are shown in Figure 4.4 and Figure 4.5 for the mainline and HVS test lane. The range of resilient moduli on the main roadway was considerably higher than on the HVS test lane, but it should be noted that the sample size was significantly larger than for the HVS test lane because of the length of the mainline sections. The frequency histogram for the southbound lane shows two distinct distributions of resilient modulus values, one with a peak in the region of 300 MPa to 400 MPa and the other in the region 1,050 MPa to 1,850 MPa. This is a result of the distribution of deflections measured on the southbound lane. The frequency histogram for the northbound lane shows a much less prominent secondary peak at 1,300 MPa. The resilient modulus values for the secondary peaks of the frequency histograms, 1,050 MPa to 1,850 MPa for the southbound lane and 1,300 MPa for the northbound lane are typical of values expected for foamed asphalt treated material.

The resilient modulus values for Row 1 on the HVS lane are still within expectations for foamed asphalt treated material but the distribution of values obtained for Row 2 is typical of untreated base layer material. Other representative values are discussed in Section 2.2, and are in the order of 1,700 MPa and 4,000 MPa for the examples cited. Typical values should be obtained for similar projects in California in an effort to assess the representivity of the HVS test lane on SR89.

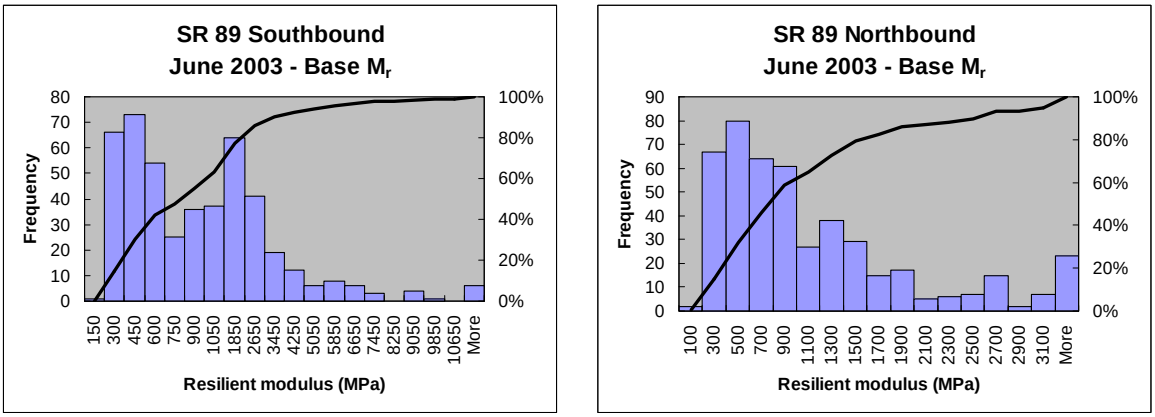

Figure 4.4: Backcalculated base resilient modulus, main roadway June 2003.

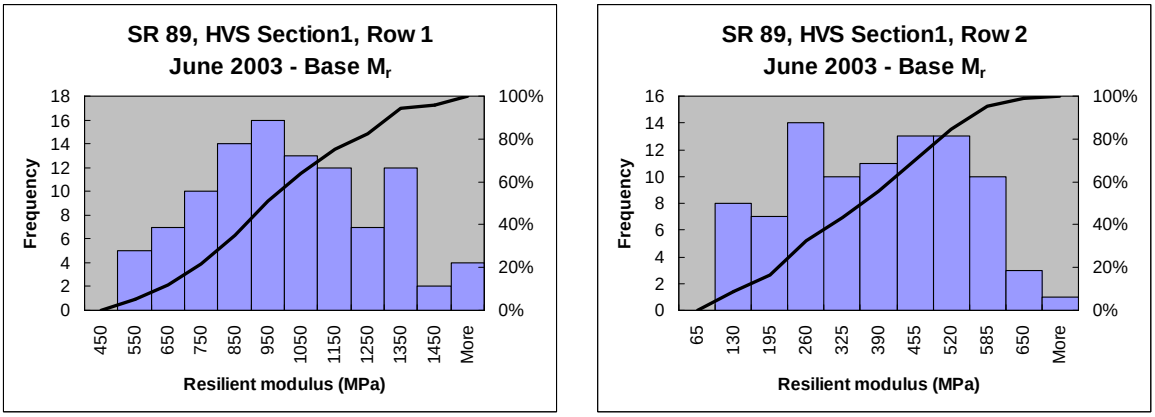

Figure 4.5: Backcalculated base resilient modulus, HVS test lane, June 2003.

Table 4.1 summarizes the mode values (values with the highest frequency of occurrence) for the FWD resilient modulus results. The base layer resilient moduli were highest in Row 1 of the HVS test lane, which was closest to the main roadway. Row 2 was through the marked HVS test sections, including Section 593FD. These data suggest a moduli gradient in the transverse direction of the turnout with the specific HVS test sections on the areas of the moduli.

Table 4.1: Backcalculated Resilient Moduli in Area of HVS Sections, June 2003

Road			Resilient moduli (MPa)
Main roadway	Southbound	Primary peak Secondary peak	300 - 450 1,050 - 1,850
	Northbound	Primary peak Secondary peak	300 - 500 1,100 - 1,300
HVS test lane	Row 1* Row 2		850 - 950 390 - 520
* Row 1 closest to the main roadway			

The modes of the FWD backcalculated subgrade resilient modulus were fairly similar for the main roadway and HVS test lane, as shown in Figure 4.6 and Figure 4.7. The northbound lane had the highest

mode between 60 MPa and 70 MPa, followed by the southbound lane with a mode between 50 MPa and 60 MPa, HVS Sections 593FD and 594FD with a mode between 55 MPa and 60 MPa and HVS Sections 595FD and 596FD with a mode between 50 MPa and 55 MPa. The top-end of the range of subgrade resilient modulus values for the main roadway was, however, considerably higher than that of the HVS test lane.

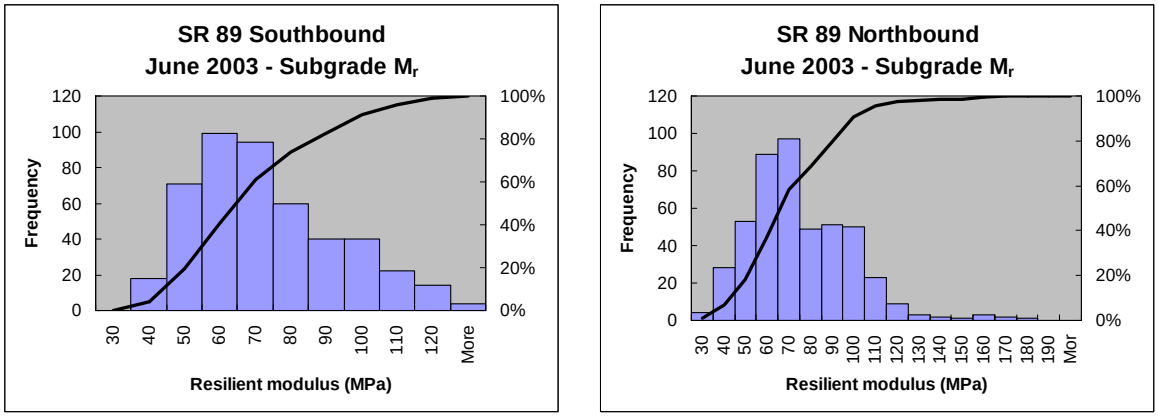

Figure 4.6: Backcalculated subgrade resilient modulus, main roadway June 2003.

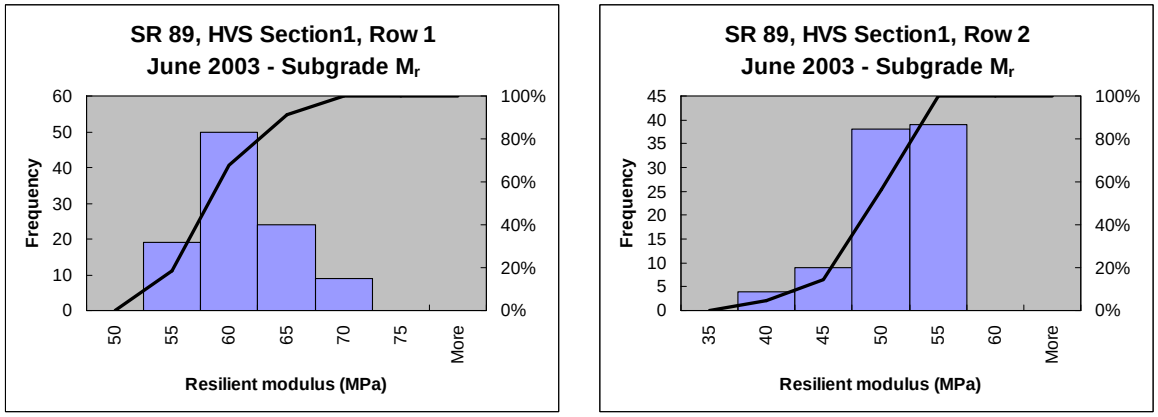

Figure 4.7: Backcalculated subgrade resilient modulus, HVS test lane June 2003.

The subgrade resilient moduli were slightly, but not unrealistically low for the decomposed granite subgrade. The support condition is fairly consistent for the main roadway and the HVS lane. The large differences in deflections discussed in the preceding section are therefore not due to differences in the support.

4.1.2 October 2003 FWD Survey

During the road closure on 29 October 2003, extensive FWD testing was performed. The frequency of the measurement points was increased to every three metres on the mainline and every meter on the

turnout selected for HVS testing. On the HVS test lane, it was only possible to measure the deflections from Section 595FD in the northerly direction. This is because the HVS was positioned on Sections 593FD and 594FD.

The peak deflections measured are illustrated in Figure 4.8 and Figure 4.9 for the two directions of the mainline and the HVS test lane.

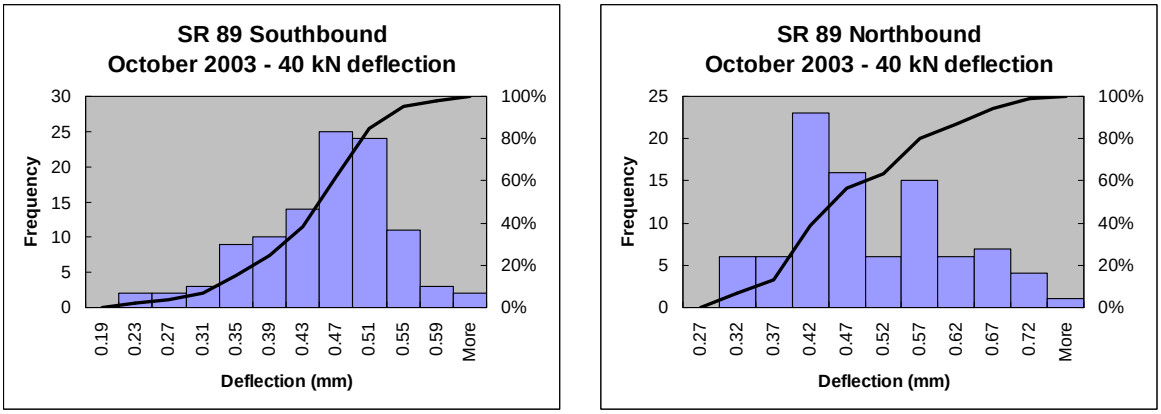

Figure 4.8: Peak FWD deflections for the main roadway during October 2003.

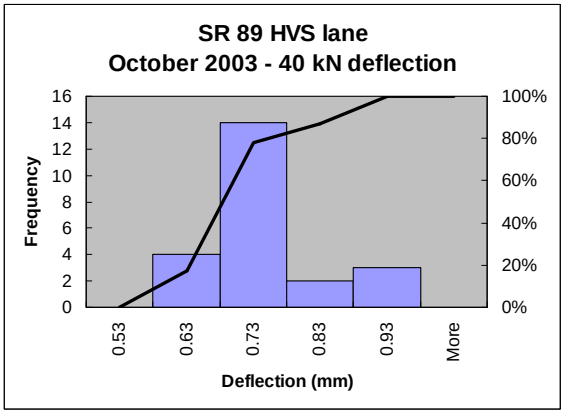

Figure 4.9: Peak FWD deflections on HVS Section 593FD during October 2003.

The peak deflections were used to backcalculate resilient moduli for the foamed asphalt treated base layer and the subgrade. Again, the best estimate of the layer thicknesses based on the test pit and coring results were used in the back-calculation procedure (see Section 4.2). The grey, clay-like material and decomposed granite observed in the test pit on the HVS lane were combined into one subgrade layer for analysis purposes.

The resilient modulus of the foamed asphalt treated base layer is illustrated in Figure 4.10 and Figure 4.11. The values for the HVS lane (Figure 4.11) are not plotted with the same scale as the mainline data. The southbound lane of the mainline has higher resilient moduli than the northbound lane. The HVS lane base layer resilient moduli were significantly lower (200 MPa - 600 MPa) than on the mainline although a secondary peak was observed between 900 MPa and 1,000 MPa. This again indicates that the base on the HVS lane was not representative of the mainline and the values were much lower than expected.

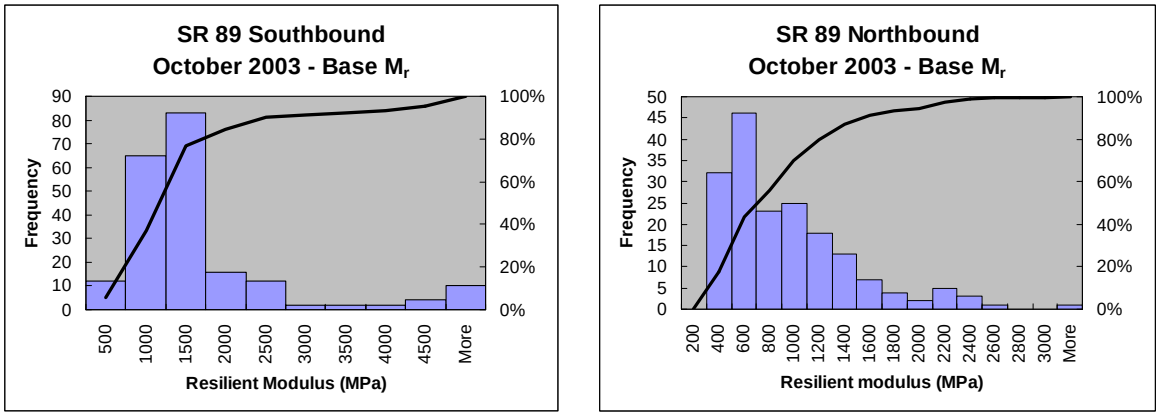

Figure 4.10: Backcalculated base resilient modulus, main roadway, October 2003.

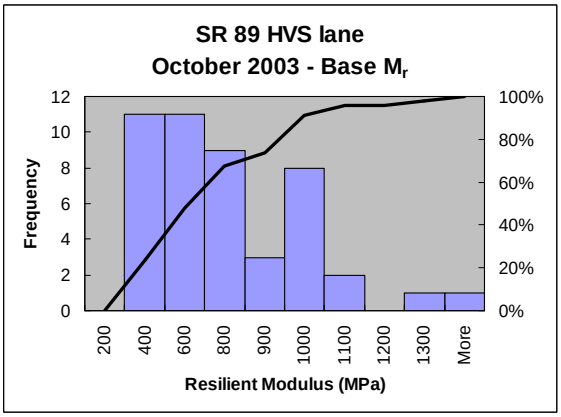

Figure 4.11: Backcalculated base resilient modulus, HVS test lane, October 2003.

The subgrade resilient moduli determined from the October 2003 survey are illustrated in Figure 4.12 and Figure 4.13. The results indicate no significant differences between the support condition of the north and southbound lanes and the HVS test lane.

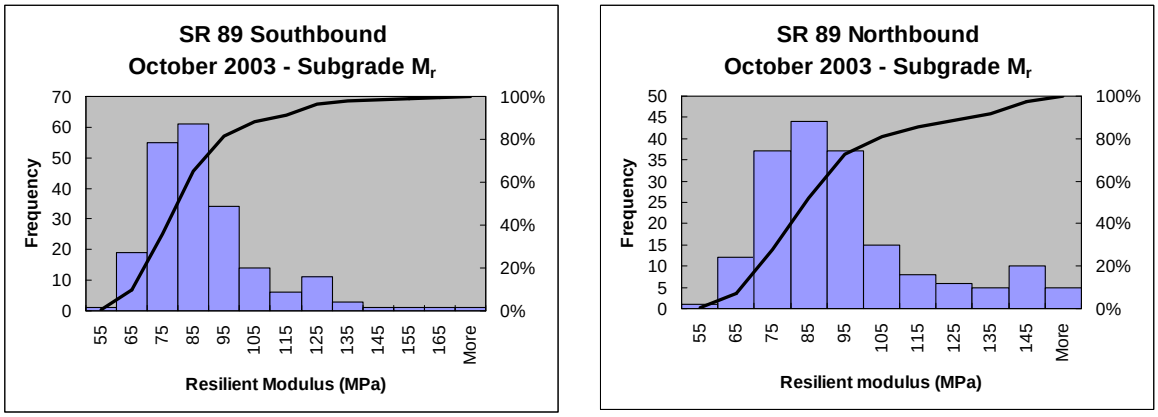

Figure 4.12: Backcalculated subgrade resilient modulus, main roadway, October 2003.

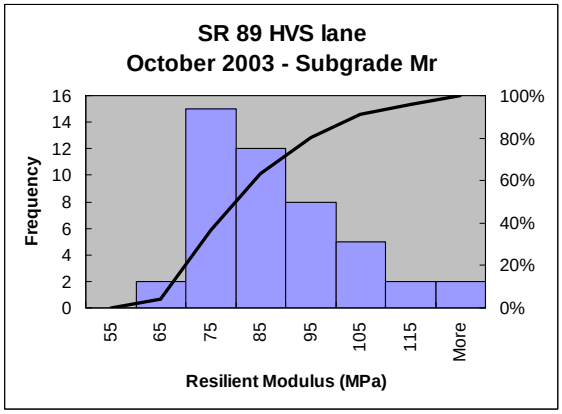

Figure 4.13: Backcalculated subgrade resilient modulus, HVS test lane, October 2003.

4.1.3 May 2004 FWD Survey

A set of FWD deflections were again recorded in May 2004 after completion of the HVS tests. Deflections were, however, recorded only on the mainline because of the test pit excavations on the HVS lane. The peak deflections measured are illustrated in Figure 4.14 for the two directions of the mainline.

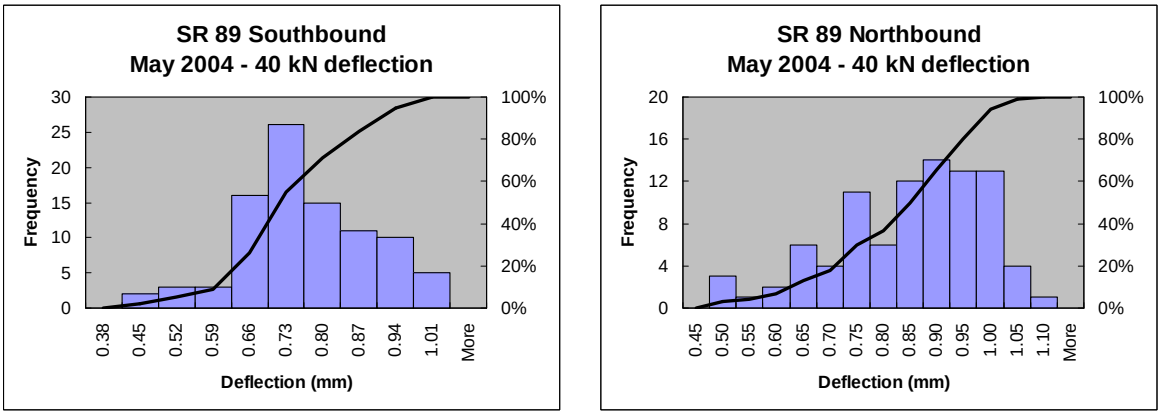

Figure 4.14: Peak FWD deflections for the main roadway during May 2004.

The peak deflections were used to backcalculate resilient moduli for the foamed asphalt treated base layer and the subgrade. Again, the best estimate of the layer thicknesses based on the test pit and coring results were used in the back-calculation procedure (see Section 4.2). The grey, clay-like material and decomposed granite were combined into one subgrade layer for analysis purposes.

The foamed asphalt treated base resilient modulus results are illustrated in Figure 4.15. The southbound lane of the mainline had higher resilient modulus values than the northbound lane.

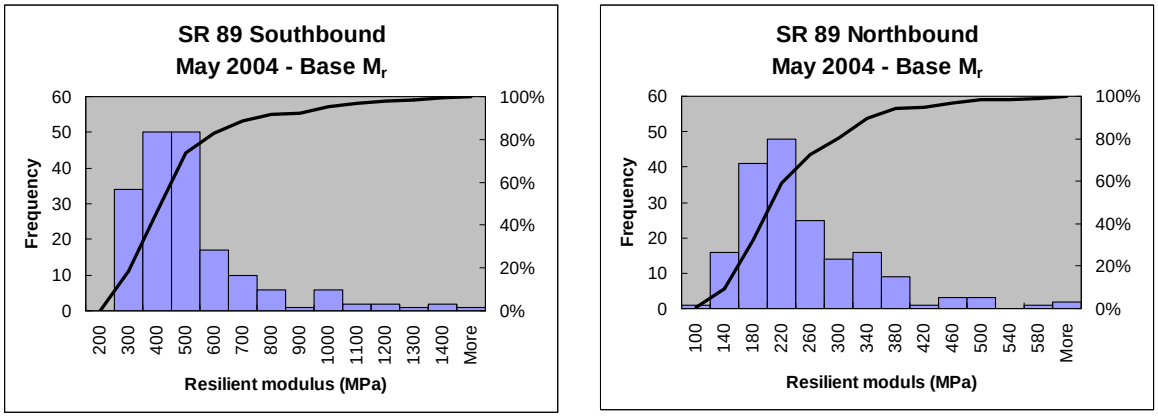

Figure 4.15: Backcalculated base resilient modulus, main roadway May 2004.

The subgrade resilient modulus values determined from the May 2004 survey are illustrated in Figure 4.16. The results indicate no significant differences between the support condition of the north and southbound lanes.

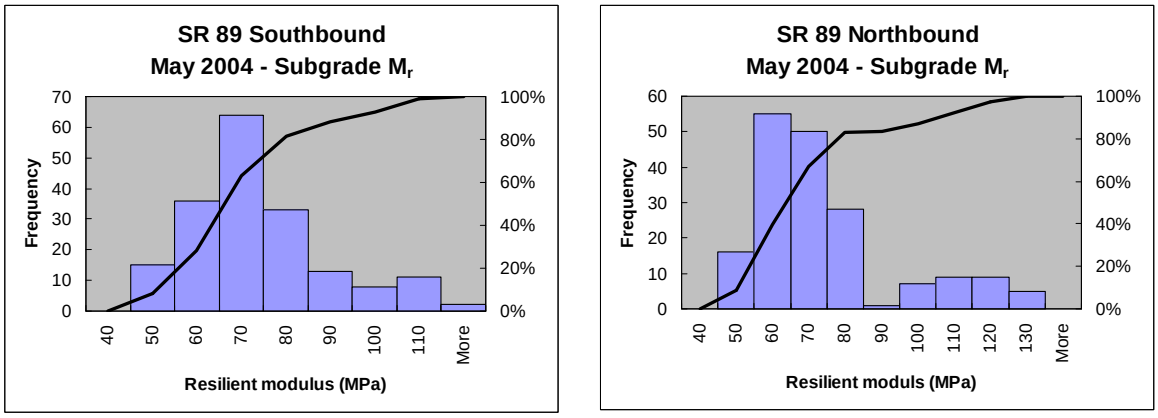

Figure 4.16: Backcalculated subgrade resilient modulus, main roadway May 2004.

4.1.4 Summary of the FWD Survey Results and Conclusions

The base layer resilient modulus results from the June 2003, October 2003 and May 2004 FWD surveys are plotted in Figure 4.17. The distribution of resilient modulus values for the southbound lane was consistently slightly higher than that of the northbound lane. The resilient modulus of the base layer of both lanes showed a significant reduction from October 2003 to May 2004. The subgrade resilient modulus did not differ substantially between the three survey periods as shown in Figure 4.18.

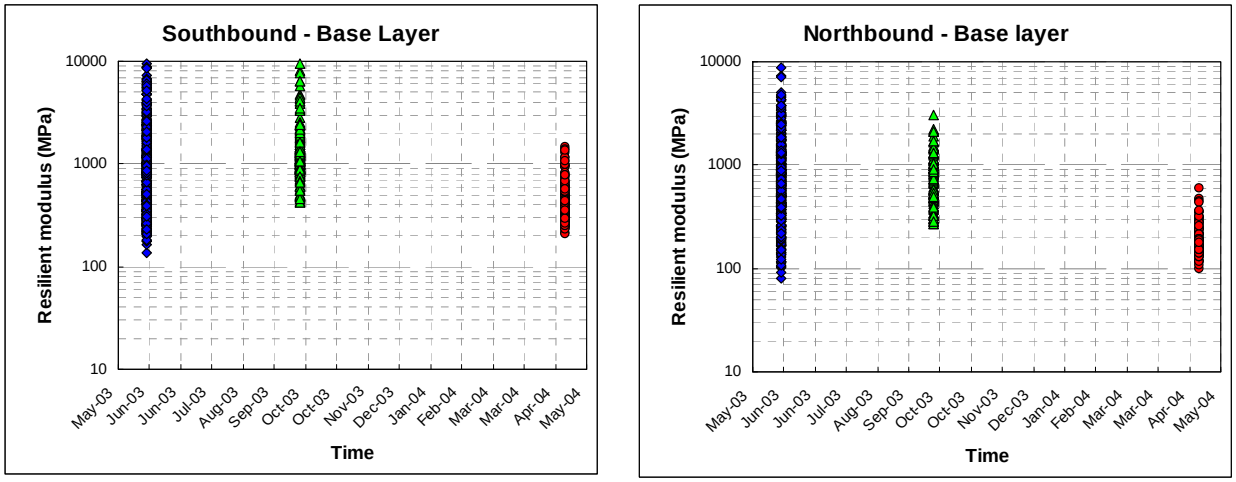

Figure 4.17: Comparison of the backcalculated base layer resilient modulus results.

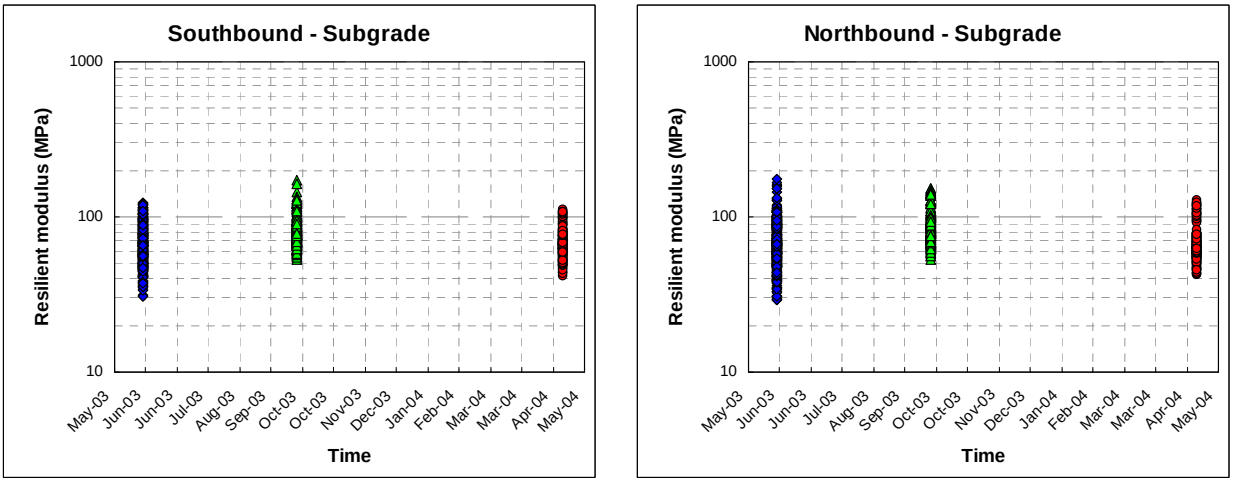

Figure 4.18: Comparison of the backcalculated subgrade resilient modulus results.

The differences in the modulus of the base layer of the main roadway and the HVS test lane determined from both the August and October 2003 FWD surveys were not attributed to differences in support. Two reasons are postulated for the differences:

- The foamed asphalt/portland cement treated material used on the HVS test lane was stockpiled for about one week before placement. It is possible that cementitious bonds (from the 1.0 percent cement filler) formed during initial construction, were broken when the material was moved from the stockpile to the HVS sections and during construction of the section.
- The base layer on the HVS test lane was not compacted in the same manner or with the same energy as on the main roadway, and hence the material had a lower density. Differences in the compaction moisture could also result in different densities being achieved.

4.2 Cores and Test Pits

During the October 2003 field testing, three cores were cut from each lane on the mainline, one core was cut from Section 593FD (the completed HVS test) and one core was cut from just outside Section 593FD. A 600 mm x 600 mm test pit was opened next to the centre-line on the southbound carriageway opposite the test pit that was opened between Stations 8 and 9 across Section 593FD. After completion of HVS testing on Sections 594FD, 595FD and 596FD, test pits were opened on the remaining three sections in May 2004.

4.2.1 Mainline Test Pit (October 2003)

The photograph in Figure 4.19 shows the asphalt concrete surfacing removed from the test pit that was excavated on the mainline. There was a good bond between the asphalt concrete surfacing and the foamed asphalt treated base. A large piece of intact reclaimed asphalt was found in the base layer during excavation as shown in Figure 4.20. The support of the foamed asphalt treated base layer in the test pit was also found to differ. The support for the southbound lane appeared to consist of decomposed granite while that of the northbound lane appeared to consist of an old oil-based pavement as shown in the photograph in Figure 4.21 (bottom of the test pit).

Moisture contents determined from samples taken from the mainline test pit in the southbound lane are shown in Table 4.2. The foamed asphalt base was slightly more moist than the grey clay layer.

Table 4.2: Moisture Contents in Southbound Test Pit

Pavement layer	SR89 southbound
Foamed asphalt base	5.5 %
Grey clay layer*	5.0 %
Subgrade	Not measured
* Grey clay layer was not the same material in the HVS lane and in the mainline test pit	

Figure 4.19: Asphalt concrete surfacing removed from the test pit on the mainline.

Figure 4.20: Intact piece of reclaimed asphalt concrete found in the mainline test pit.

Figure 4.21: Bottom of mainline test pit showing old oil-based pavement.

4.2.2 593FD Test Pit (October 2003)

The photograph in Figure 4.22 shows the asphalt concrete surfacing layer removed from the test pit excavated on Section 593FD. There appeared to have been a good bond between the asphalt concrete surfacing and the foamed asphalt treated base layer.

A grey colored material that appeared to have high clay content was found between the foamed asphalt treated base layer and decomposed granite subgrade as shown by the photographs in Figure 4.23. This material tended to break out in flaky pieces as shown in Figure 4.23(b) and Figure 4.24. Similar material was also noticed during the drilling of the holes for MDD installation.

Figure 4.25 shows the completed test pit on Section 593FD. The asphalt concrete surfacing, foamed asphalt treated base layer, grey clay-like material, and decomposed granite subgrade layers are marked with string in the test pit. Figure 4.26 shows the profile measured in the partial test pit. The foamed asphalt treated base layer increased in thickness from the caravan to the traffic side. Table 4.3 summarizes the average values of the layer thicknesses measured in the test pit.

Figure 4.22: Good bond between asphalt concrete and foam asphalt base layer on Section 593FD.

(a) Grey colored material found below the base layer on the HVS lane

(b) The material below the base layer broke out in flaky pieces

Figure 4.23: Grey, clay like material found below the base layer on Section 593FD.

Figure 4.24: Flaky, clay like material from below the base layer on Section 593FD.

Figure 4.25: Test pit Section 593FD after HVS trafficking.

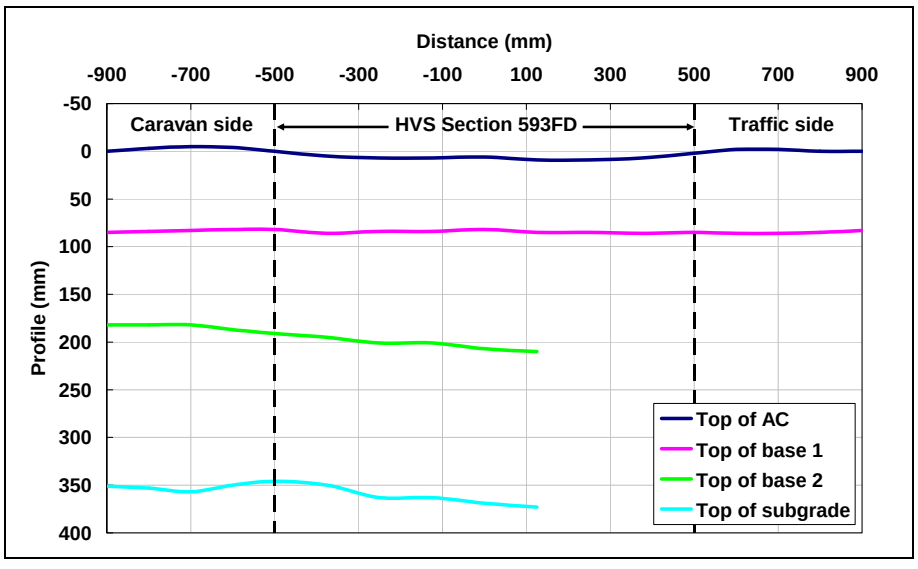

Figure 4.26: Test pit profile on Section 593FD.

Table 4.3: Average layer thickness from the test pit on Section 593FD

Layer	Average thickness for all readings (mm)	Average thickness on HVS section (mm)
Asphalt concrete surfacing	82	79
Foamed asphalt base layer	110	117
Grey, clay-like layer	164	160

Material was obtained from the test pits, and was used to determine the oven-dried moisture contents. The results are shown in Table 4.4. In the foamed asphalt treated reclaimed asphalt, the moisture contents ranged between 5.0 percent and 5.8 percent (except for HVS, CS), which is the same range measured in the mainline test pit (Table 4.2). There is no explanation for the higher moisture content on the caravan side (CS) of the HVS lane. The material below the base of the HVS test pit appeared to contain clay, which would typically have a higher moisture content. The subgrade moisture content was also fairly high, which is expected for a fine-grained material.

Table 4.4: Moisture Contents in the Test Pit on Section 593FD

Pavement layer	Moisture content (%)		
	593FD CS	593FD inside	593FD TS
Foam asphalt base	6.5 %	5.8 %	5.0 %
Grey clay	Not measured	9.4 %	Not measured
Subgrade	Not measured	7.9 %	Not measured

4.2.3 594FD Test Pit (May 2004)

The photograph in Figure 4.27 shows the asphalt concrete surfacing layer removed from the test pit in Section 594FD. Again, there appeared to be a good bond between the asphalt concrete surfacing and the foamed asphalt treated base layer. However, there did appear to be some lamination near the top of the foamed asphalt treated base layer.

Figure 4.27: Bond between asphalt concrete surfacing and the treated base on Section 594FD.

A photograph of a section of the 594FD test pit with the layer interfaces marked with string is shown in Figure 4.28. Grey clay-like material layer was again found underneath the foamed asphalt layer. On this section, the subgrade appeared to comprise of two materials, somewhat randomly placed. The lighter material was sandy weathered granite, while the darker material appeared to have more clay particles. It is thought that the materials are essentially the same, but were procured from different areas when the turnout was constructed. This is discussed in Section 4.2.4.

Figure 4.28: Test pit on Section 594FD after HVS trafficking.

Table 4.5 summarizes the average values of the layer thicknesses measured in the test pit and Figure 4.29 shows the profile measured in the partial test pit. The foamed asphalt treated layer increased in thickness from the caravan to traffic sides, similar to Section 593FD. Little rutting was apparent on the surface of this section.

Table 4.5: Average Layer Thickness from the Test Pit on Section 594FD

Layer	Average thickness for all readings (mm)	Average thickness on HVS section (mm)
Asphalt concrete surfacing	80	77
Foamed asphalt base layer	97	98
Grey, clay-like layer	126	123

Material was collected from the test pits, and was used to determine the oven-dried moisture contents. The results are shown in Table 4.6. In the foamed asphalt base, the moisture contents ranged between 6.2 percent and 7.0 percent. The moisture content in the grey clay layer increased from 9.2 percent on the caravan side to 10.2 percent on the traffic side and in the subgrade the moisture content increased from 9.6 percent on the caravan side to 13.2 percent on the centerline of the section. A moisture gradient is observed for all three layers with an increase in moisture content towards the mainline of SR 89.

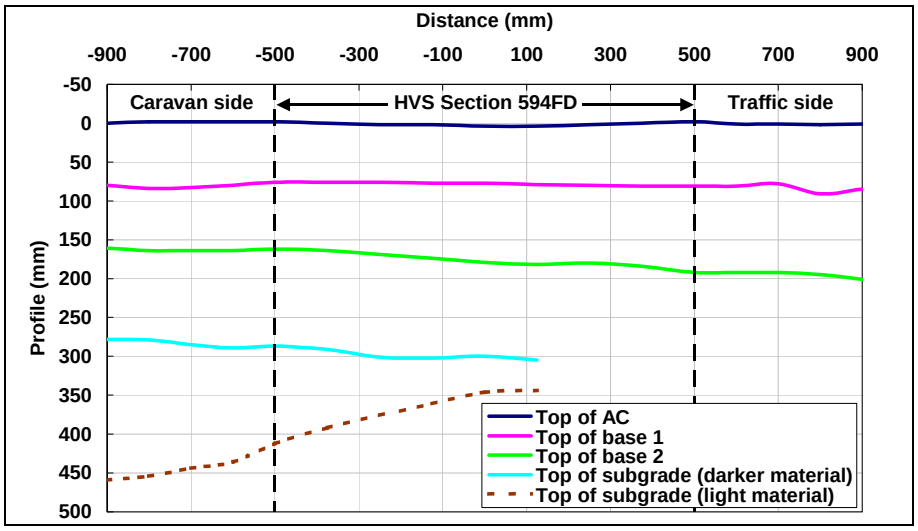

Figure 4.29: Test pit profile on Section 594FD.

Table 4.6: Moisture Contents in the Test Pit on Section 594FD

Pavement layer	Moisture content (%)		
	594FD CS	594FD inside	594FD TS
Foamed asphalt base	6.2	6.2	7.0
Grey, clay-like layer	9.2	9.6	10.2
Subgrade	9.6 (dark)	13.2 (light)	Not measured

4.2.4 595FD Test Pit

The photograph in Figure 4.30 shows the asphalt concrete surfacing layer removed from the test pit excavated on Section 595FD. This section was cracked through the slab, and the slabs broke up when lifted out of the test pit. The slabs from outside the trafficked area remained intact.

Figure 4.30: Asphalt surfacing from Section 595FD.

A photograph of a section of the 595FD test pit with the layer interfaces marked with string is shown in Figure 4.31. The grey clay-like material layer was again found below the foamed asphalt layer and materials in the subgrade appear to have been mixed as shown in Figure 4.32.

Figure 4.31: Test pit on Section 595FD after HVS trafficking.

Figure 4.32: Two materials in subgrade on Section 595FD.

Figure 4.33 shows the profile measured in the test pit and Table 4.7 summarizes the average values of the layer thicknesses measured in the test pit. The rutting in the pavement is evident in the test pit profile, and appears to occur in all the layers. The "humps" on the side of the test sections caused by the rutting are also evident.

Table 4.7: Average Layer Thickness Results from the Test Pit on Section 595FD

Layer	Average thickness for all readings (mm)	Average thickness on HVS section (mm)
Asphalt concrete surfacing	81	80
Foamed asphalt treated base layer	77	72
Grey, clay-like layer	132	130

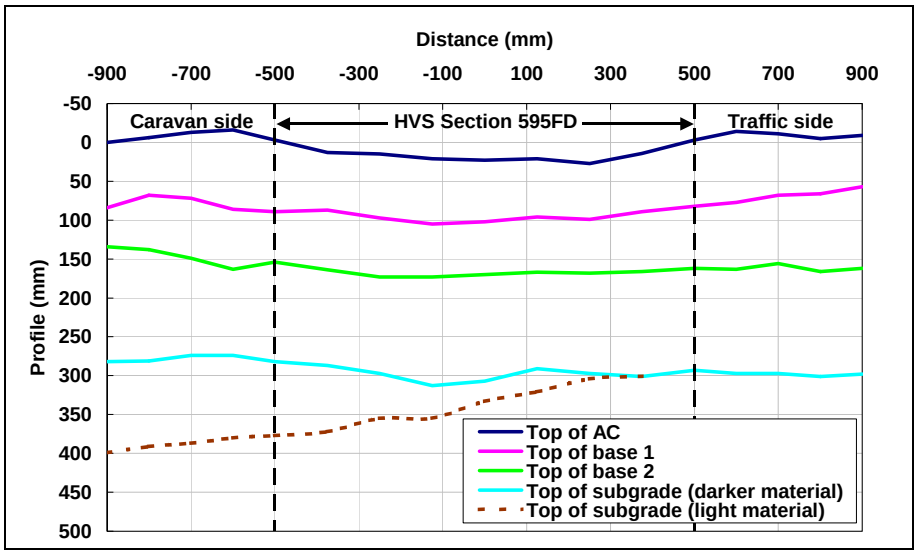

Figure 4.33: Test pit profile on Section 595FD.

Material was obtained from the test pits, and was used to determine the oven-dried moisture contents. The results are shown in Table 4.8. In the foamed asphalt base, the moisture contents range between 6.3 and 8.0 per cent. The moisture content in the grey clay layer varied between 9.9 and 10.8 percent with the lowest moisture content inside the HVS test section. The subgrade moisture content varied from 12.0 to 24.3 percent. The moisture content of all the layers is lower on the inside of the HVS test section than on the outside. In general, the moisture contents are extremely high, although no water was introduced artificially during the test.

Table 4.8: Moisture Contents from Samples Taken in Test Pit on Section 595FD

Layer	Moisture content (%)		
	595FD CS	595FD inside	595FD TS
Foamed asphalt base	8.0	6.3	8.0
Grey, clay-like layer	10.8	9.9	10.2
Subgrade (darker material)	24.3 (dark)	12.0 (light)	21.8 (dark)

4.2.5 596FD Test pit

A test pit was opened on the part of Section 596FD that had severe cracking and upward movement on the sides of the test section. When the surfacing was removed, a mud puddle was observed on the side of the caravan side of the test section, illustrated in Figure 4.34. This demonstrates that the water applied to the surface reached the base layer. A large amount of the base material was pushed to the sides of the test section because of this water. This is shown in Figure 4.35 and in the profile in Figure 4.36. Deformation in the layers underneath the base is not evident from the profiles. Average layer thicknesses in the test pit are provided in Table 4.9.

Figure 4.34: Mud between the AC surfacing and treated base, on the side of Section 596FD.

Figure 4.35: Test pit on the completed Section 596FD.

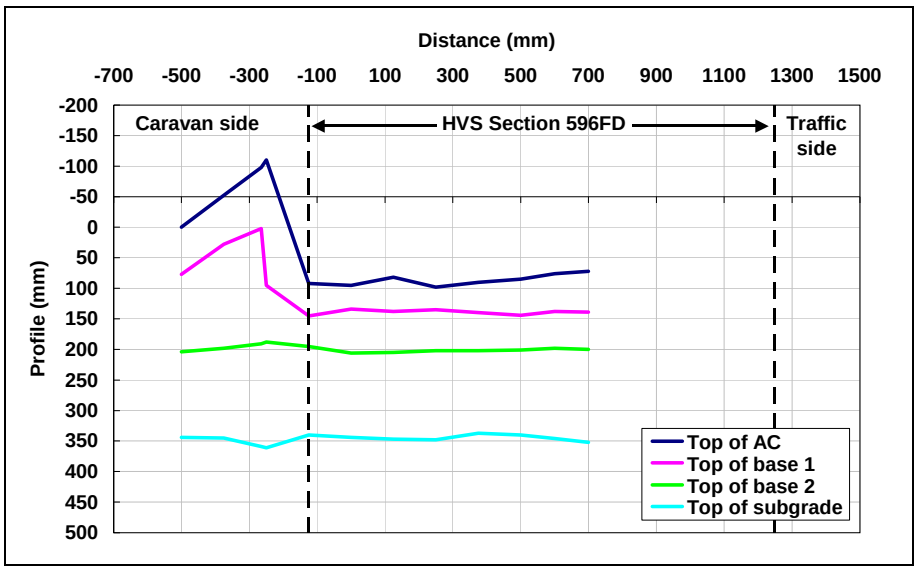

Figure 4.36: Test pit profile on Section 596FD.

Table 4.9: Average Layer Thickness Results from the Test Pit on Section 596FD

Layer	Average thickness on HVS section (mm)	Thickness on section with maximum upward surface movement (mm)
Asphalt concrete surfacing	53	100
Foamed asphalt base	62	189
Grey, clay-like layer	143	168

It appears as if the thickness of the asphalt concrete surfacing was less on the 595FD test than on the previous tests, which were all greater than 75 mm. The surfacing punched into the moist foamed asphalt treated base layer, and the interface was difficult to determine.

No moisture content samples were taken in the 596FD test pit.

4.2.6 Northbound Lane Cores (October 2003)

Figure 4.37 shows the two 100 mm cores (Cores 1 and 2) taken from the northbound lane in October 2003. The asphalt concrete surfacing layer was not bonded to the foamed asphalt treated base layer on both of these cores. The asphalt concrete thicknesses were 64 mm and 62 mm for Core 1 and Core 2 respectively. The foamed asphalt treated portion of Core 1 was 130 mm thick and the intact portion of the foamed asphalt treated material from Core 2 was 110 mm thick.

(a) Core 1 taken from the northbound lane

(b) Core 2 taken from the northbound lane

Figure 4.37: 100 mm cores taken from the northbound lane.

Figure 4.38 shows the 150 mm core taken from the northbound lane (Core 3). The asphalt concrete surfacing was not bonded to the foamed asphalt treated layer. The thickness of the asphalt concrete layer was 56 mm on Core 3 and the foamed asphalt treated material thickness was 230 mm. Figure 4.38(b) shows Core 3 after being air-dried with the reclaimed asphalt pavement (RAP) clearly visible.

(a) Core 3, wet (b) Core 3, air-dried

Figure 4.38: 150 mm core taken from the northbound lane.

4.2.7 Southbound Lane Cores (October 2003)

Figure 4.39 shows the two 100 mm cores (Cores 4 and 5) taken from the southbound lane. The asphalt concrete surfacing layer was well bonded to the foamed asphalt treated base layer on both cores. The asphalt concrete thicknesses were 40 mm and 42 mm on Core 4 and Core 5 respectively. The foamed asphalt treated portion was 140 mm to 150 mm thick on Core 4 and 185 mm thick on Core 5.

Figure 4.40 shows the 150 mm core taken from the southbound lane (Core 6). The asphalt concrete surfacing was well bonded to the foamed asphalt treated layer. The thickness of the asphalt concrete layer was 49 mm on Core 6 and the foamed asphalt treated material thickness was 220 mm.

(a) Core 4 taken from the southbound lane

(b) Core 5 taken from the southbound lane

Figure 4.39: 100 mm cores taken from the southbound lane.

Figure 4.40: 150 mm core taken from the southbound lane.

4.2.8 HVS lane Cores (October 2003)

The photographs in Figure 4.41 show cores taken from inside Section 593FD and immediately next to section 593FD. The foamed asphalt treated base appears to have disintegrated under the effect of HVS trafficking as shown by the loose material from Core 13, taken inside the HVS test section. The thicknesses of the asphalt concrete layer were 85 mm on Core 13 and 86 mm on Core 14. The foamed asphalt treated base on Core 14, taken next to the HVS section, came out intact and bonded to the asphalt concrete surfacing layer, but the foamed asphalt treated portion was only 40 mm thick.

(a) Core 13 taken from the HVS test section

(b) Core 14 taken next to the HVS test section

Figure 4.41: Cores taken from and next to Section 593FD.

The asphalt concrete and foamed asphalt treated cores were tested in the Caltrans laboratory. Air-void contents were determined on the asphalt concrete and unconfined compressive strengths (UCS), moisture contents, and asphalt binder contents were determined on the foamed asphalt treated cores. The results are summarized in Table 4.10 and

Table 4.11. The asphalt concrete air voids ranged from 5.1 percent to 8.3 percent, with an average of 6.5 percent. There was no discernable difference between the air-void contents on the mainline and the HVS section.

The moisture contents of the foamed asphalt treated cores were lower than those measured from samples removed from the test pit. It is possible that some drying occurred between extraction and measurement of the moisture content. The binder content determined from the cores indicates a much higher binder concentration than the 2.5 percent foamed asphalt introduced during recycling. This is not surprising

because the original binder in the asphalt concrete layer before recycling was still present, and is included in the total binder content. The highest binder content was measured on a core removed near HVS Section 593FD on the mainline (Core #6). This may imply that more foamed asphalt was added to this area than the 2.5 percent design value.

Table 4.10: Asphalt Concrete Core Measurements

Core number	Location	Height (mm)	Diameter (mm)	Specific gravity (g/cm^3)	Air-void content (%)
1	Northbound	64	102	2.33	6.5
2	Northbound	64	102	2.29	8.3
3	Northbound	54	152	2.33	6.5
4	Southbound	39	102	2.34	6.1
5	Southbound	45	102	2.37	5.1
6	Southbound	44	150	2.31	7.4
13	593FD	87	149	2.36	5.4
14	Next to 593FD	83	149	2.33	6.5
* Calculated using maximum specific gravity = 2.496 g/cm^3 (AASHTO T209)					

Table 4.11: Foamed Asphalt Treated Base Core Measurements

Core number	Location	Height (mm)	Diameter (mm)	UCS (kPa)	Moisture content (%)	Binder content[1] (%)
1[A]	Northbound	105	101	2746	2.40	6.1
2[A,2,3]	Northbound	111	101	1725	4.10	6.5
3[A]	Northbound	107	149	4375	1.20	6.6
3[B,2]	Northbound	103	149	3215	1.80	6.7
4[A]	Southbound	103	101	5120	1.20	6.2
5[A,2]	Southbound	90	102	4264	1.50	7.9
5[B]	Southbound	96	102	(4)	2.60	7.6
6[A]	Southbound	103	149	4968	1.80	8.4
6[B,2]	Southbound	103	149	3657	2.70	8.5
13[A]	593FD	No core, material broken up			2.20	8.3
14[A]	Next to 593FD	90	149	2836	3.30	8.5

[A] Top of core after cut or whole core
[B] Bottom section of core after cut
[1] Determined from extractions
[2] Cores cut to separate
[3] Outside surface area damaged by water when core extracted
[4] Core broke

The UCS values fell within a large range, however, the values are dependant on the moisture content, as illustrated in Figure 4.42. It does, however, appear from the figure that the UCS of the southbound base layer material was higher than the northbound. The material in the HVS section also had a relatively high UCS. The grey clay layer could not be extracted in a core. In the HVS section, the core collapsed, indicating that the foamed asphalt base probably weakened under the HVS loading.

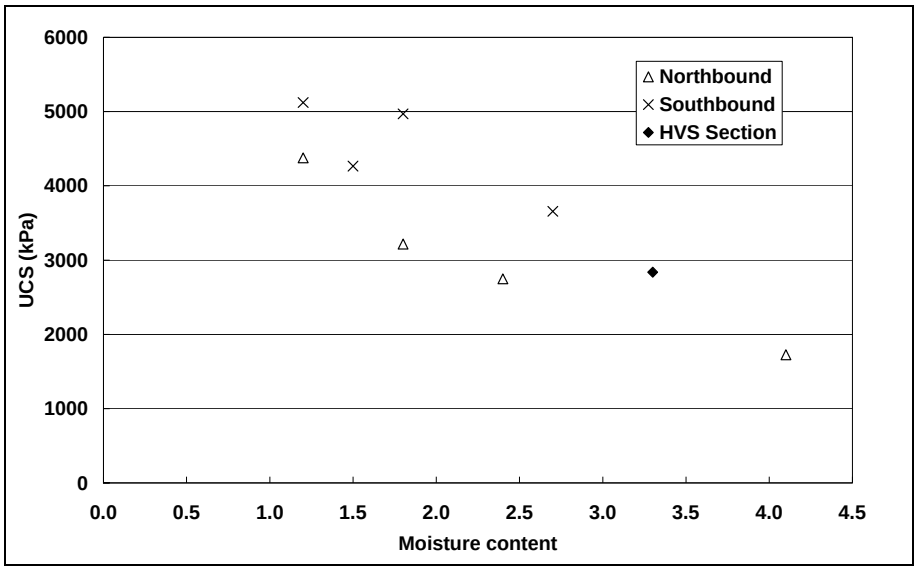

Figure 4.42: UCS as a function of moisture content of foamed asphalt treated cores.

4.3 Dynamic Cone Penetrometer Test Results

Dynamic Cone Penetrometer (DCP) tests were completed at various stages throughout the project. Tests were completed by Caltrans prior to rehabilitation. After rehabilitation, the first DCP tests on the HVS test lane were done on July 11 and July 31. Extensive testing on the mainline in the vicinity of the HVS tests was done in October 2003. DCP tests were also done on the HVS test lane at the time of opening the test pits on Sections 594FD and 595FD.

4.3.1 DCP Results after Rehabilitation (July and October 2003)

The layout of the DCP tests performed after rehabilitation is illustrated in Figure 3.4. All DCP tests were done from the top of the base after drilling though the asphalt concrete.

Figure 4.43 shows the DCP penetration rates for the foamed asphalt (upper base), grey clay layer (lower base) and subgrade of the HVS lane plotted against longitudinal position. There was a vertical strength gradient in the base layer and the base was separated into the upper base and grey clay layer for this reason. The existence of two completely different layers was later confirmed in the test pit. The foamed asphalt base was stronger than the grey clay layer. Penetration rates of approximately 2.0 mm per blow are typically expected on stabilized materials. The penetration rates of the foamed asphalt base, and even more so the grey clay layer, were higher than this typical value. The penetration rates through the subgrade also show a strength gradient in the longitudinal direction of the HVS lane. Section 539FD was located between zero and 10 m, and was therefore on the strongest part of the subgrade.

The agreement between the DCP results taken in July and October for the foamed asphalt base and subgrade indicates that these pavement layers did not change significantly during this period. The DCP penetration rate for the grey clay layer on the HVS lane did, however, reduce significantly from July to October. The material of this layer was a grey, clay-like material and the increased DCP strength of this material may be attributed to drying out of the material during this period. The condition of the subgrade improved towards Section 595FD.

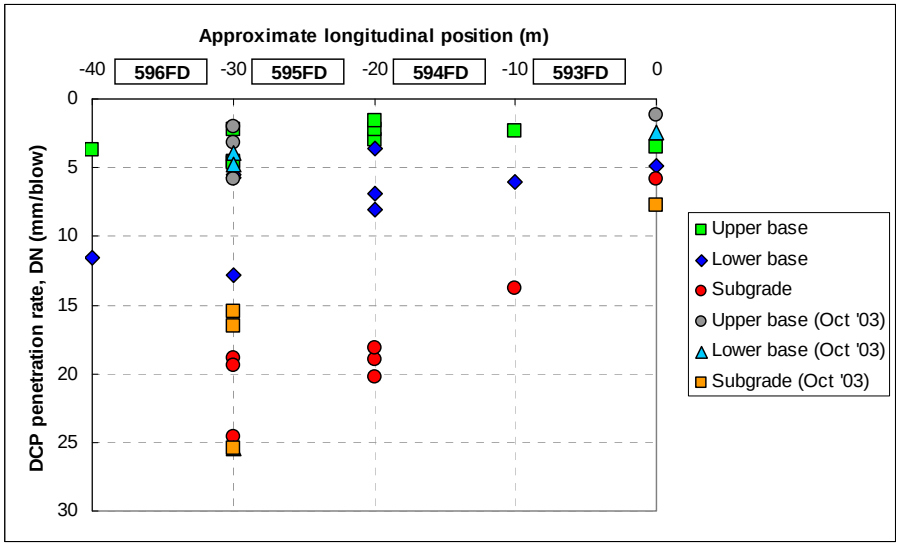

Figure 4.43: DCP results for the HVS lane.

July 2003 DCP Analyses

Figure 4.44 shows the average layer strength diagram for the combined DCP results collected on the HVS lane in July 2003. The required layer strength diagram for medium traffic is plotted as a reference. The penetration rates of the individual DCP readings were consistent for the top 100 mm of the pavement. Below 100 mm to a depth of 400 mm there was more variation in the penetration rates of the individual readings and below 400 mm the penetration rates were again consistent although rather high. Comparing the layer strength diagrams of the individual readings and the average layer strength diagram with the required layer strength diagram for medium traffic showed that the upper 450 mm of the pavement was not adequate for medium traffic with the actual layer strength diagrams plotting to the right of the required layer strength diagram.

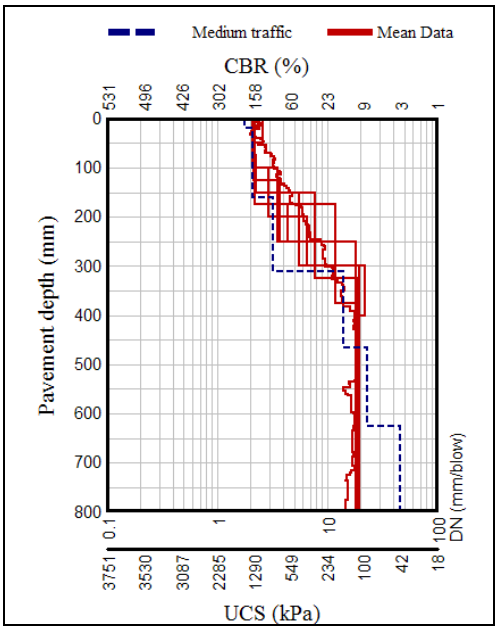

Figure 4.44: Average DCP layer strength for the HVS lane in July 2003.

Table 4.12 provides a summary of the average DCP penetration rates for all the DCP tests in the HVS lane in July 2003. Based on the results presented, it appears that only the upper 100 mm of the base layer was effectively stabilized by the foamed asphalt treatment.

Table 4.12: Average DCP Analysis for all DCP Tests in July 2003

Layer (mm)	Penetration rate (mm/blow)	CBR (%)	UCS (kPa)
0 – 100	2.67	118	995
100 – 200	4.63	59	Not tested
200 – 300	8.15	29	Not tested
300 – 400	13.59	15	Not tested
400 – 800	17.18	11	Not tested

<u>October 2003 DCP Analyses</u>

- Southbound Lane - Figure 4.45 shows the average layer strength diagram for the combined DCP results collected on the southbound lane in October 2003. The required layer strength diagram for medium traffic is plotted as a reference. The penetration rates of the individual DCP readings were consistent for the top 200 mm of the pavement. Below 200 mm to a depth of 350 mm there was more variation in the penetration rates of the individual readings and below 350 mm the penetration rates were again consistent. Comparing the layer strength diagrams of the individual readings and the average layer strength diagram with the required layer strength diagram for medium traffic shows that the upper 200 mm of the pavement far exceeded the requirement for medium traffic with the actual layer strength diagrams plotting well to the left of the required layer strength diagram.

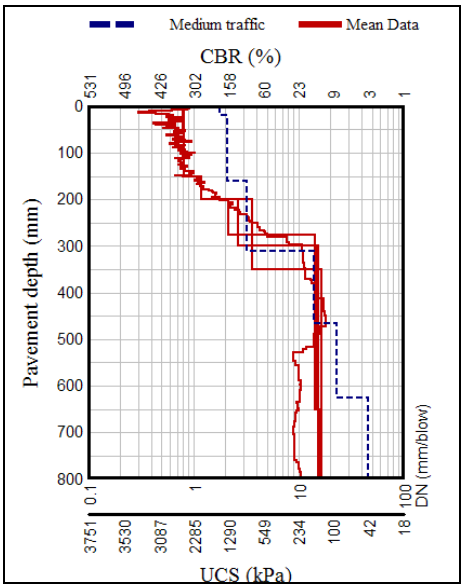

Figure 4.45: Average DCP layer strength for the southbound lane in October 2003.

Table 4.13 provides a summary of the average DCP penetration rates for all the DCP tests done on the southbound lane in October 2003. Based on the results presented in the table, it appears that the upper 200 mm of the base layer was well stabilized by the foamed asphalt treatment.

Table 4.13: Average DCP Analysis in the Southbound Lane in October 2003

Layer (mm)	Penetration rate (mm/blow)	CBR (%)	UCS (kPa)
0 – 150	0.74	Not tested	2634
150 – 200	1.36	Not tested	1847
200 – 300	4.49	61	Not tested
300 – 800	12.80	16	Not tested

- Northbound Lane - Figure 4.46 shows the average layer strength diagram for the combined DCP results collected on the northbound lane in October 2003. The required layer strength diagram for medium traffic is plotted as a reference. The penetration rates of the individual DCP readings were fairly consistent for the top 200 mm of the pavement. The DCP also consistently showed a slightly weaker layer of about 25 mm to 50 mm at the top of the base. Below 200 mm to a depth of 400 mm there was more variation in the penetration rates of the individual readings and below 400 mm the penetration rates were again consistent. Comparing the layer strength diagrams of the individual readings and the average layer strength diagram with the required layer strength diagram for medium traffic shows that the upper 250 mm of the pavement satisfies the requirement for medium traffic with the actual layer strength diagrams plotting slightly to the left of the required layer strength diagram. Table 4.14 provides a summary of the average DCP penetration rates for

all the DCP tests done on the northbound lane in October 2003. Based on the results presented, it appears that the upper 200 mm of the base layer was stabilized by the foamed asphalt treatment.

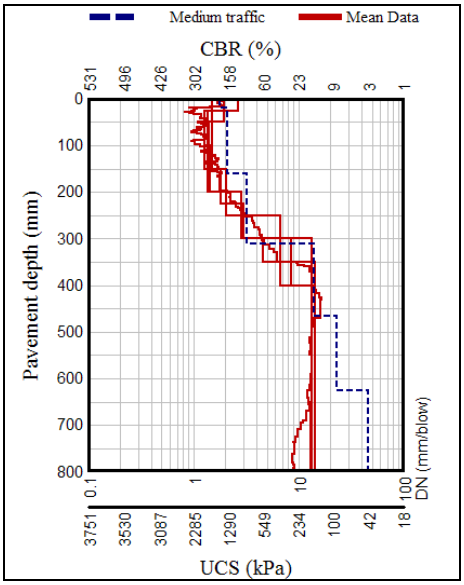

Figure 4.46: Average DCP layer strength diagram for northbound lane in October 2003.

Table 4.14: Average DCP Analysis on the Northbound Lane in October 2003

Layer (mm)	Penetration rate (mm/blow)	CBR (%)	UCS (kPa)
0 – 25	1.54	Not tested	1678
25 – 150	1.30	Not tested	1913
150 – 250	2.18	Not tested	1253
250 – 350	4.82	56	Not tested
350 – 800	13.64	15	Not tested

4.3.2 May 2004 DCP Analyses

Figure 4.47 shows the layer strength diagrams for the DCP tests done on the caravan and traffic sides of Section 594FD. Table 4.15 provides a summary of the average layer penetration rate (DN) and CBR values derived form the DCP tests. Figure 4.48 and Table 4.16 provide the corresponding results for Section 595FD.

Table 4.15: Results from the DCP Analysis of Tests Next to Section 594FD

Layer (mm)	Caravan side		Traffic side	
	Penetration rate (mm/blow)	CBR (%)	Penetration rate (mm/blow)	CBR (%)
0 – 100	3.5	82	3.0	101
100 – 220	4.5	59	4.3	64
220 – 300	7.7	30	6.9	35
300 – 400	8.2	28	13.9	15
400 – 800	16.2	12	8.6	27

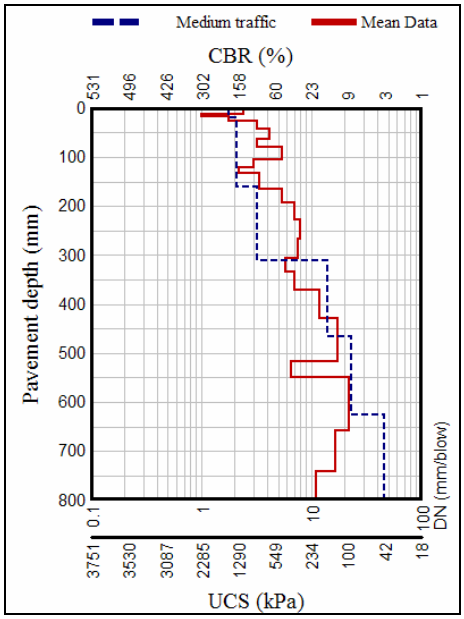

(a) Caravan side

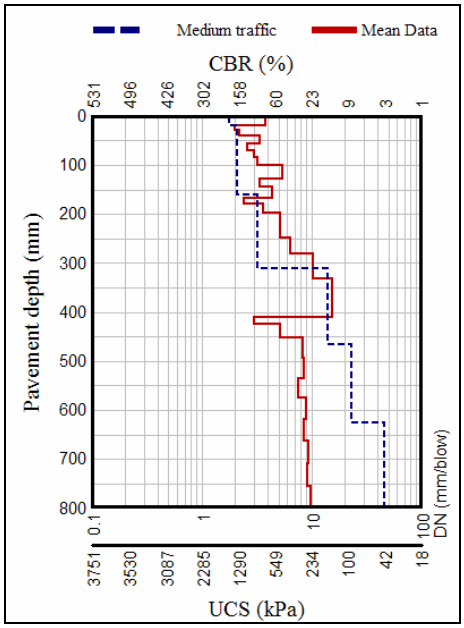

(b) Traffic side

Figure 4.47: DCP test results next to Section 594FD

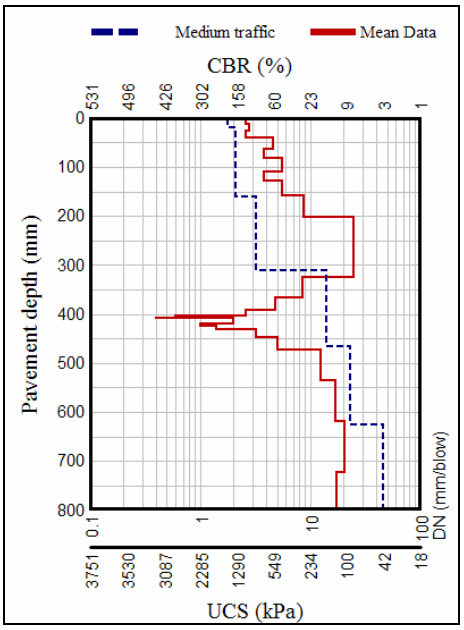

(a) Caravan side

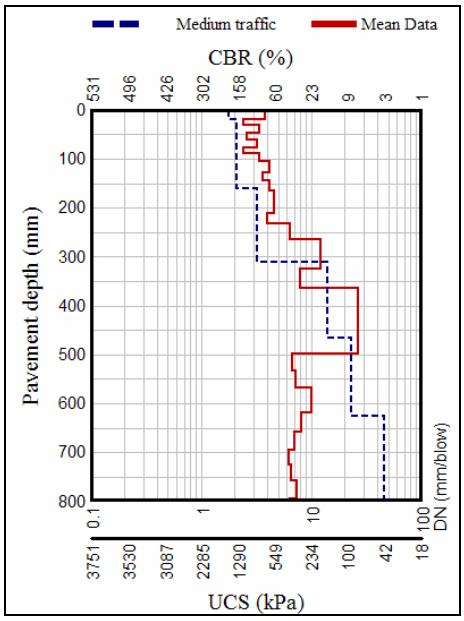

(b) Traffic side

Figure 4.48: DCP test results next to Section 595FD.

Table 4.16: Results from the DCP Analysis of Tests Next to Section 595FD

Layer (mm)	Caravan side		Traffic side	
	Penetration rate (mm/blow)	CBR (%)	Penetration rate (mm/blow)	CBR (%)
0 – 70	3.4	86	3.2	95
70 – 200 (70 – 220)*	6.2	40	3.9	71
200 – 300 (220 – 370)*	24.4	7	9.7	23
300 – 400 (370 – 500)*	10.9	20	26.3	6
400 – 800 (500 – 800)*	14.7	13	7.6	31
* Layer boundaries for the traffic side				

A weak layer was shown by the DCP on Section 595FD, 200 mm to 300 mm deep on the caravan side and 370 mm to 500 mm deep on the traffic side. This weak layer was not observed during the July 2003 DCP survey and these points were not trafficked by the HVS. The only possible explanation for the change in the condition of this layer is an increase in moisture content of this layer. This is supported by the moisture content data presented in Table 4.8 for Section 595FD. Other than this, the base layer had a slightly higher penetration rate and lower CBR than during the July 2003 survey and the properties of the material below the base to a depth of 200 mm remained consistent with the July 2003 results. The 400 mm to 800 mm deep subgrade measurements improved with depth on the traffic side.

4.4 Nuclear Density Gauge Results

The data discussed in this section were determined from nuclear density gauge surface backscatter and depth-probe measurements. Depth-probe measurements were obtained by drilling a hole through the pavement structure and placing the probe in the hole at 50 mm, 100 mm, 150 mm and 200 mm depths. The surface measurements were taken at most of the nuclear density gauge points and the DCP points, as marked in Figure 3.8. The depth measurements were taken at the nuclear density gauge points, as marked. Readings were also taken in both the mainline and HVS test pits.

4.4.1 Surface Backscatter Data

The surface backscatter data were collected in the asphalt mode. The results are shown in Figure 4.49. The densities of the southbound direction are consistent, ranging between 2,200 kg/m^3 and 2,300 kg/m^3. Some of the results from the northbound direction were significantly lower than this range and are considered unrealistic. A weak interlayer was observed between the asphalt concrete surfacing and foamed asphalt base from all the cores taken from the northbound lane and the DCP results, which may have influenced the backscatter reading sufficiently to result in the low density results.

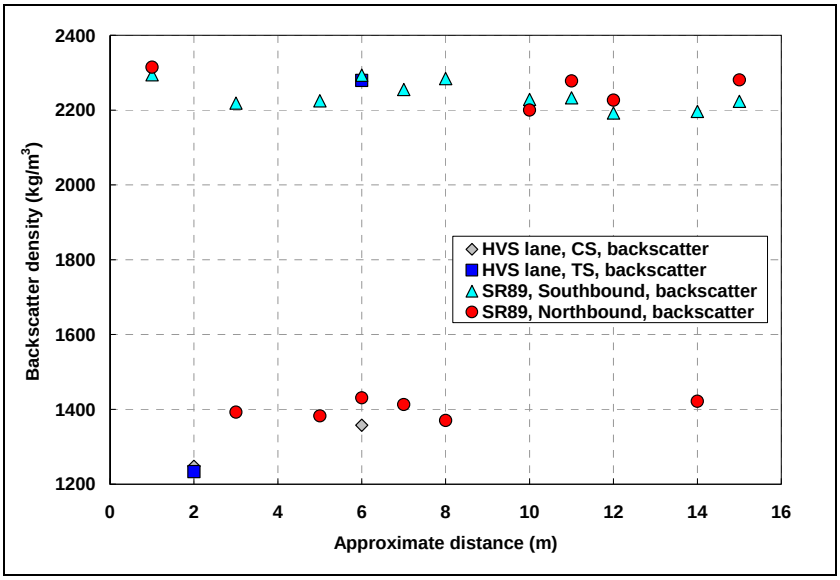

Figure 4.49: Density from backscatter mode on top of asphalt concrete.

The gravimetric densities determined from the asphalt concrete cores (Table 4.10) are plotted in Figure 4.50 for comparison. The gravimetric densities are slightly higher than the corresponding densities determined using the nuclear density gauge in backscatter mode, and none of the low densities obvious in Figure 4.49 were found.

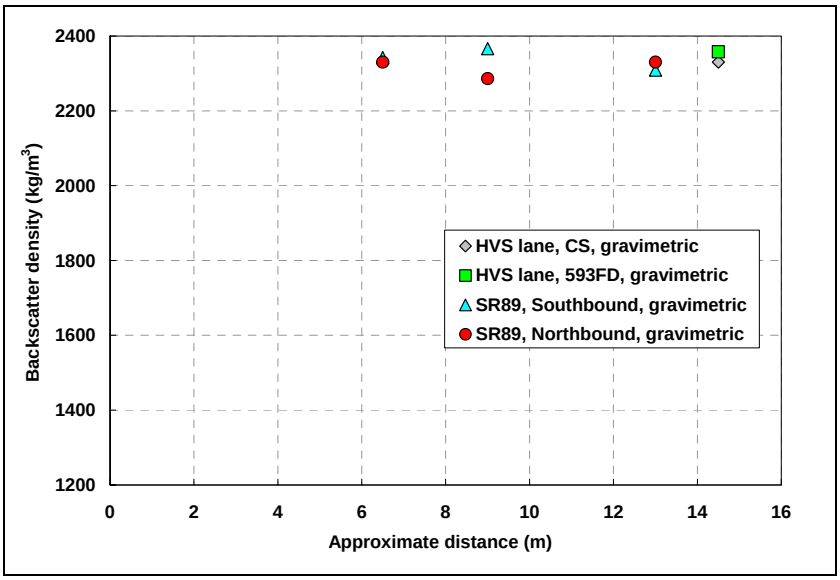

Figure 4.50: Gravimetric density determined from cores.

4.4.2 Depth Measurements

The measurements taken at depth were determined using both the asphalt (0 to 50 mm) and soil (> 200 mm). In the soil mode, the wet density, dry density and moisture content were measured. Figure 4.51 shows the density results and Figure 4.52 shows the moisture contents. In the figure, the marker represents the average value, and the line ranges from the minimum to maximum reading. At a depth of 50 mm, the measurements taken in the asphalt mode were used. These measurements correspond well with the wet density measurements in the soil mode. At 100 mm, 150 mm and 200 mm depths, the dry density results from the soil mode are shown.

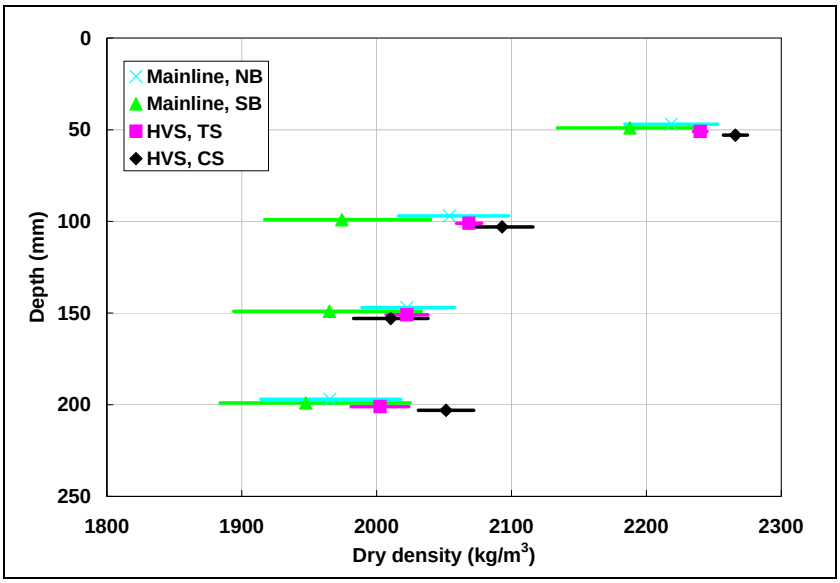

Figure 4.51: Nuclear gauge determined dry density.

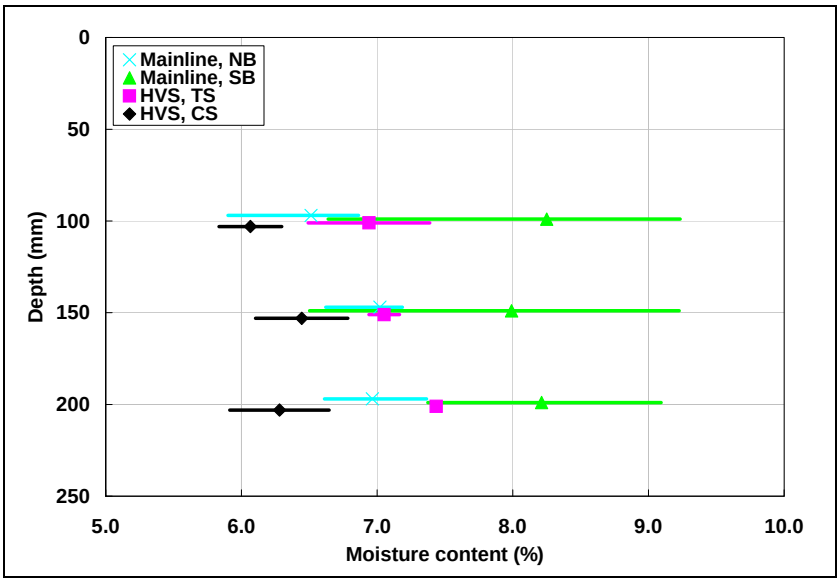

Figure 4.52: Nuclear gauge determined moisture content.

The density results show that southbound SR89 had the lowest base material density, but the highest moisture content. Values less than 2,100 kg/m^3 are considered low for a foamed asphalt base, while typical values exceed 2,100 kg/m^3. At 100 mm and 150 mm depths, the northbound SR89 lane and the HVS lane had comparable densities. At these depths the moisture content of the HVS lane, caravan side (CS) was lower than the other locations. The results from FWD and DCP tests show that the southbound lane was the strongest lane, which did not agree with the nuclear density results. The binder extractions on the cores show that the southbound lane had a higher binder content within the foamed asphalt base layer, which may explain why the cores remained intact. This also explains the high nuclear gauge moisture content, because of the presence of hydrogen in the asphalt which will in turn result in an under-estimate of the dry density.

The thickness of the asphalt concrete layer varied across the lanes. The HVS lane had the thickest asphalt concrete (85 mm); the northbound lane asphalt concrete was 61 mm thick and the southbound lane 44 mm thick. The density readings at depth provide an average density between the probe depth and the device, and are therefore heavily influenced by the thickness and density of the asphalt concrete. The thicker asphalt concrete on the northbound and HVS lanes was probably the reason for the higher density values. Unfortunately it was not possible to obtain moisture content samples from the northbound lane, and therefore the actual moisture contents could not be compared.

4.5 Summary and Conclusions

Table 4.17 summarizes the information obtained from the FWD, test pits, coring and DCP testing. Figure 4.53 shows a graphical representation of these results. There is fair agreement between the conclusions made from the DCP results and observations from the cores and test pit.

The southbound lane of the mainline appeared to be representative of a well-constructed foamed asphalt treated pavement with good bond between the base and asphalt, and sufficient base layer thickness. The base layer was also effectively stabilized. The northbound lane of the mainline was also well constructed with sufficient base thickness but there appeared to be a weak interlayer between the base and surfacing layer, attributed to poor compaction.

Unfortunately, the pavement structure of the HVS test lane could not be regarded as being representative of the pavement structure of the mainline. The foamed asphalt treated base layer was only estimated to be 100 mm thick and the imported subbase material immediately below the base layer was of low quality. The DCP results and back-calculations based on the layer thicknesses from the test pit indicate that the 100 mm thick base on the HVS lane was properly stabilized.

The following specific points were noted to assist in the interpretation of the HVS results:

- The thickness of the foamed asphalt base was estimated to be only 100 mm on the HVS sections;
- The foamed asphalt base had an underlying layer of weak clay-like material;
- The density of the foamed asphalt treated base was acceptable;
- The moisture content of the HVS test sections appeared to have increased between October 2003 and May 2004. This increase was significant in the subgrade and more so towards Section 595FD.
- The subgrade condition was weak and weakened in the direction from Section 593FD towards Section 596FD.

In conclusion, the HVS test sections were not representative of the main roadway, and are not representative of typical foamed asphalt treated sections. This is demonstrated by comparing the data between the main roadway and the HVS sections. The HVS tests are therefore, optimistically, testing the worst case. The field and laboratory testing aided in identifying the causes of the differences between the main roadway and the HVS sections.

After the field investigations, it was recommended that the HVS testing on SR89 be completed. It is however, also recommended that another HVS site is investigated where the behavior will be more representative of that of typical foamed asphalt treated pavements. Such a test should be planned prior to construction, to ensure the construction is representative and to ensure appropriate data is collected from the design stage, through construction, and during and after HVS testing. Where possible, the HVS test should be placed on the main roadway, with the traffic detoured onto the bypass. This is particularly important for full-depth reclamation projects, where the construction of a new bypass is not representative if new material has to be brought in.

Table 4.17: Summary of the Test Pit, Core and DCP Test Results

Data source and parameter	Layer	Lane		
		HVS	Southbound	Northbound
Resilient modulus (October 2003 FWD data)	Asphalt concrete	1,950 MPa	1,950 MPa	1,950 MPa
	Foamed asphalt treated base	649 MPa	1,574 MPa	846 MPa
	Subgrade	83 MPa	83 MPa	89 MPa
Test pit thickness	Asphalt concrete	77 - 82 mm		
	Foamed asphalt treated base	110 - 119 mm		
	Grey, clay-like material	161 - 164 mm		
Core thickness	Asphalt concrete	85 - 86 mm	40 - 49 mm	56 - 64 mm
	Foamed asphalt treated base	Undetermined	220 mm	230 mm
Unconfined Compressive Strength (UCS), measured on cores	Foamed asphalt treated base	2,836 kPa	4,264 - 5,120 kPa	1,725 - 4,375 kPa
Unconfined Compressive Strength (UCS), DCP derived strength	Foamed asphalt treated base	995 kPa	1,847 - 2,634 kPa	1,253 - 1,913 kPa
California Bearing Ratio (CBR), DCP derived strength	Subbase	29 - 59 %	61 %	56 %
	Decomposed granite subgrade	15 %	16 %	15 %
Nuclear density	0 - 50 mm	2,253 kg/m^3	2,188 kg/m^3	2,219 kg/m^3
	50 mm - 100 mm	2,081 kg/m^3	1,974 kg/m^3	2,054 kg/m^3
	100 mm - 150 mm	2,017 kg/m^3	1,965 kg/m^3	2,023 kg/m^3
	150 mm - 200 mm	2,027 kg/m^3	1,948 kg/m^3	1,965 kg/m^3

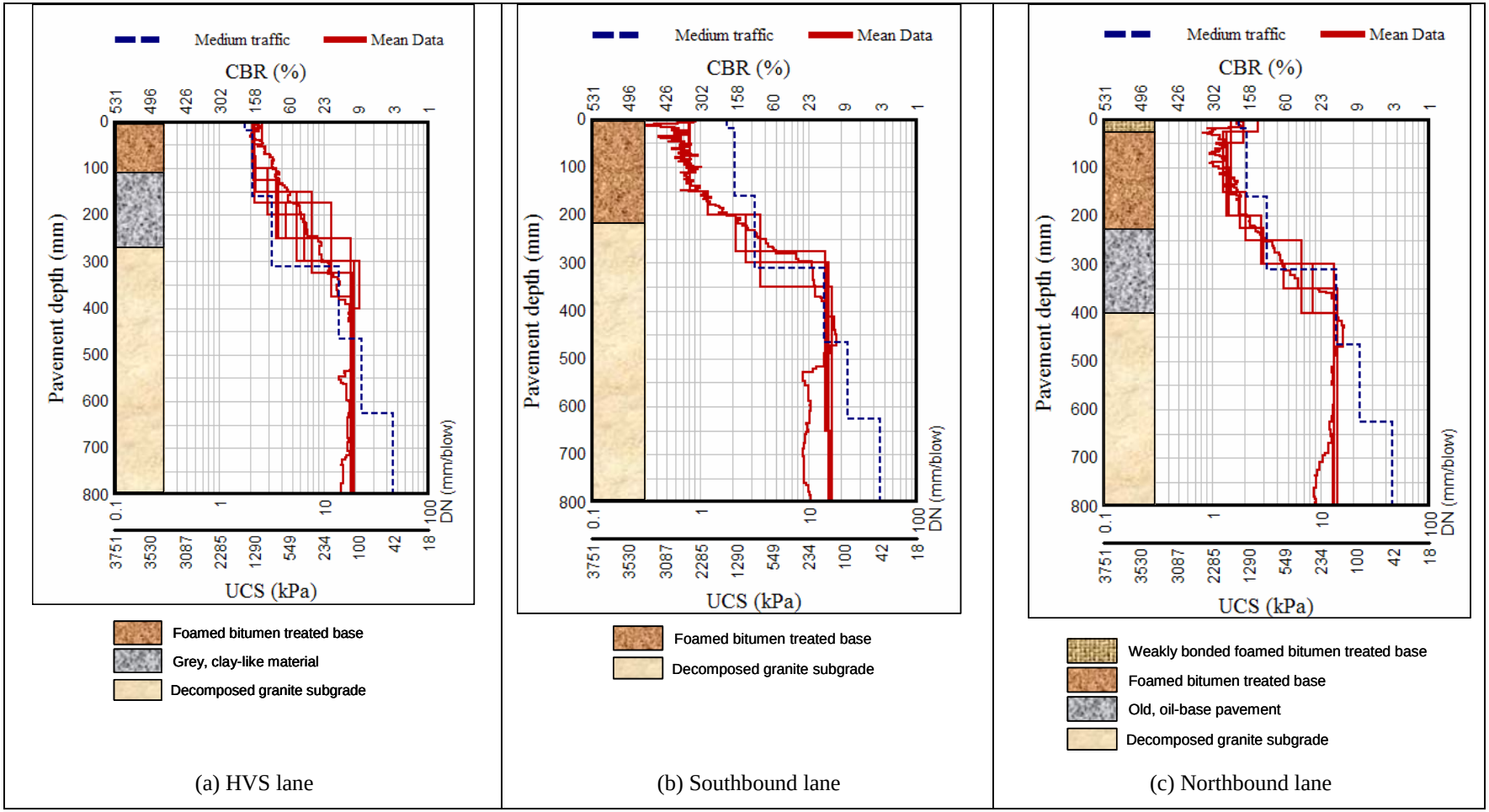

Figure 4.53: Summary of the DCP, coring and test pit results.

5. DATA SUMMARY

5.1 Introduction

The data for each HVS test section (Sections 593FD through 596FD) are presented according to the following outline:

- Environmental data
  - Rain and snowfall data
  - Ambient and pavement temperature data
- Surface response data
  - Visual distress
  - Road Surface Deflectometer (RSD) data
  - Straightedge and Laser Profilometer data (surface profile)
- Depth response data
  - Depth deflection data (MDD deflections)
  - Backcalculated resilient moduli for the pavement layers

5.2 HVS Test 593FD

5.2.1 Environmental Data

Rainfall

No rainfall data were collected during the test on Section 596FD and no snow fell during the test.

Pavement Temperature

Pavement and ambient temperatures were collected inside the temperature control box during the times at which data were recorded. A summary of the data is shown in Figure 5.1. Although the ambient temperature varied considerably during the test, the pavement surface temperature, asphalt concrete temperature (25 mm deep) and the temperature in the foamed bitumen treated base (measured at 150 mm depth) varied in a band around 20°C for most of the test.

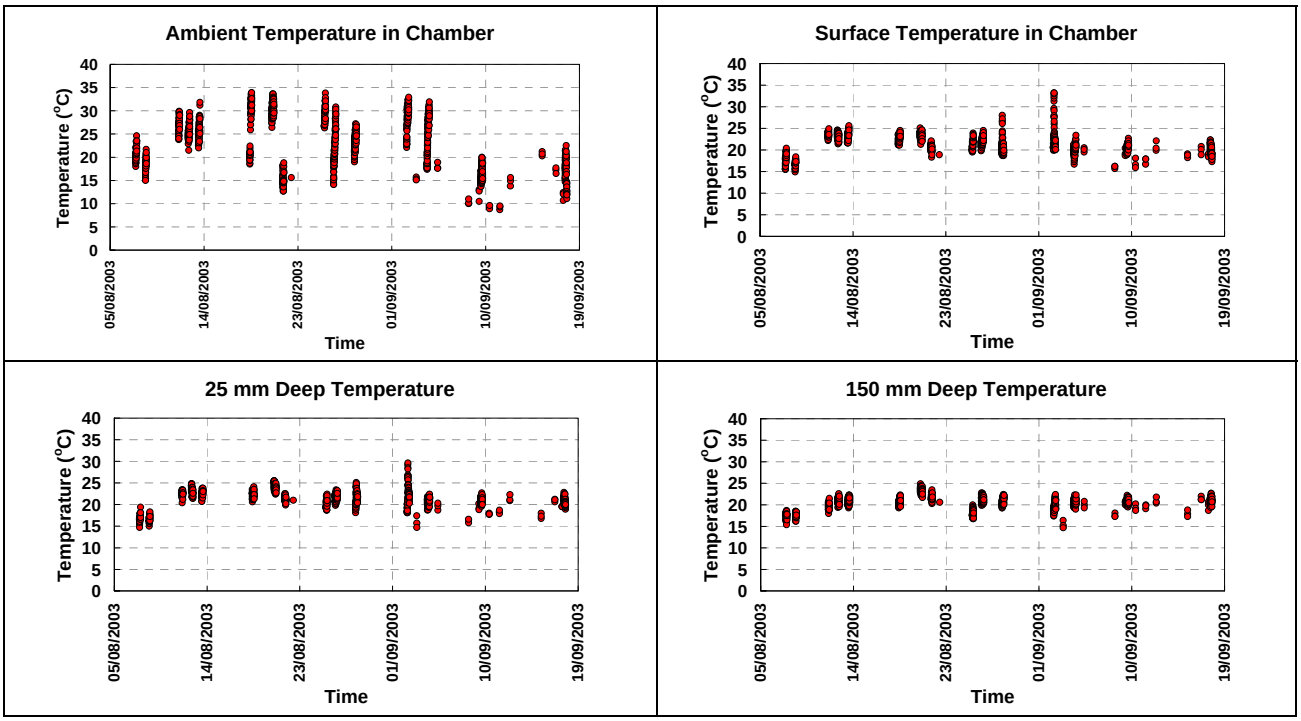

Figure 5.1: Ambient and pavement temperatures from Section 593FD.

5.2.2 Surface Response Data

Visual Distress

Figure 5.2 shows the visual condition of Section 593FD at the start and completion of the test. Except for the surface rut, no other visual distress was observed on completion of the test.

(a) Start of test after 10 repetitions at 60 kN (b) End of test after 300,000 repetitions

Figure 5.2: Visual condition of Section 593FD at the start and end of the test.

Surface Deflection (RSD)

Figure 5.3 through Figure 5.5 illustrate the average peak deflection on the centerline, and on the traffic and caravan sides, for the 60 kN, 90 kN and 80 kN test loads, respectively. The magnitude of the deflections was extremely high, which is indicative of a weak pavement structure. The deflections

increased in the early stages of the test, although the increase was not that significant. Under the 80 kN test load, the deflections did not change markedly during the test. The deflections across the section from the caravan side to the traffic side were in the same range, and neither side had consistently higher or lower deflections. The deflections increased with increasing load, but decreased briefly after the 90 kN to 80 kN load change.

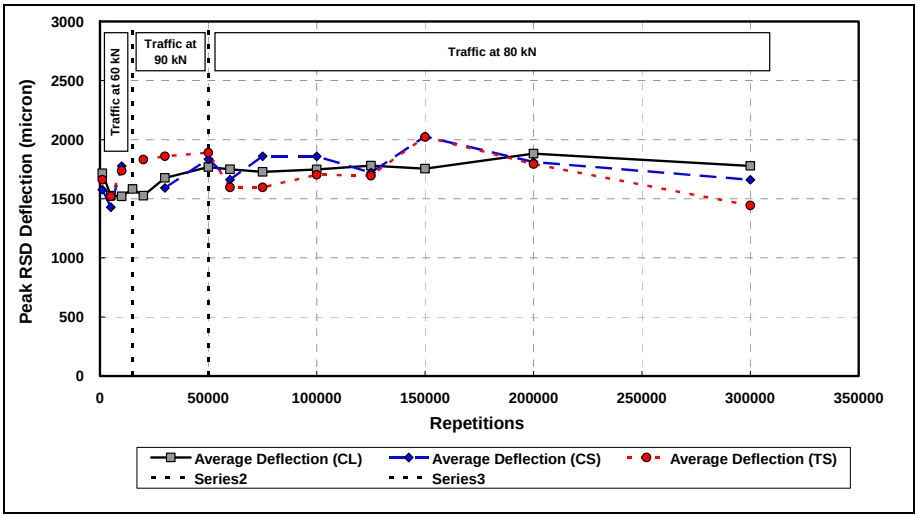

Figure 5.3: RSD peak deflections under 60 kN loading on Section 593FD.

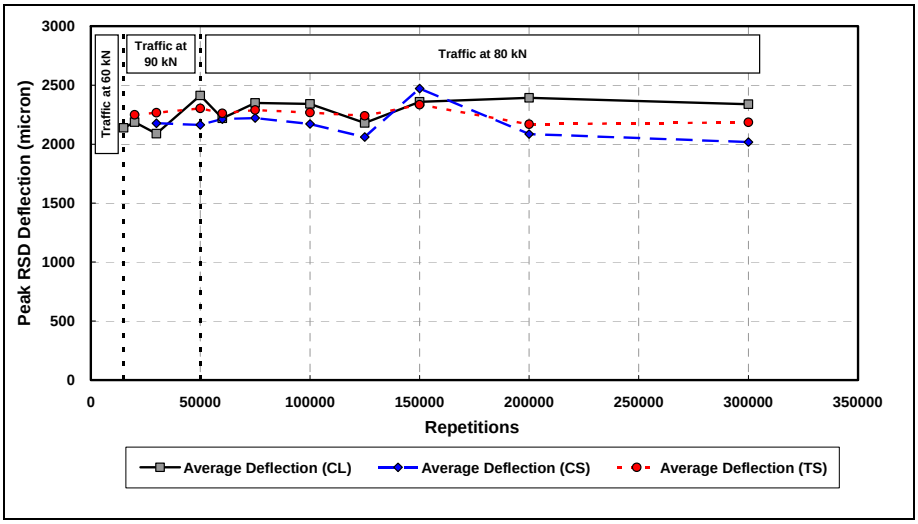

Figure 5.4: RSD peak deflections under 90 kN loading on Section 593FD.

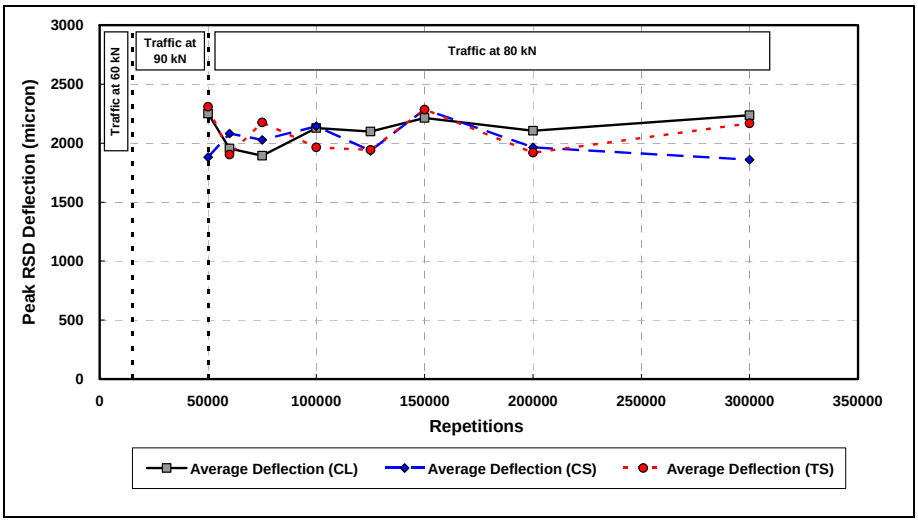

Figure 5.5: RSD peak deflections under 80 kN loading on Section 593FD.

Figure 5.6 shows a plot of the variation of the RSD 60 kN deflection along the centerline of the section. Lower deflections were experienced on the side of the test section that corresponded to the highest densities (Section 4.4) and lowest DCP penetration rates (Section 4.3). These results again illustrate the variation in the pavement condition across the HVS sections.

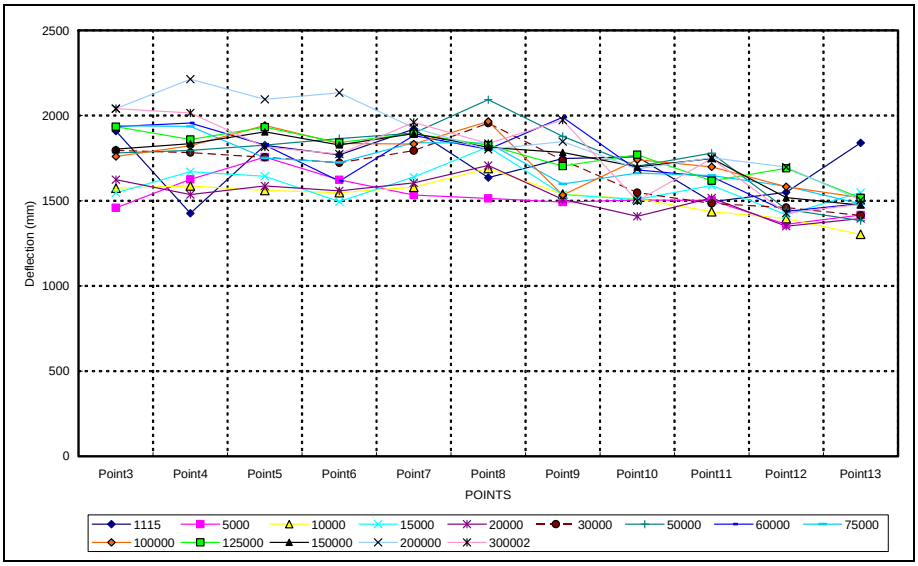

Figure 5.6: Centerline RSD deflections along Section 593FD (60 kN loading).

Surface Profile

Straightedge measurements were not taken during most of the test on Section 593FD. Only two measurements were taken, which is insufficient to provide insight into the behavior of the section. Laser profilometer readings were taken at regular intervals and Figure 5.7 shows the accumulation of rut during the test. Three rut measurements are shown, the average rut, the average maximum rut, and the maximum

rut. The average rut is the average rut (from the original surface) across the whole section excluding the turnaround areas (Stations 2 through 14). The maximum average rut is the average of the maximum rut at each longitudinal measuring point between Stations 2 and 14.

The average maximum rut is representative of how the rut would be recorded on a road project and is therefore used for the interpretation of the results. The average maximum rut accumulated quickly at the start of the test and the embedment exceeded 10 mm in the first 100,000 repetitions, which is indicative of a weak section. A stable linear rate of rutting was reached beyond 100,000 repetitions and the terminal rut depth of 12.5 mm was reached after approximately 250,000 load repetitions.

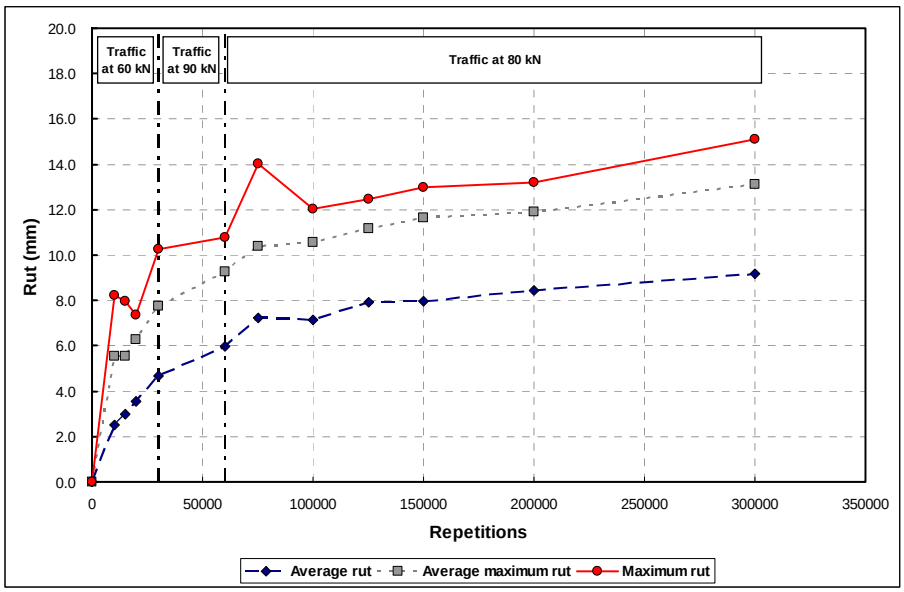

Figure 5.7: Laser profilometer rut accumulation, Section 593FD.

Figure 5.8 shows contour plots of the laser profilometer rut early during the test and at the end of the test. The rut on most of Section 593FD was between 10 mm and 15 mm at the end of the test. A ridge formed across the section at Station 12 (6.0 m). The reason for the lower rutting on this ridge is not apparent.

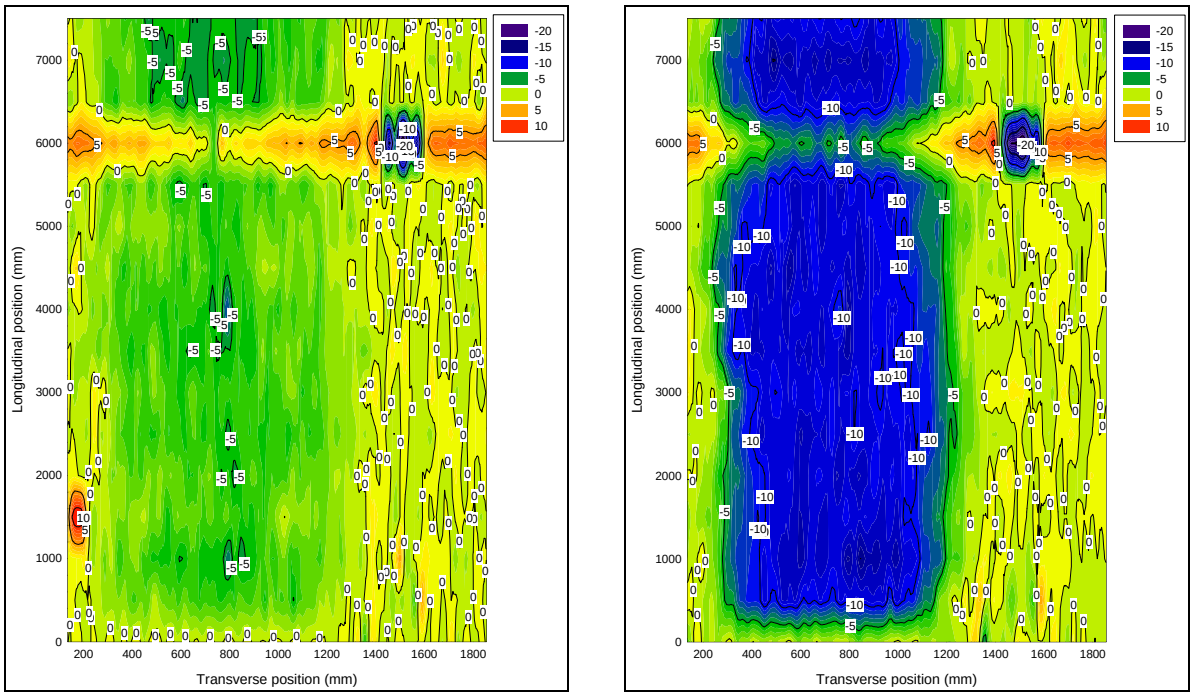

(a) Start of test (b) End of test

Figure 5.8: Laser profilometer rut profiles on Section 593FD.

5.2.3 Depth Response Data

Depth Deflection (MDD)

Details of the MDD positions and instrumentation depths for Section 593FD are shown in Figure 3.5 and Figure 3.6. A spreadsheet template was used for the first level processing of the MDD depth deflection data. Selected results are presented in this section to highlight the response of the test section during the HVS test.

Figure 5.9(a) and (b) show the 60 kN and 80 kN depth deflection data for MDD4 plotted for the duration of the test. The top-cap depth deflection data show a similar trend to the RSD deflection data except for the 80 kN deflection load.

It is possible to investigate the origin of the deflection in the pavement by plotting the depth deflection data from Figure 5.9 against the instrumentation depth of the MDD modules and calculating the vertical elastic strain for each of the pavement layers from the slope of these deflection profiles. This process results in the MDD deflection profiles shown in Figure 5.10(a) and (b) and the 60 kN and 80 kN vertical elastic strain history for each pavement layer, as shown in Figure 5.11(a) and (b).

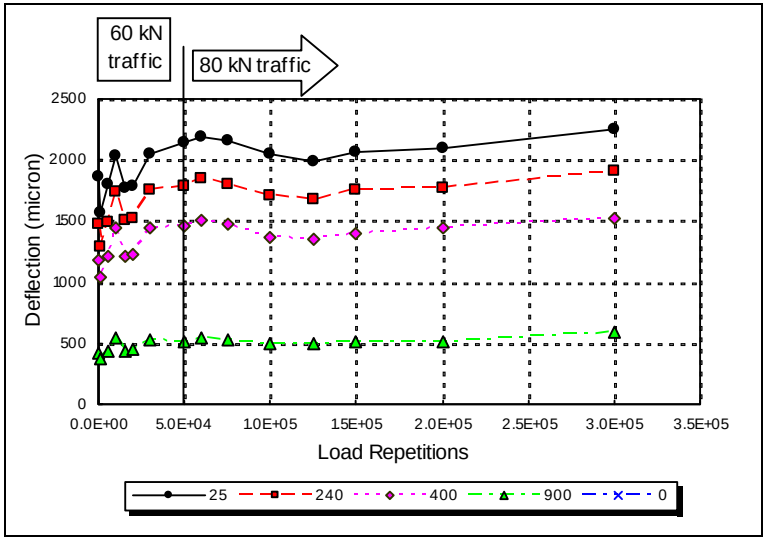

(a) 60 kN MDD deflection for the duration of test 593FD

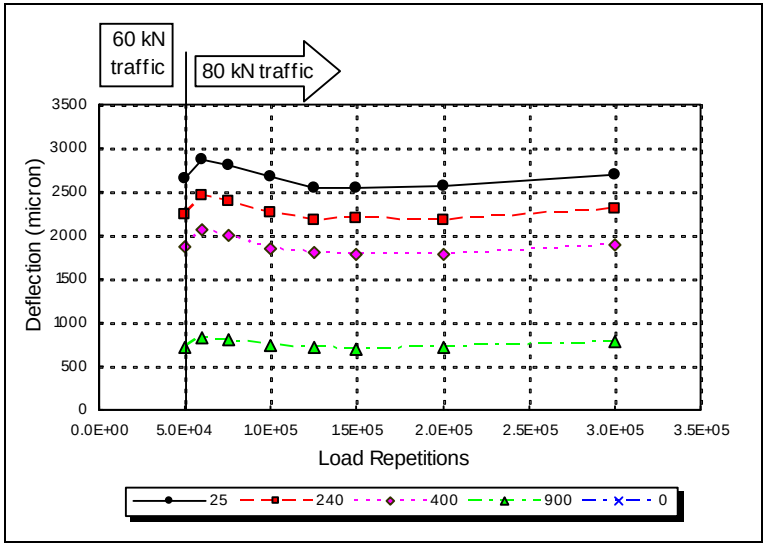

(b) 80 kN MDD deflection for the duration of test 593FD

Figure 5.9: 60 kN and 80 kN MDD data for Section 593FD.

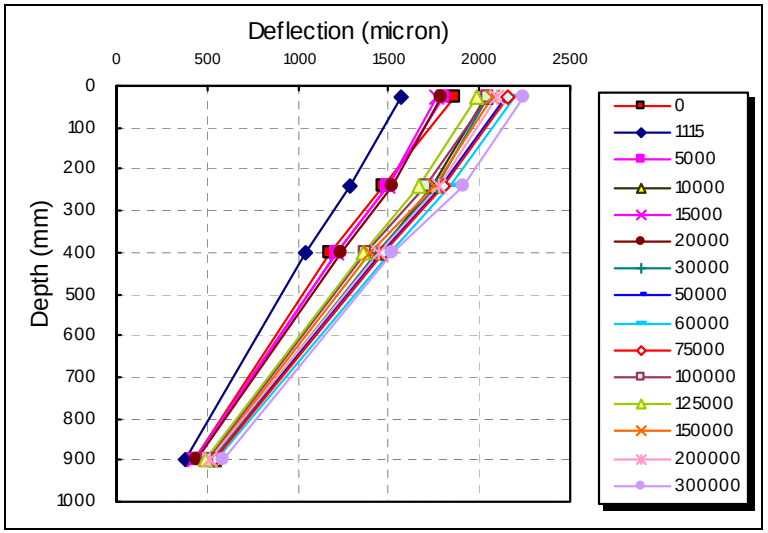

(a) 60 kN MDD deflection profiles for Section 593FD

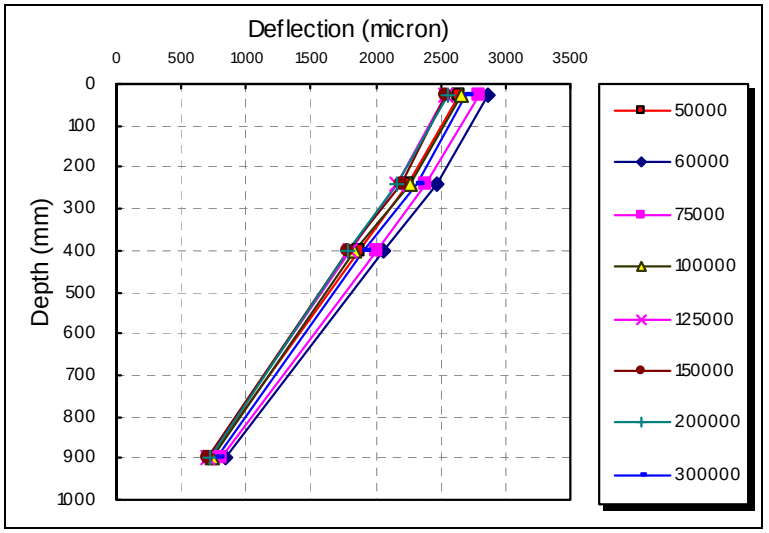

(b) 80 kN MDD deflection profiles for Section 593FD

Figure 5.10: 60 kN and 80 kN MDD profiles for Section 593FD.

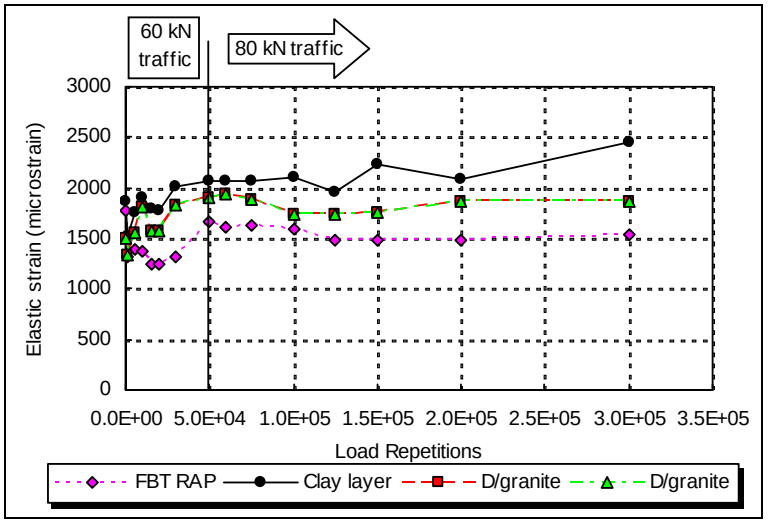

(a) Vertical elastic strain history calculated from the 60 kN MDD data for Section 593FD

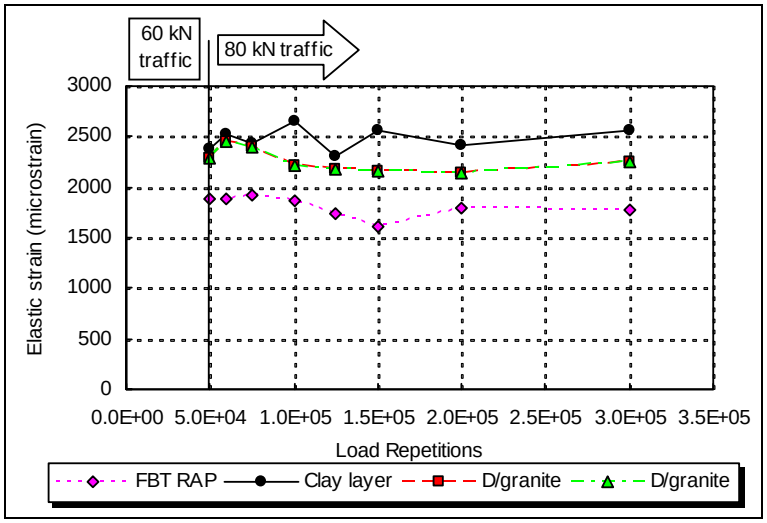

(b) Vertical elastic strain history calculated from the 80 kN MDD data for Section 593FD

Figure 5.11: Vertical elastic strain for the 60 kN and 80 kN loads on Section 593FD.

The elastic strain results from all the MDDs indicate that the grey, clay layer below the base layer contributed the largest portion of the elastic deflection. The combined asphalt concrete and foamed bitumen treated base layer had the lowest elastic strain. The contribution from the individual layers remained fairly consistent during the test. However, these deflection and elastic strain data need to be normalized for the effect of stress to enable a meaningful assessment of the resilient response of the individual pavement layers. This is achieved by doing a back-calculation of the resilient modulus values of the individual pavement layers.

Backcalculated Base Layer Resilient Modulus Values

The depth deflection data for each MDD stack were used in a linear-elastic routine to backcalculate the resilient modulus for the pavement layers. Figure 5.12 through Figure 5.14 show the resilient modulus for the foamed bitumen treated base layer backcalculated from the 60 kN, 90 kN and 80 kN deflection data respectively. The resilient modulus values were well below the expected range of values for foamed bitumen treated material (Section 2). This may in part be attributed to the combination of asphalt concrete, foamed bitumen treated reclaimed asphalt and clay material between the top-cap and 240 mm deep MDD modules.

Permanent Deformation (MDD)

The MDD permanent deformation data were too erratic for modeling of the plastic deformation of the base layer. This is attributed to difficulties experienced during the installation of the MDDs.

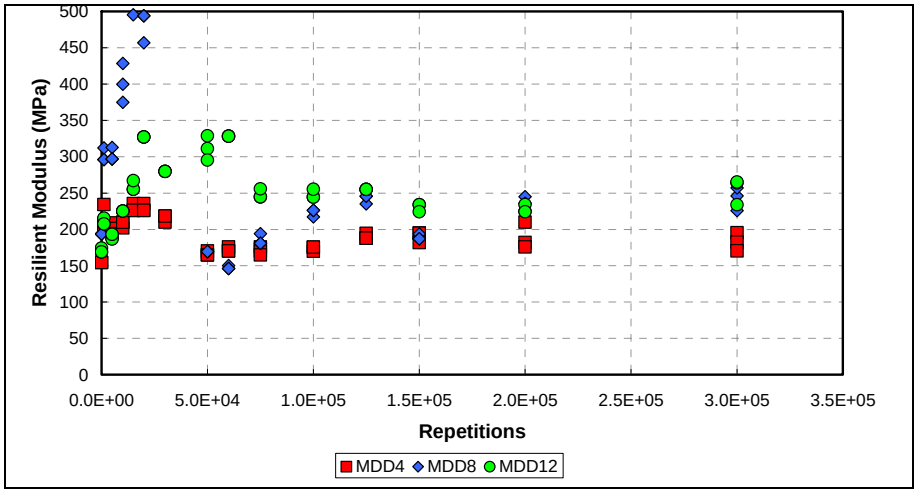

Figure 5.12: 60 kN resilient modulus results for the treated base layer of Section 593FD.

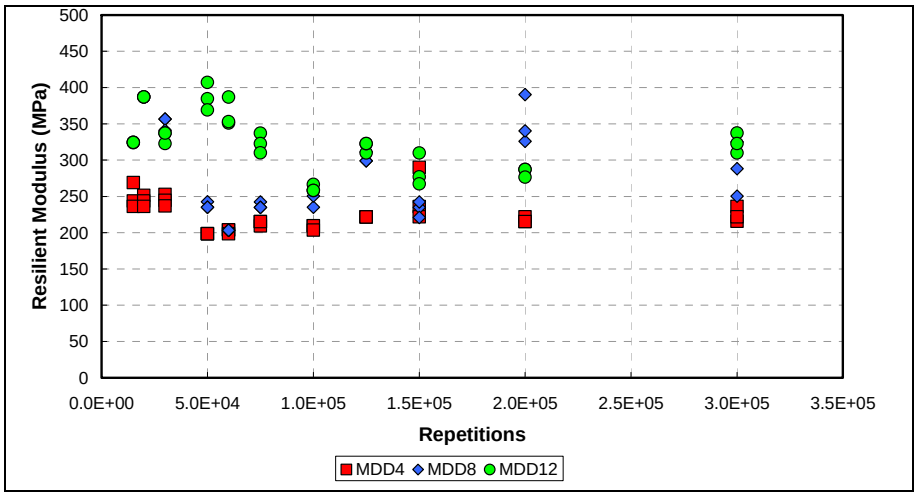

Figure 5.13: 60 kN resilient modulus results for the treated base layer of Section 593FD.

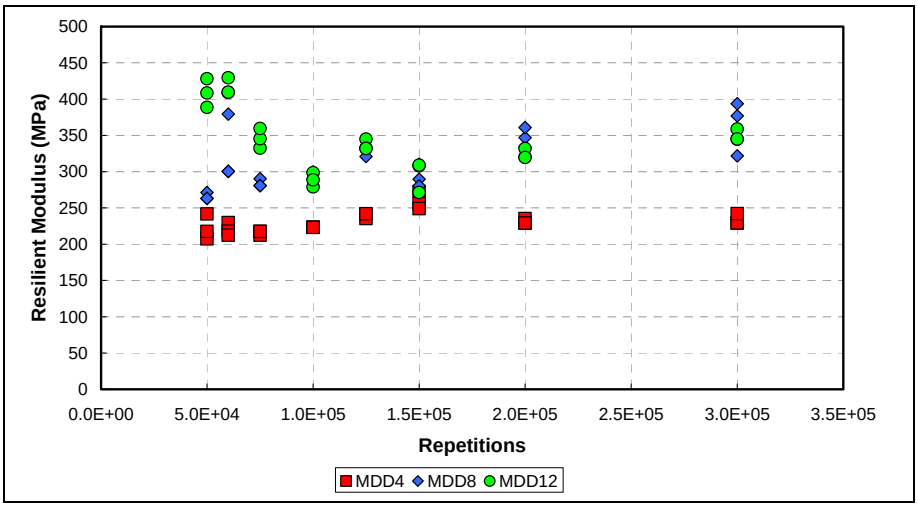

Figure 5.14: 80 kN resilient modulus results for the treated base layer of Section 593FD.

5.2.4 Observations from Section 593FD

The following observations were made regarding the response of Section 593FD:

- The temperature in the foamed bitumen treated, reclaimed asphalt concrete base varied around 20°C for the duration of the test.
- Visual distress was limited to surface rutting at the end of the test with no visible fatigue cracking.
- The elastic deflection of the test section was extremely high for a newly constructed pavement with a stabilized base layer. The high values of deflection were observed for the RSD and all three MDD stacks.
- The resilient modulus of the base layer was unexpectedly low (compared with expected values from Section 2.2). This may be partly attributed to the layer of clay-like material that was

combined with the asphalt concrete and stabilized base between the topcap and 240 mm-deep MDD modules. The MDD installation was carried out according to the design layer thicknesses, but the actual thickness determined from test pits was substantially less.

- The test section reached a terminal rut of 12.5 mm after about 250,000 load repetitions and a rut between 10 mm and 15 mm along the section at the end of the test. Problems with the MDD permanent displacement readings prevented any analysis to determine the origin of the plastic deformation, but the surface and profilometer rut measurements are used later in the report to estimate the pavement bearing capacity in terms of rutting.

5.3 HVS Test 594FD

5.3.1 Environmental Data

Rainfall

No rainfall data were collected during the test on Section 594FD but significant snow fell during the test as shown in Figure 5.15.

Figure 5.15: Snowfall during test 594FD.

Pavement Temperature

Pavement and ambient temperatures were collected inside the temperature control box during the times at which data were recorded. A summary of the data is shown in Figure 5.16. The ambient temperature reduced considerably during the test. The pavement surface temperature, asphalt concrete temperature (25 mm deep) and the temperature in the foamed bitumen treated base (measured at 150 mm) appeared less affected by the cold weather and varied between 10 and 20 C for the latter part of the test.

5.3.2 Surface Response Data

Visual Distress

Figure 5.17 shows the visual condition of Section 594FD upon completion of the test. Substantial cracking of the asphalt concrete layer was observed.

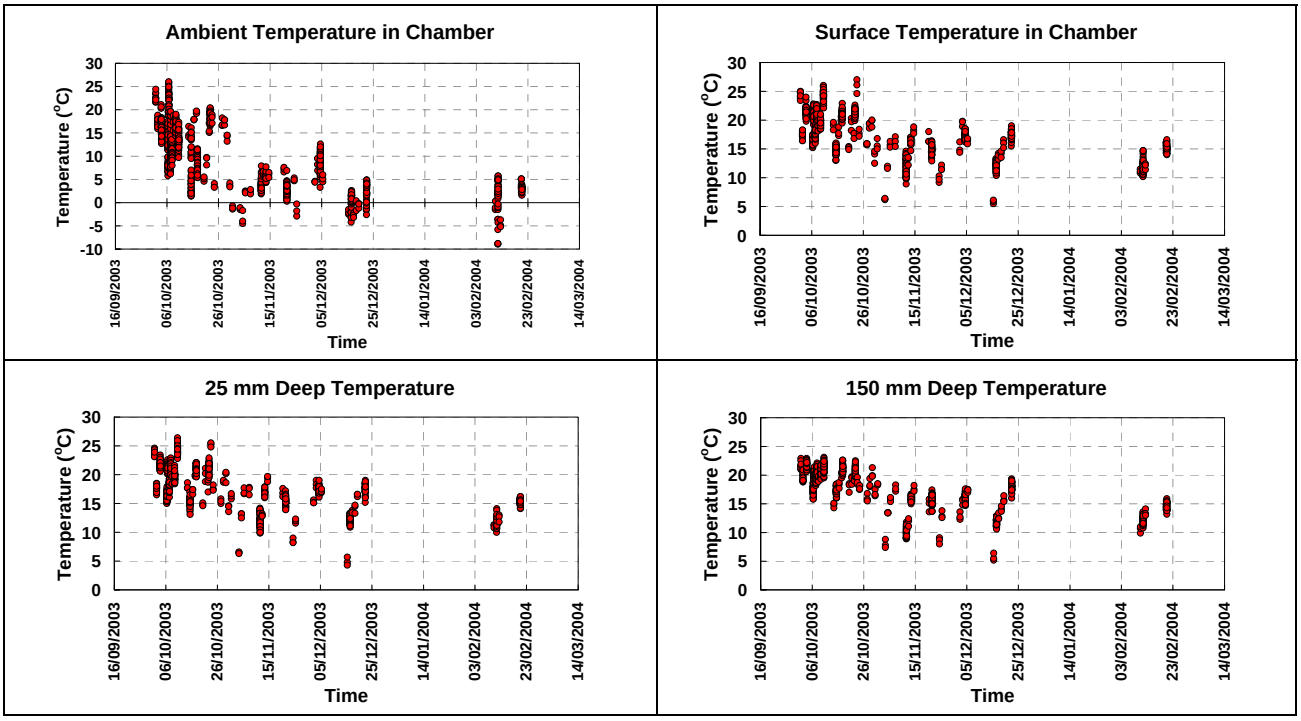

Figure 5.16: Ambient and pavement temperatures from Section 594FD.

Figure 5.17: Visual condition of Section 594FD at the end of the test.

Surface Deflection (RSD)

Figure 5.18 shows the average peak deflection on the centerline, traffic and caravan sides for the 60 kN test load. The magnitude of the deflections was again high. The deflections remained below 1.5 mm for

the initial stages of the test but started increasing from about 400,000 repetitions onwards. The increase in deflection could have been caused by the fatigue damage of the surfacing layer under the relatively cold conditions. The onset of the increase in deflection will be investigated with radius of curvature calculations from the RSD deflection bowls during the second level analysis of the HVS data.

The deflections across the section from the caravan to the traffic side were in the same range, and neither side had consistently higher or lower deflections. Deflection was also consistent along the length of the section.

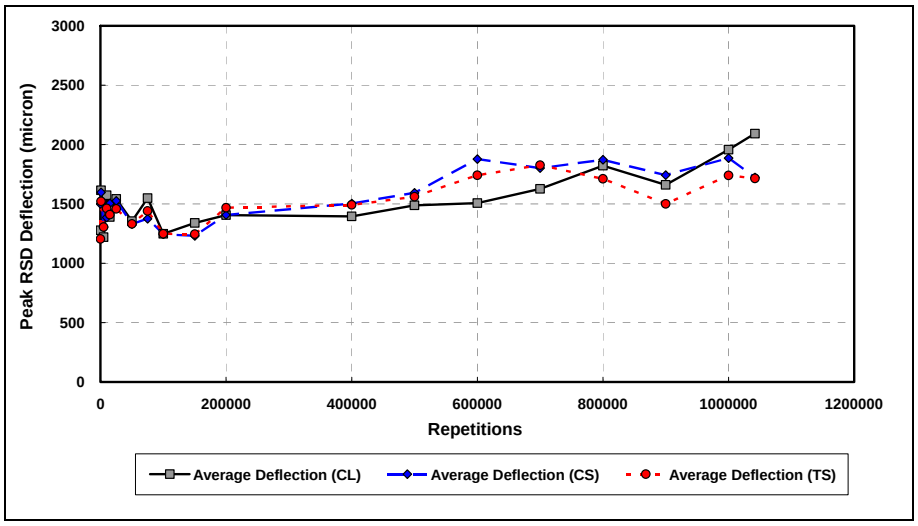

Figure 5.18: RSD peak deflections under 60 kN loading on Section 594FD.

Surface Profile

Straightedge measurements were taken during the test on Section 594FD and the accumulation of rut based on these measurements is shown in Figure 5.19. There was an increase in rut rate from 600,000 repetitions onwards. This increase could be related to the increase in elastic deflection discussed in the preceding section. The test section reached a terminal rut of 12.5 mm after about 930,000 load repetitions at 60 kN.

Laser profilometer readings were also taken on Section 594FD and Figure 5.20 shows the accumulation of rut during the test based on these measurements. Three rut measurements are shown, the average rut, the average maximum rut, and the maximum rut according to the definitions used in Section 5.2.2.

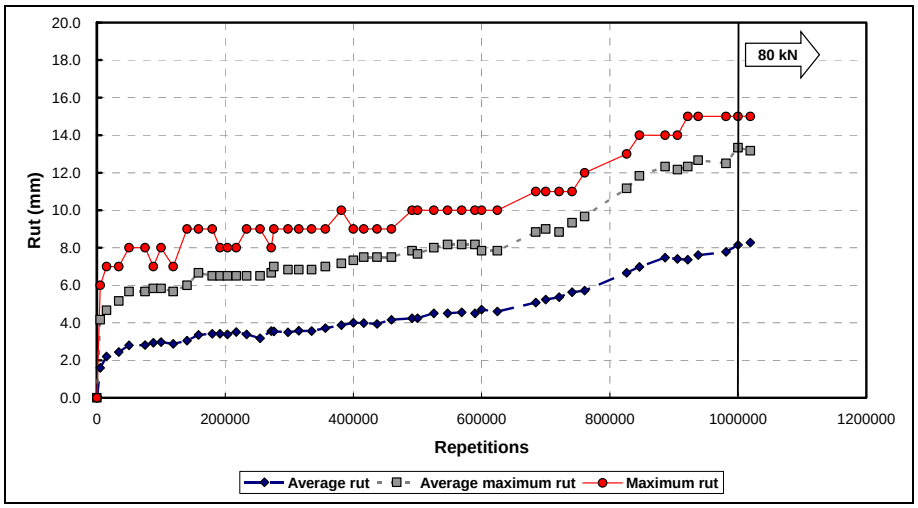

Figure 5.19: Straightedge rut accumulation for Section 594FD.

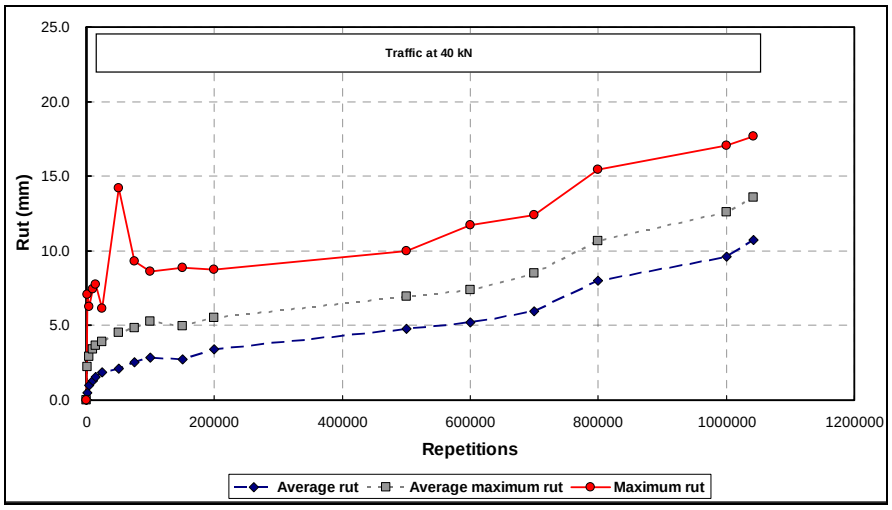

Figure 5.20: Laser profilometer rut accumulation for Section 594FD.

The average maximum rut was used for the interpretation of the results. The embedment was less than that of Section 593FD and only reached about 5.0 mm after 100,000 repetitions. A stable linear rate of rutting was reached beyond 100,000 repetitions and again the rut rate increased beyond 600,000 repetitions. The terminal rut depth of 12.5 mm was reached after approximately one million load repetitions.

Figure 5.21 shows contour plots of the laser profilometer rut early during the test, at 600,000 repetitions and at the end of the test. The rut over most of Section 594FD was between 10 mm and 15 mm at the end of the test.

5.3.3 Depth Response Data

Depth Deflection (MDD)

Figure 5.22 shows the 60 kN depth deflection data for MDD12 plotted for the duration of testing on Section 594FD. Unfortunately the deflections from MDDs 4 and 8 were not reliable and had to be discarded. The top-cap depth deflection data show a similar trend to the RSD deflection data with an increase in elastic deflection from 400,000 repetitions onwards.

A plot of the depth deflection data from Figure 5.22 against the instrumentation depth of the MDD modules was used to calculate the vertical elastic strain for each of the pavement layers from the slope of the deflection profiles. These results are shown in Figure 5.23. The vertical elastic strain history for each pavement layer is shown in Figure 5.24.

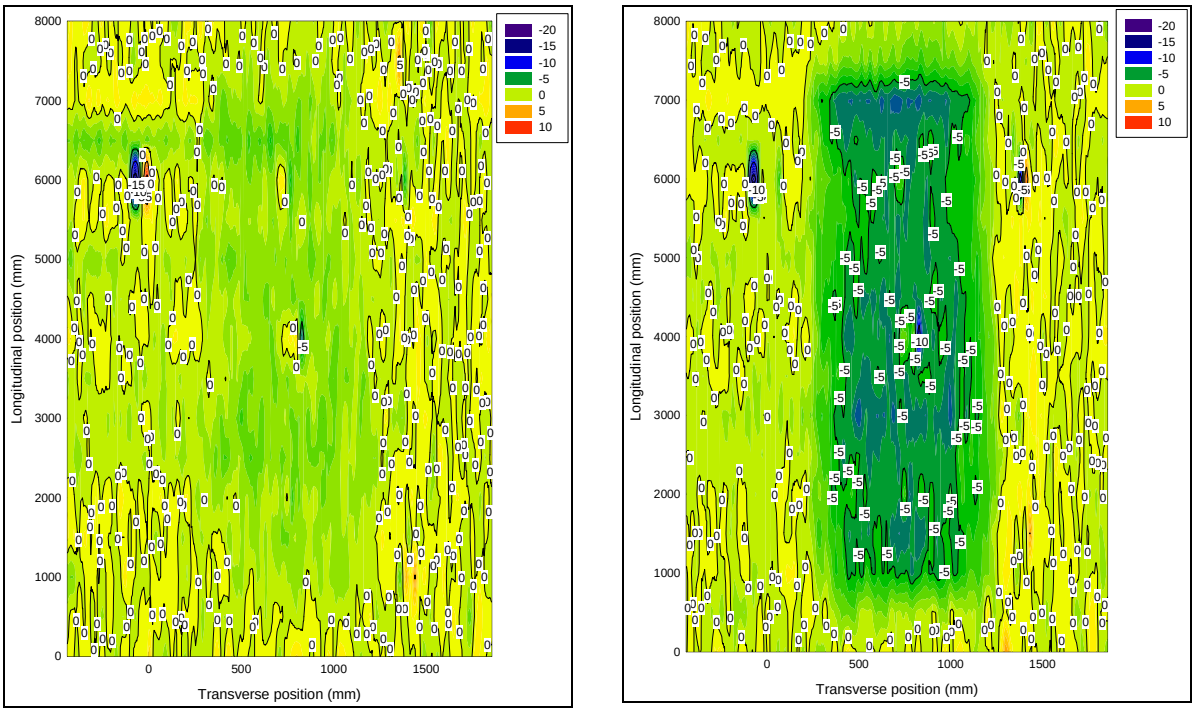

(a) 10,000 repetitions

(b) 600,000 repetitions

Figure 5.21: Laser profilometer rut profiles for Section 594FD.

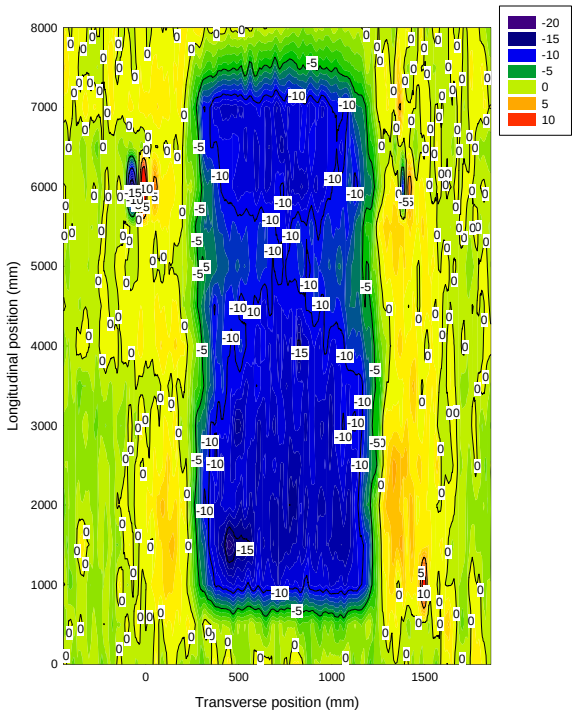

(c) End of the test, 1,042 million repetitions

Figure 5.21: Laser profilometer rut profiles for Section 594FD *(continued)*.

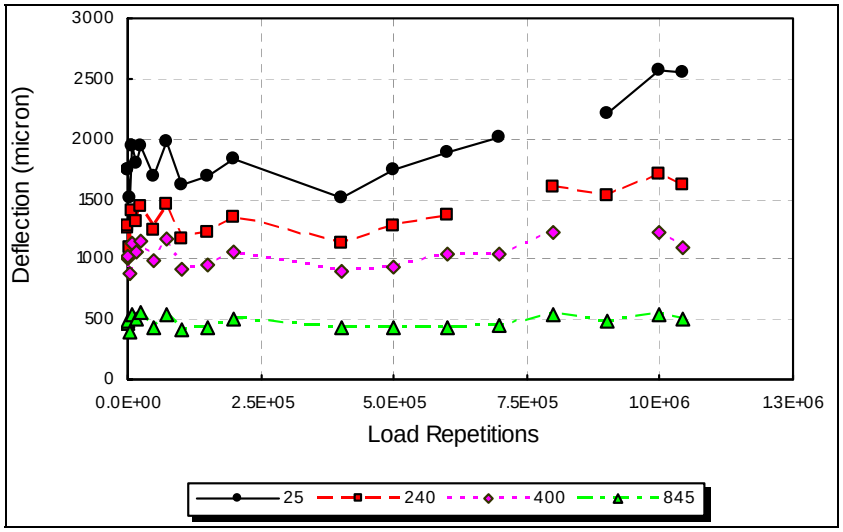

Figure 5.22: 60 kN depth deflection data for Section 594FD.

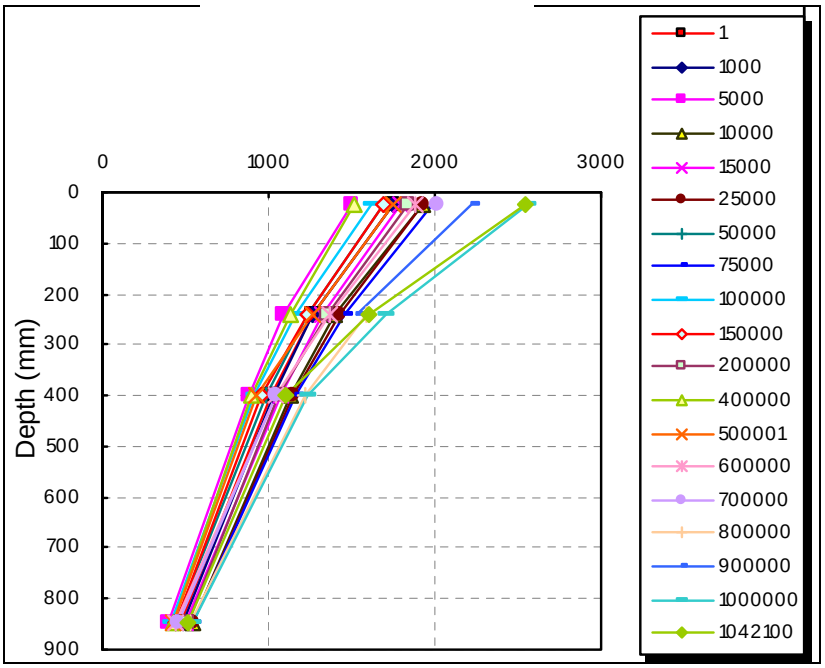

Figure 5.23: 60 kN MDD depth deflection profiles for Section 594FD.

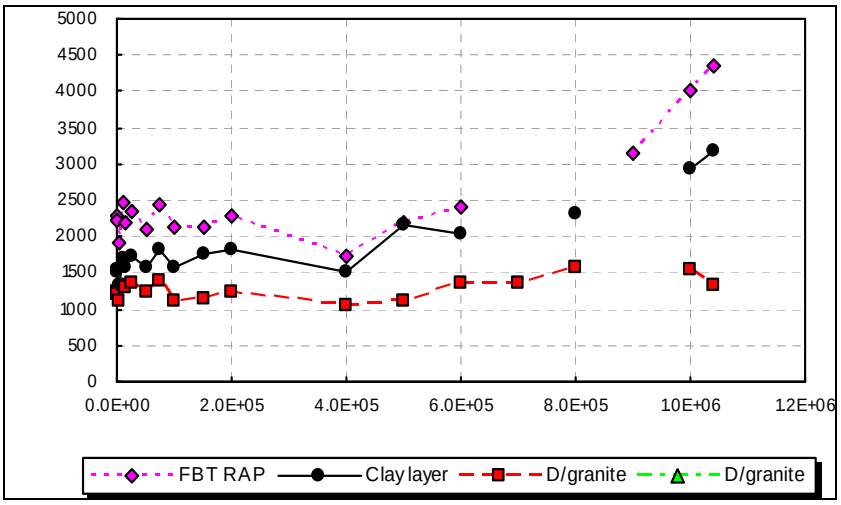

Figure 5.24: Vertical elastic strain data for 60 kN load on Section 594FD.

It is interesting to note that the combined asphalt concrete and foamed bitumen treated base layer contributed the most to the elastic strain and the elastic strain of these combined layers increased the most during the test. All the layers showed an increase in elastic strain from 400,000 repetitions onwards.

Backcalculated Base Layer Resilient Modulus Values

The depth deflection data for each MDD stack were used in a linear-elastic routine to backcalculate the resilient modulus for the pavement layers. Figure 5.25 shows the resilient modulus for the foamed

bitumen treated base layer backcalculated from the 60 kN deflection data. The resilient modulus values are well below the expected range of values for foamed bitumen treated material. This may in part be attributed to the combination of asphalt concrete, foamed bitumen treated reclaimed asphalt, and clay material between the top-cap and 200 mm deep MDD modules. The resilient modulus of the base layer showed a significant reduction from 400,000 repetitions onwards to reach very low values around 60 MPa at the end of the test.

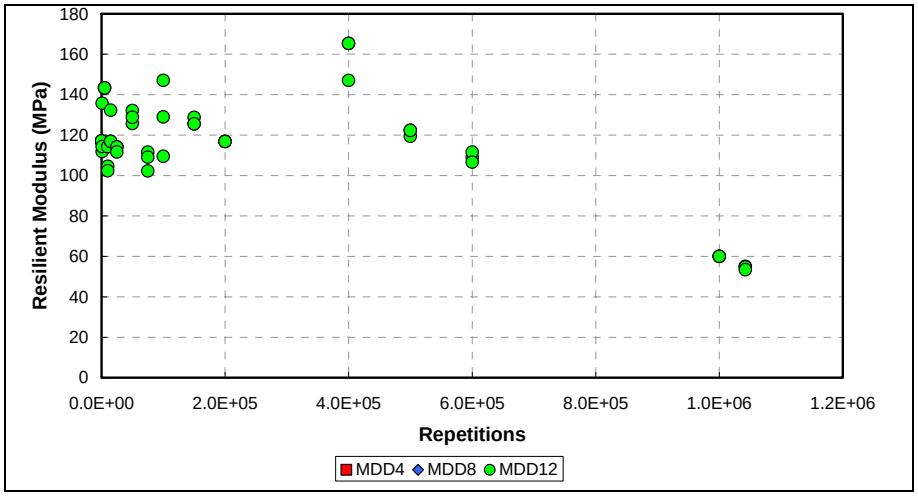

Figure 5.25: 60 kN resilient modulus results for the base layer on Section 594FD.

In-depth Permanent Deformation (MDD)

As for Section 593FD, the MDD permanent deformation data were too erratic to be used for modeling of the plastic deformation of the base layer.

5.3.4 Observations from Test 594FD

The following observations were made regarding the response of Section 594FD:

- The temperature in the foamed bitumen treated, reclaimed asphalt concrete base varied between 10°C and 20°C for the duration of the test, while the ambient temperature went below freezing point (0°C).
- Fatigue cracks were clearly visible at the end of the test.
- The elastic deflection of the test section was extremely high for a newly constructed pavement with a stabilized base layer. The high values of deflection were observed for the RSD and MDD12. Both the RSD and MDD topcap deflection increased from 400,000 repetitions onward.
- The resilient modulus of the base layer was unexpectedly low (compare with expected values from Section 2.2) and reduced drastically from 400,000 repetitions onward. This reduction in base layer modulus coincides with an increase in the elastic deflection.

- The straightedge and laser profilometer average maximum rut rate increased from 400,000 repetitions onward.
- The test section reached a terminal rut of 12.5 mm after approximately one million 60 kN load repetitions, with rut depth varying between 10 mm and 15 mm along the section at the end of the test. Problems with the MDD permanent displacement readings prevented any analysis to determine the origin of the plastic deformation.
- The different types of measurements taken on Section 594FD all show 400,000 load repetitions to be a significant point at which a change occurred in the pavement behavior. It is not possible to identify the exact cause of this change but it may have been a combination of surfacing fatigue and water from melting snow entering the pavement through the fatigue cracks.

5.4 HVS Test 595FD

5.4.1 Environmental Data

Rainfall

No rainfall data were collected during the test on Section 595FD and no significant snow fell during the test.

Pavement Temperature

Pavement and ambient temperatures were collected inside the temperature control box during the times at which data were recorded. A summary of the data is shown in Figure 5.26. The ambient temperature remained below 20°C during the test. The intention was to control the temperature of the base layer at 10°C during the test. The pavement surface temperature, asphalt concrete temperature (25 mm deep) and the temperature in the foamed bitumen treated base (measured at 150 mm depth) ranged between 5°C and 15°C for most of the test.

5.4.2 Surface Response Data

Visual Distress

Figure 5.27 shows the visual condition of Section 595FD at the end of the test. Significant rutting occurred in the vicinity of Stations 8 and 9 and extensive fatigue occurred over the full length of the section. The appearance of fatigue cracks on the surface of the test section occurred at about 100,000 load repetitions.

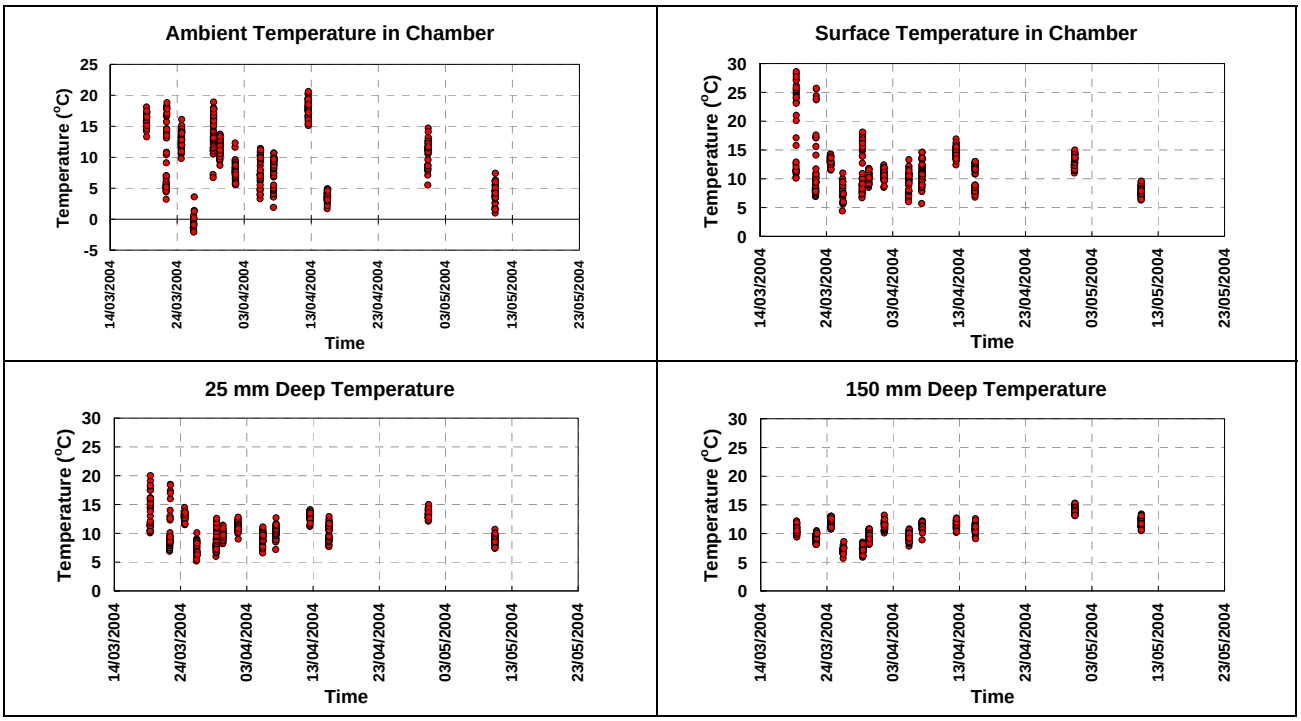

Figure 5.26: Ambient and pavement temperatures for Section 595FD.

(a) Rut on Section 595FD at end of test (b) Extensive fatigue of Section 595FD at end of test

Figure 5.27: Visual condition of Section 595FD at the end of the test.

Surface Deflection (RSD)

Figure 5.28 shows the average peak deflection on the centerline, traffic and caravan sides, for the 60 kN test load. The deflection started at 1.5 mm and increased to levels between 2.0 and 2.5 mm within 50,000 load repetitions. The magnitude of these deflections was extremely high. Given these high levels of deflection, the radius of curvature was probably very small which would have been detrimental to the fatigue life of the surfacing layer. The radius of curvature will be calculated from the RSD deflection bowls during the second level analysis of the HVS data and compared to the radius of curvature for the other test sections.

The deflections across the section from the caravan to the traffic side were in the same range, and neither side has consistently higher or lower deflections. Figure 5.29 shows the RSD deflection plotted along the length of the section. The section can be divided into three distinct segments:

- An area from Station 3 to Station 7 with an initial deflection of about 1.5 mm,
- An area from Station 10 to Station 13 with an initial deflection of about 1.0 mm; and
- A transitional area from Station 7 to Station 10. The deflection in this transitional area increased the most during the test and was also the area showing the highest rut.

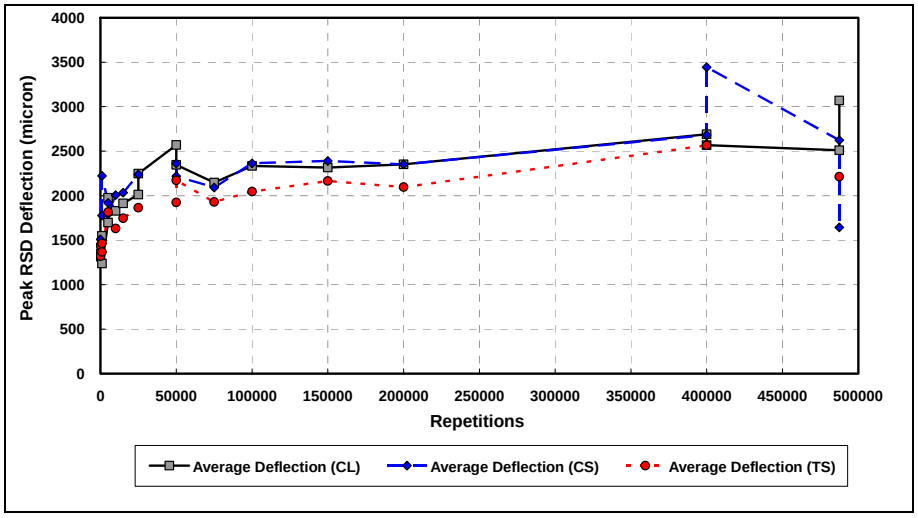

Figure 5.28: RSD peak deflections under 60 kN loading on Section 595FD.

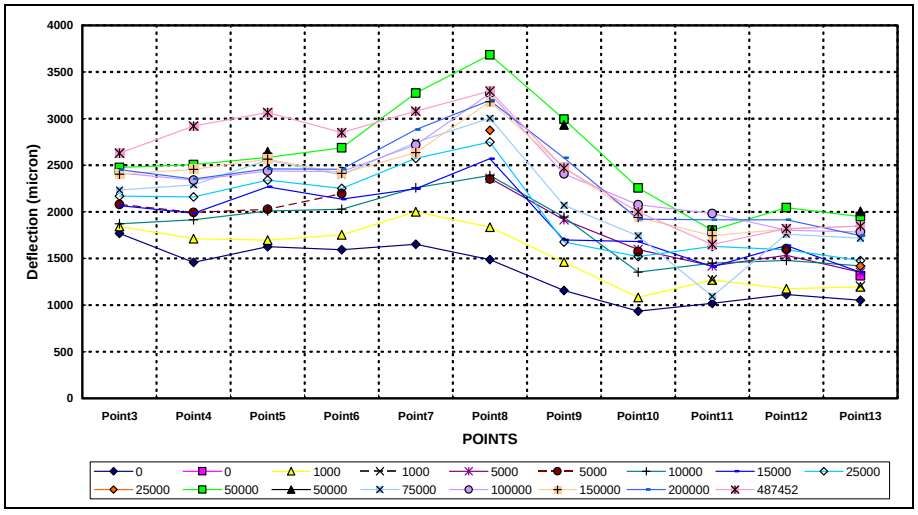

Figure 5.29: RSD peak deflections under 60 kN loading on Section 595FD.

Surface Profile

Straightedge measurements were taken during the test on Section 595FD and the accumulation of rut based on these measurements is shown in Figure 5.30. The test section reached a terminal rut of 12.5 mm after about 850,000 load repetitions at 60 kN.

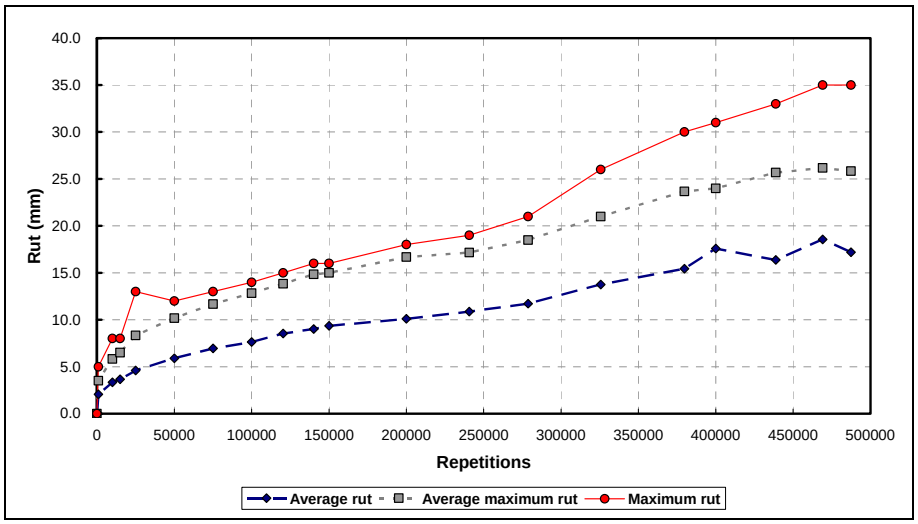

Figure 5.30: Straightedge rut accumulation for Section 595FD.

Laser profilometer readings were taken on Section 595FD and Figure 5.31 shows the accumulation of rut during the test. The average rut, average maximum rut, and maximum rut are shown. The average maximum rut was again used for the interpretation of the results. The embedment was substantial and reached almost 13 mm (terminal rut) after 100,000 repetitions before settling into a stable linear rate of rutting.

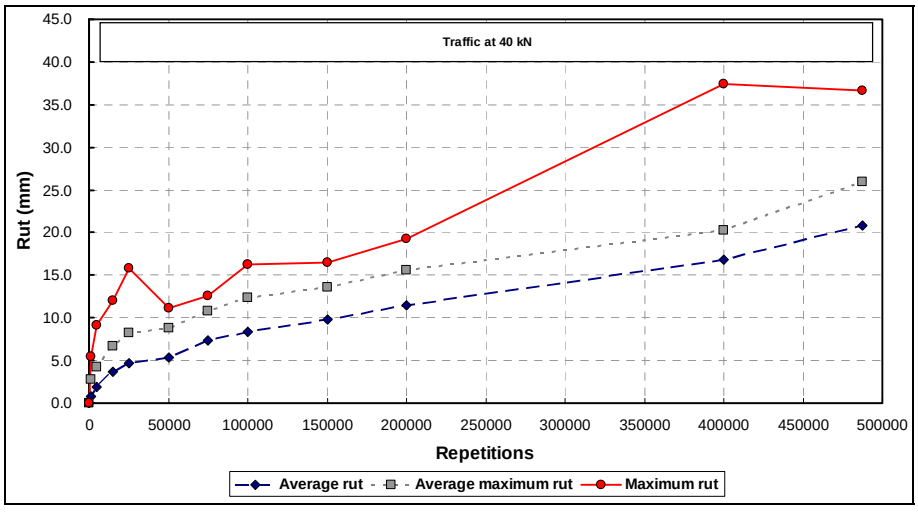

Figure 5.31: Laser profilometer rut accumulation for Section 595FD.

Figure 5.32 shows contour plots of the laser profilometer rut early during the test, at 100,000 repetitions and at the end of the test. The rut on most of Section 595FD was between 10 mm and 15 mm at 100,000 load repetitions. A fairly large area of the section had a rut exceeding 20 mm at the end of the test with the area in the vicinity of Stations 8 and 9 showing initial signs of shear failure with heaving next to the section.

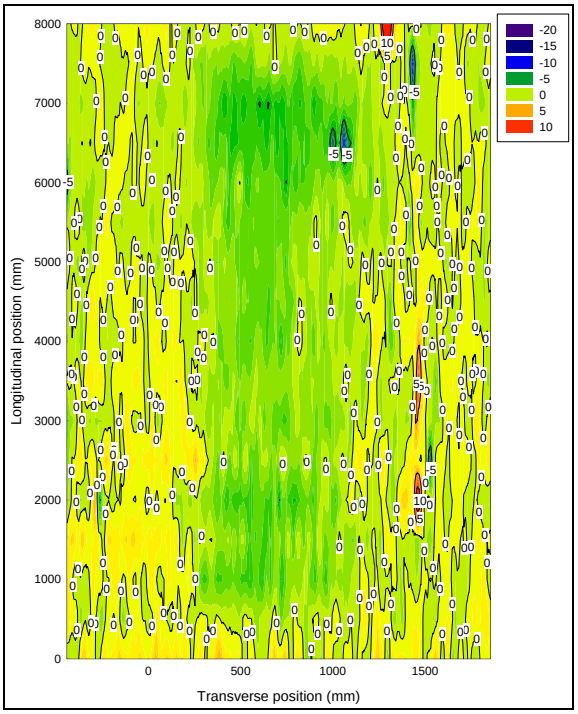

(a) 5,000 repetitions

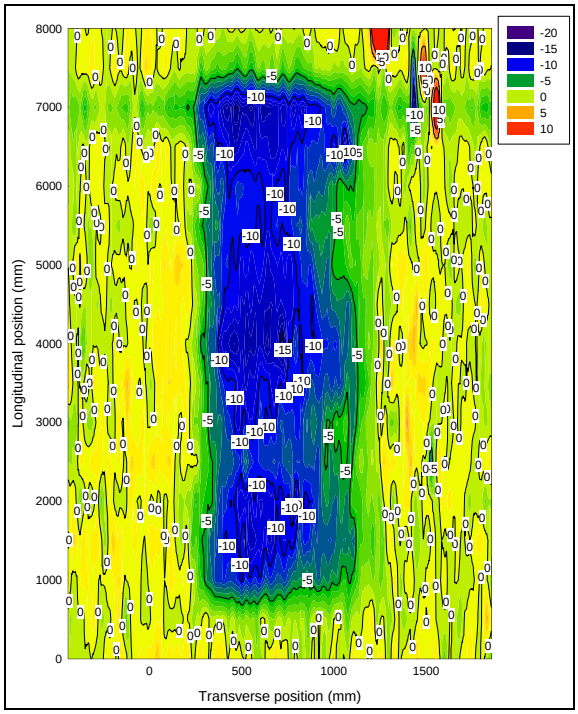

(b) 100,000 repetitions

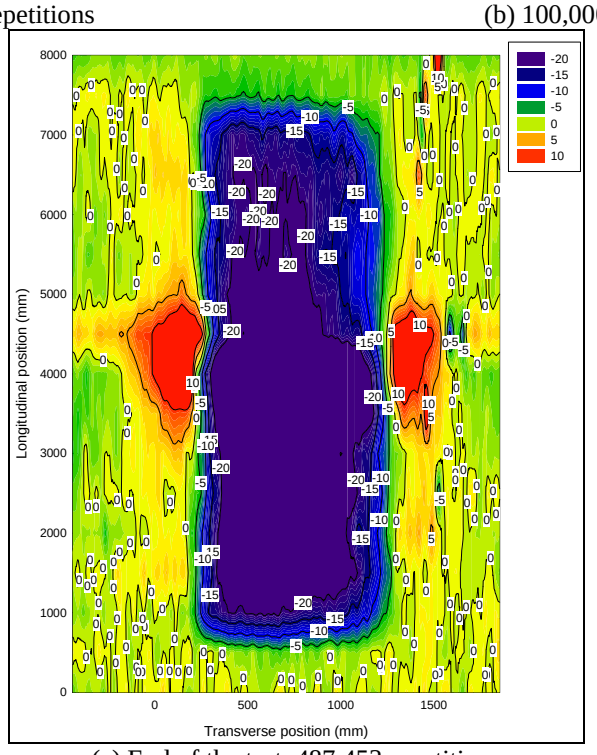

(c) End of the test, 487,453 repetitions

Figure 5.32: Laser profilometer rut profiles for Section 595FD.

5.4.3 Depth Response Data

Depth Deflection Data (MDD)

Figure 5.33 shows the 60 kN depth deflection data for MDD12 plotted for the duration of HVS testing on Section 595FD. Unfortunately the deflections from MDD4 and MDD8 were not reliable and had to be discarded. The topcap depth deflection data show a similar trend to the RSD deflection data but were significantly higher. Given the high levels of peak deflection, the RSD supports were probably within the deflection bowl resulting in a lower deflection reading from the RSD. Conversely, the anchor for the MDD was at a depth of 3.0 m at which point the influence of the load was probably dissipated.

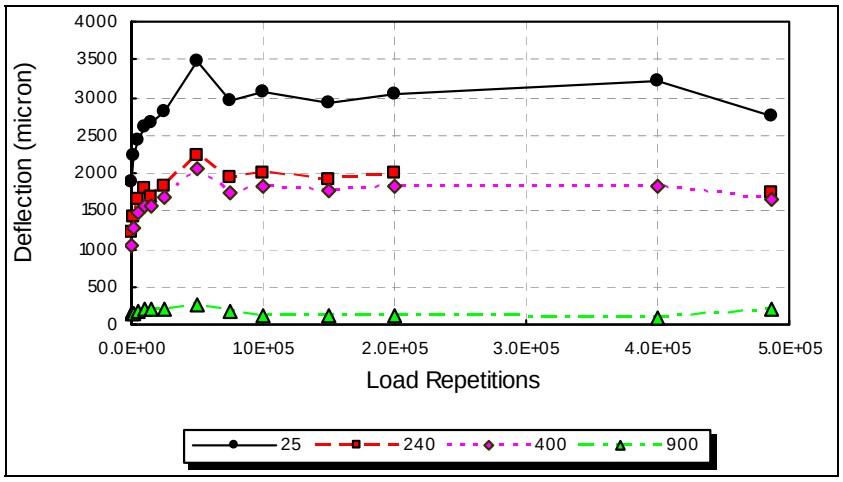

Figure 5.33: 60 kN depth deflection data for Section 595FD.

A plot of the depth deflection data from Figure 5.33 against the instrumentation depth of the MDD modules was used to calculate the vertical elastic strain for each of the pavement layers from the slope of the deflection profiles. These results are shown in Figure 5.34. The vertical elastic strain history for each pavement layer is shown in Figure 5.35.

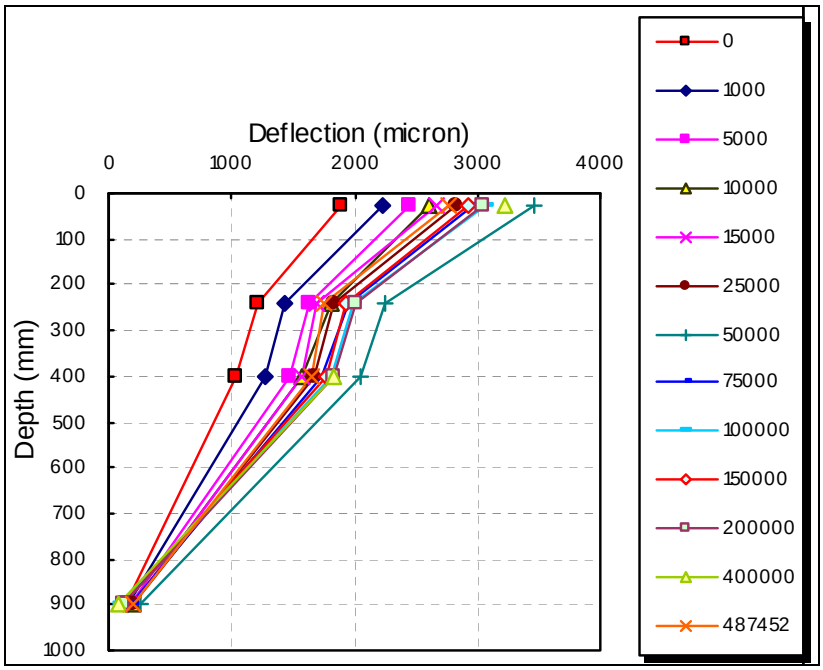

Figure 5.34: 60 kN MDD depth deflection profiles for Section 595FD.

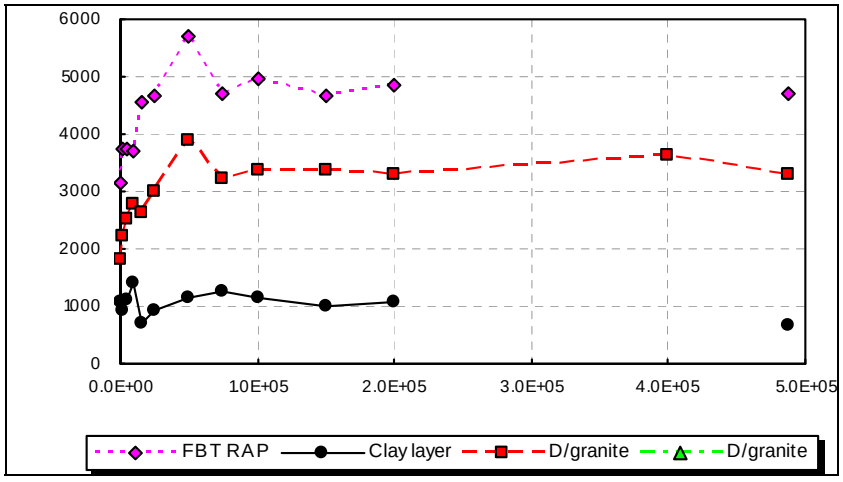

Figure 5.35: Vertical elastic strain data for the 60 kN test loads on Section 595FD.

It is interesting to note that the combined asphalt concrete and foamed bitumen treated base layer contributed the most to the elastic strain. The vertical elastic strain of all the layers remained fairly consistent from about 75,000 repetitions onwards. Normalization of the deflection and elastic strain data for the effect of stress is discussed below.

Backcalculated Base Layer Resilient Modulus Values

The depth deflection data for each MDD stack were used in a linear-elastic routine to backcalculate the resilient modulus for the pavement layers. Figure 4.36 shows the resilient modulus for the foamed bitumen treated base layer backcalculated from the 60 kN deflection data. The resilient modulus values were well below the expected range of values for foamed bitumen treated material. This may in part be attributed to the combination of asphalt concrete, foamed bitumen treated reclaimed asphalt and clay material between the topcap and the MDD modules at 200 mm. The resilient modulus of the base layer showed a significant reduction from the start of the test to reach very low values around 60 MPa from 25,000 repetitions onwards.

Permanent Deformation (MDD)

As for the other sections, the MDD permanent displacement data were too erratic to be used for modeling of the plastic deformation of the base layer.

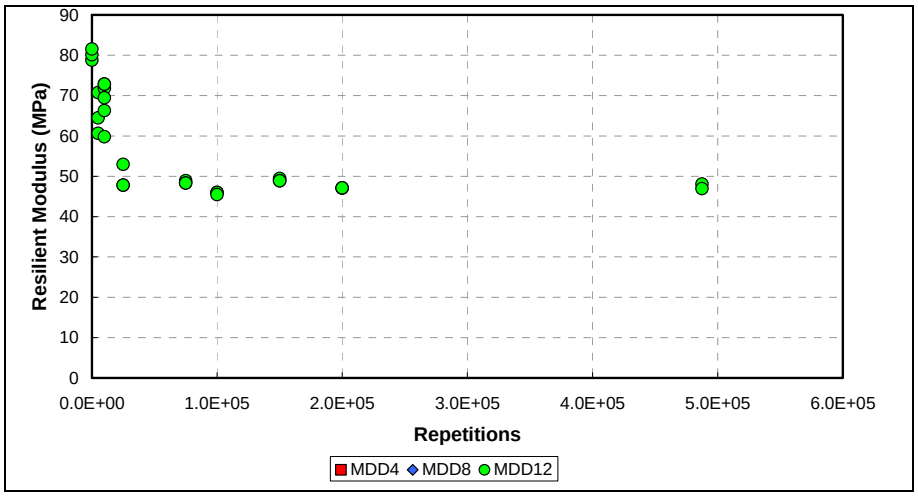

Figure 5.36: 60 kN resilient modulus results for the treated base layer of Section 595FD.

5.4.4 Observations from Test 595FD

The following observations are made regarding the response of Section 595FD:

- The temperature in the foamed bitumen treated, reclaimed asphalt concrete base was controlled between 5°C and 15°C for the duration of the test, while the ambient temperature varied considerably.
- Fatigue cracks were observed early during the test and the full area of the test section was cracked at the end of the test. An area of shear failure was observed in the vicinity of Stations 8 and 9 at the end of the test.

- The elastic deflection of the test section was extremely high for a newly constructed pavement with a stabilized base layer. The high values of deflection were observed for the RSD and MDD12. The area with the highest deflection in the vicinity of Station 8 coincided with the area with the highest rut and where a shear failure started to develop.
- The resilient modulus of the base layer was unexpectedly low (compared with expected values from Section 2.2) and reduced significantly from the start of the test. This reduction in base layer modulus coincided with an increase in the elastic deflection. Such low base layer resilient modulus values will contribute in combination with the low temperatures to the early fatigue of the asphalt concrete surfacing which was observed on Section 595FD.
- The rut exceeded 12.5 mm from 100,000 repetitions onwards and exceeded 20 mm at the end of the test. Heaving next to the section started to occur towards the end of the test. Problems with the MDD permanent displacement readings prevented any analysis to determine the origin of the plastic deformation.
- The combined very low resilient modulus of the base layer and high rut rate suggest that the base layer moisture content may have been high. It is for this reason that nuclear density and moisture content readings are recommended at regular intervals during the test.

5.5 HVS Test 596FD

5.5.1 Environmental Data

Rainfall

No rainfall data were collected during the test on Section 596FD and no significant snow fell during the test.

Pavement Temperature

Pavement and ambient temperatures were collected inside the temperature control box during the times at which data were recorded. A summary of the data is shown in Figure 5.37. The ambient temperature only exceeded 20 C on one occasion during the test. The pavement surface temperature, asphalt concrete temperature (25 mm deep) and the temperature in the foamed bitumen treated base (measured at 150 mm) varied around 15 C for most of the test.

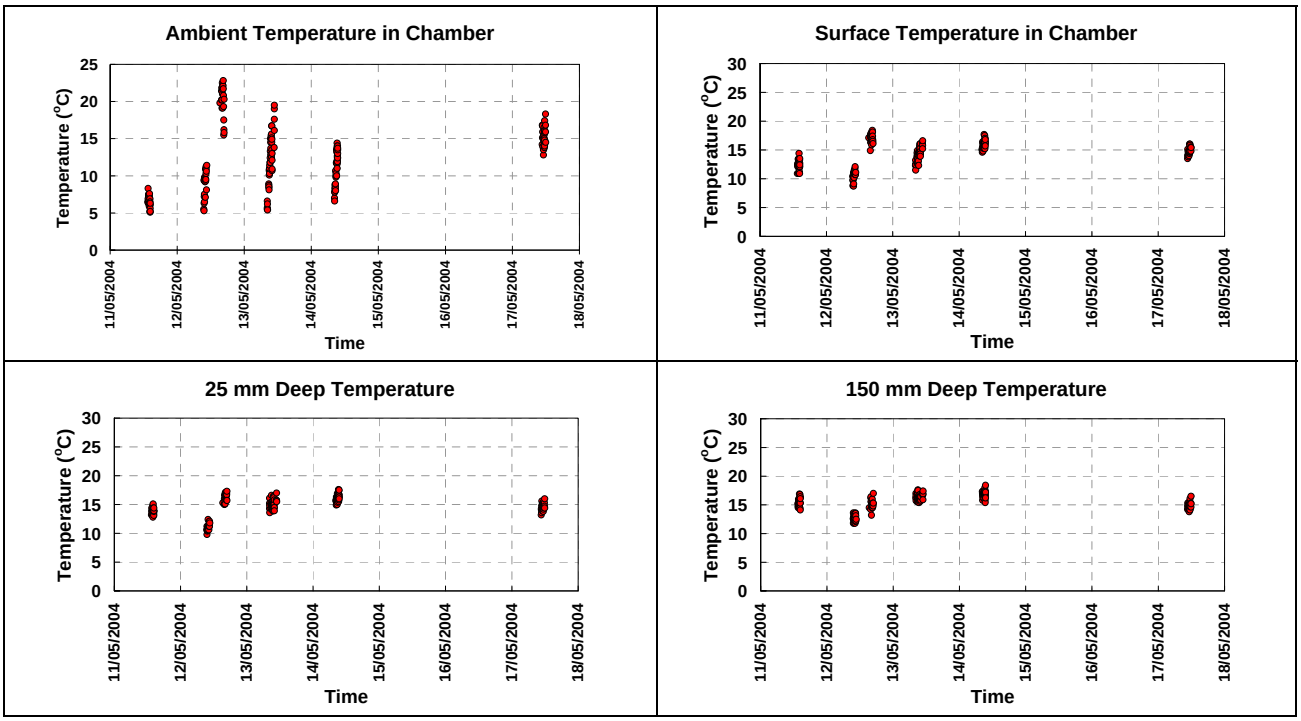

Figure 5.37: Ambient and pavement temperatures for Section 596FD.

5.5.2 Surface Response Data

Visual Distress

Figure 5.38 shows the visual condition of Section 596FD at the end of the test. Shear failure with extensive alligator cracking occurred in the vicinity of Stations 7 and 8. Water was applied to the section during the test and fines pumped from the base were observed on the surface at the end of the test.

(a) Shear failure between Stations 7 and 8 (b) Extensive alligator cracking and pumping

Figure 5.38: Visual condition of Section 596FD at the end of the test.

Road Surface Deflection (RSD)

Figure 5.39 shows the average peak deflection on the centerline, traffic and caravan sides for the 60 kN test load. The deflection started at 1.5 mm and increased to levels between 2.0 mm and 2.5 mm within 5,000 load repetitions. The deflection remained at these levels until about 15,000 repetitions, after which average deflections increased to 3.5 mm. The magnitude of these deflections is extremely high. Given these high levels of deflection, the radius of curvature was probably very small which would have been detrimental to the fatigue life of the surfacing layer.

The deflections across the section from the caravan to the traffic side are in the same range, and neither side had consistently higher or lower deflections. Figure 5.40 shows the RSD deflection plotted along the length of the section. Although fairly uniform initially, the deflection in the vicinity of Station 7 increased to extremely high values towards the end of the test.

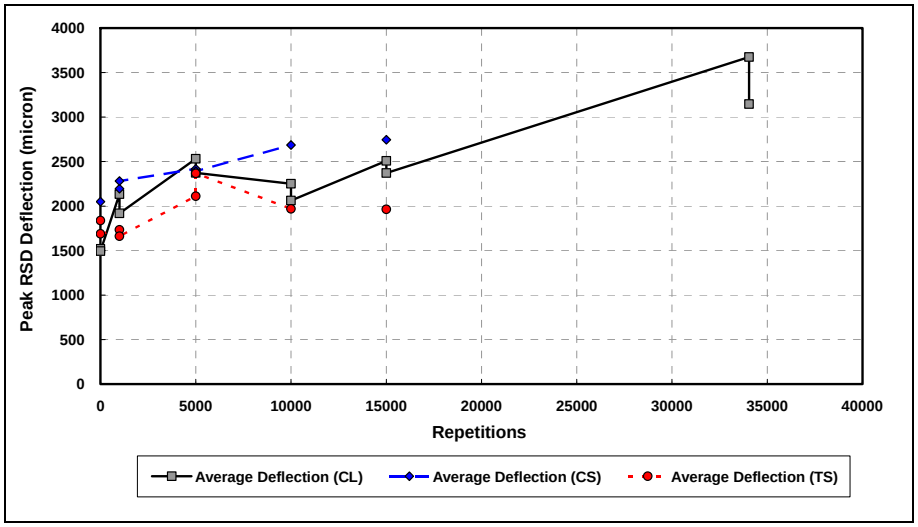

Figure 5.39: RSD peak deflections under 60 kN loading on Section 596FD.

Surface Profile

Straightedge measurements were taken during the early staged of testing on Section 596FD. However, final straightedge readings could not be taken due to the shear failure on the section. The accumulation of rut based on the straightedge measurements is shown in Figure 5.41.

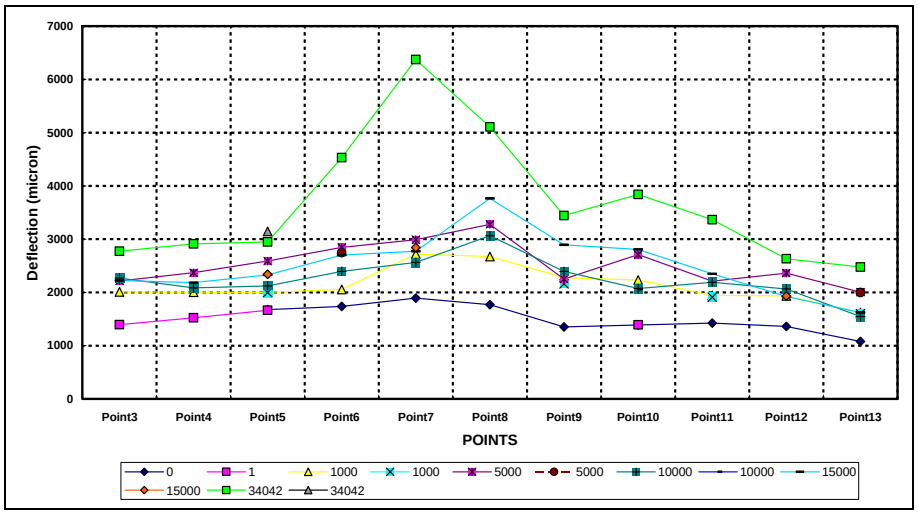

Figure 5.40: RSD peak deflections under 60 kN loading on Section 596FD.

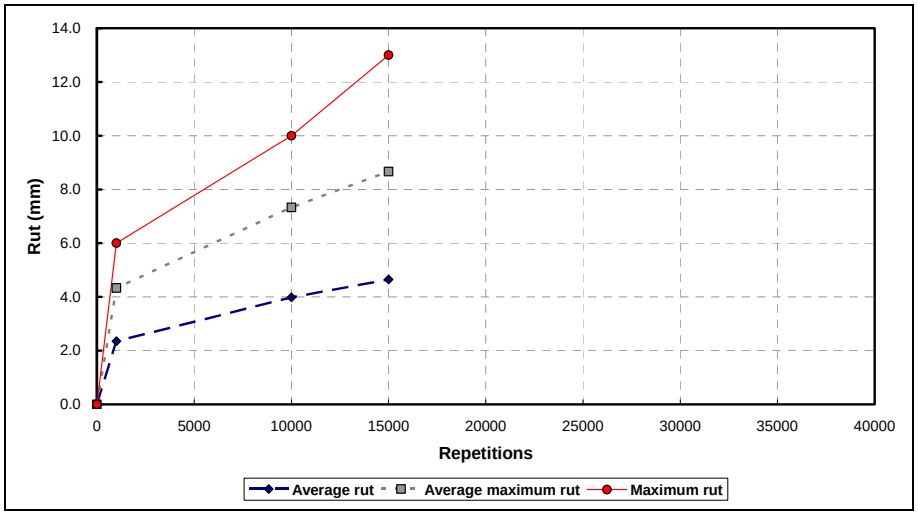

Figure 5.41: Straightedge rut accumulation on Section 596FD.

Laser profilometer readings were taken on Section 596FD and Figure 5.42 shows the accumulation of rut during the test based on the measurements. The average rut, average maximum rut, and maximum rut are shown.

The average maximum rut was used for the interpretation of the results. The terminal rut depth of 12.5 mm was reached after approximately 20,000 load repetitions. The deepest rut on the section at the end of the test was 75 mm.

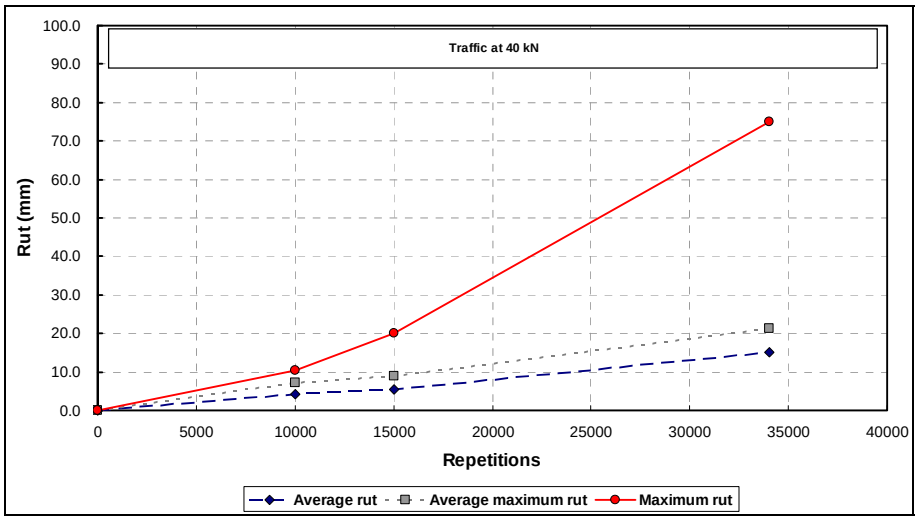

Figure 5.42: Laser profilometer rut accumulation for Section 596FD.

Figure 5.43 shows contour plots of the laser profilometer rut early during the test and at the end of the test. The rut on most of Section 596FD was between 5 mm and 10 mm at 10,000 load repetitions. A fairly large portion of the section had a rut exceeding 20 mm at the end of the test with the area in the vicinity of Station 7 showing extensive shear failure with heaving of material next to the section.

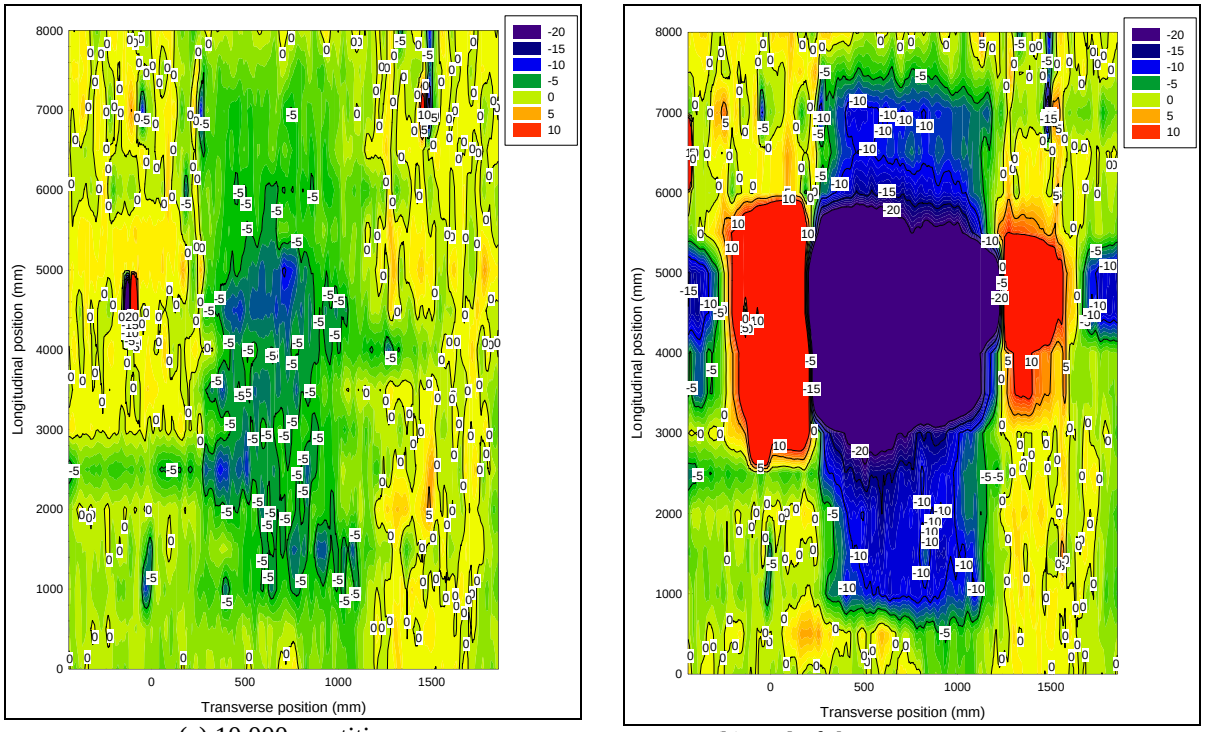

(a) 10,000 repetitions (b) End of the test, 34,042 repetitions

Figure 5.43: Laser profilometer rut profiles for Section 596FD.

5.5.3 Depth Response Data

No MDD systems were installed on Section 596FD.

5.5.4 Observations from Test 596FD

The following observations are made regarding the response of Section 596FD:

- The temperature in the foamed bitumen treated, reclaimed asphalt concrete base fluctuated around 15°C for the duration of the test while the ambient temperature varied considerably.
- The full area of the test section was cracked at the end of the test and fines pumped from the base were observed on the surface. An area of shear failure was observed in the vicinity of Station 7 on the section at the end of the test.
- The elastic deflection of the test section was extremely high for a newly constructed pavement with a stabilized base layer. The area in the vicinity of Station 7 with the highest deflection towards the end of the test coincided with the area where a shear failure developed;
- The rut exceeded 12.5 mm from 20,000 repetitions onwards and exceeded 20 mm at the end of the test. A shear failure in the vicinity of Station 7 resulted in individual surface deformation results of 75 mm.
- The results from Section 596FD indicate that the pavement was extremely sensitive to moisture.

6. DISCUSSION OF HVS TEST RESULTS

This section provides an overview of the HVS test results for the following aspects of material and pavement behavior:

- The resilient modulus of the foamed asphalt treated base layer material obtained from back-calculation of the MDD deflection data;
- The modes of distress of the HVS test sections; and
- Pavement bearing capacity estimates based on the surface rutting of the test sections;

6.1 Base Layer Resilient Modulus Results

A summary of the base layer resilient modulus results of the HVS test sections are provided in Table 6.1.

Table 6.1: Summary of the Base Layer Resilient Modulus Results

Section number	Resilient modulus (MPa)		Comment
	Initial value	End value	
593FD	150 - 350	150 - 250	Initial high values for MDD8 believed to be a calibration problem
594FD	100 - 160	60	The resilient modulus of the base layer remained consistent up to 400,000 repetitions. A clear reduction is observed beyond 400,000 repetitions
595FD	60 - 80	50	Extremely low values for base layer material

All the base layer resilient modulus results were extremely low for foamed bitumen treated material. This may be a result of the combination of the foamed asphalt treated base and a portion of the clay-like material between the two top MDD modules. Regardless of this, there was a clear change in the elastic response of the test sections from about 400,000 load repetitions on Section 594FD. This period coincided with the onset of very low ambient temperatures and snowfalls in early November 2003.

6.2 Modes of Distress of the Test Sections

The mode of distress of the test sections before the onset of winter consisted of gradual deformation of the pavement resulting in a surface rut with limited fatigue cracking. After the winter, the mode changed to a more rapid rate of rutting. On Sections 595FD and 596FD, tested after the winter, shear failure of the base layer occurred in certain locations. The sections tested after the winter also showed extensive fatigue cracking but this was probably caused by the weak base and subbase layers (low resilient modulus) with large plastic strains generating high tensile strains in the asphalt surfacing layer.

6.3 Pavement Bearing Capacity Estimates

The straightedge and laser profilometer rut data were used for estimating the pavement bearing capacity (repetitions to 12.5 mm rut) for a range of testing conditions. A non-linear model of the type shown in Equation 6.1 below was fitted to the rut data using non-linear regression analysis. Once the regression coefficients were known, the number of load repetitions to 12.5 mm rut (bearing capacity) was solved. The rut data for Section 594FD was split at 400,000 load repetitions and the function given by the non-linear equation was fitted to the data preceding 400,000 load repetitions. A linear function was fitted to the data from 400,000 repetitions onward.

$$Rut = mN + a\left(1 - e^{-bN}\right) \quad (6.1)$$

Where: Rut = Surface rut (mm);
N = Load repetitions;
a, b, and m = Regression coefficients.

The parameters "a" and "m" in the above equation have physical interpretations. Parameter "a" represents the amount of embedment that occurs during the initial load repetitions and parameter "m" represents the eventual linear rut rate.

Figure 6.1 through Figure 6.4 show the model fitted to the data of the individual HVS tests. It is clear from these plots that the model adequately represents the rut data. Table 6.2 provides a summary of the rut model data and bearing capacity estimates. Figure 6.5 shows the effect of axle load on pavement bearing capacity under favorable conditions in the fall of 2003. Figure 6.6 through Figure 6.8 show seasonal effects on the embedment parameter, linear rut rate, and pavement bearing capacity, respectively.

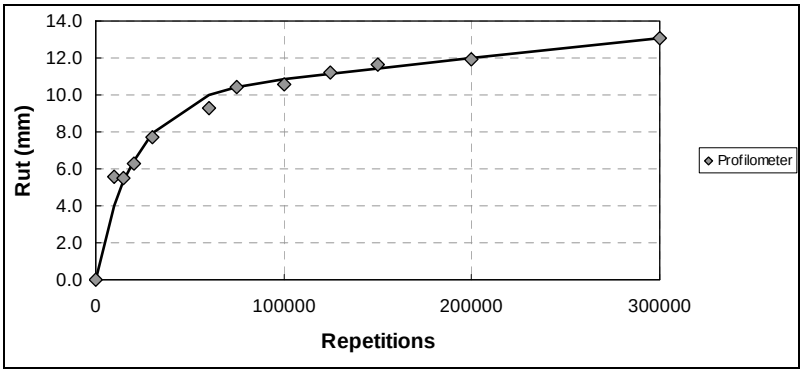

Figure 6.1: Non-linear rut models for Section 593FD.

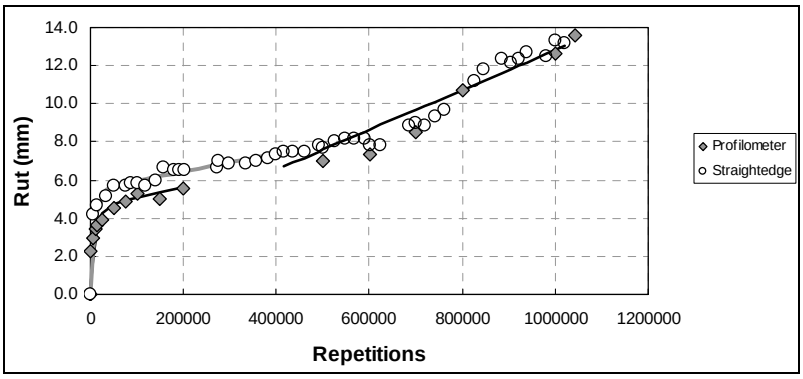

Figure 6.2: Non-linear rut models for Section 594FD.

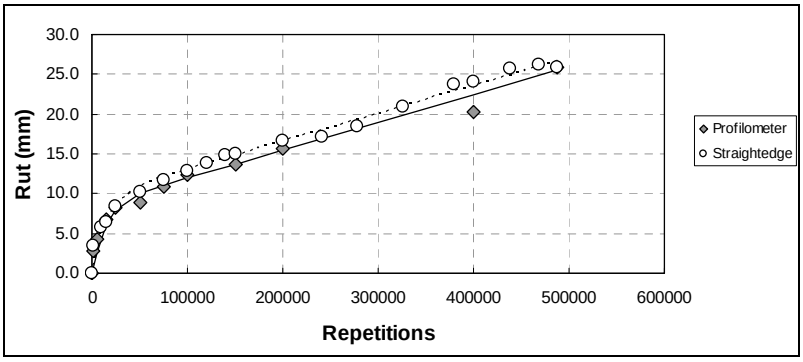

Figure 6.3: Non-linear rut models for Section 595FD.

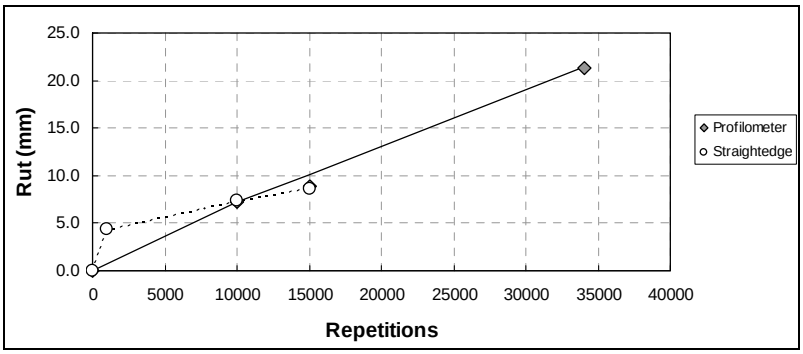

Figure 6.4: Non-linear rut models for Section 596FD.

Table 6.2: Summary of Rut Model Data

Section	Half-axle load (kN)	Season	Instrument					
			Straightedge			Profilometer		
			Embedment (mm)	Rut rate (mm/million repetitions)	Bearing capacity (repetitions)	Embedment (mm)	Rut rate (mm/million repetitions)	Bearing capacity (repetitions)
593FD	80	Fall	-	-	-	9.8	11.0	245,000
594FD[1]	60	Fall	5.5	4.7	1,490,000	4.5	5.7	1,400,000
594FD[2]	60	Winter	2.4	10.5	969,000	-	-	-
595FD	60	Spring	9.6	35.0	83,600	8.5	35.0	114,000
596FD	60	Spring with surface water	4.6	270.0	29,300	1.3	590.0	19,000

[1] Rut data preceding 400,000 repetitions [2] Rut data after 400,000 repetitions

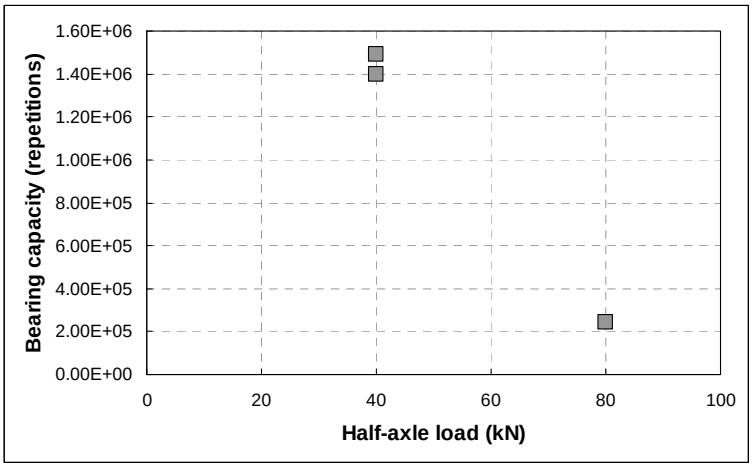

Figure 6.5: Effect of axle load on pavement bearing capacity.

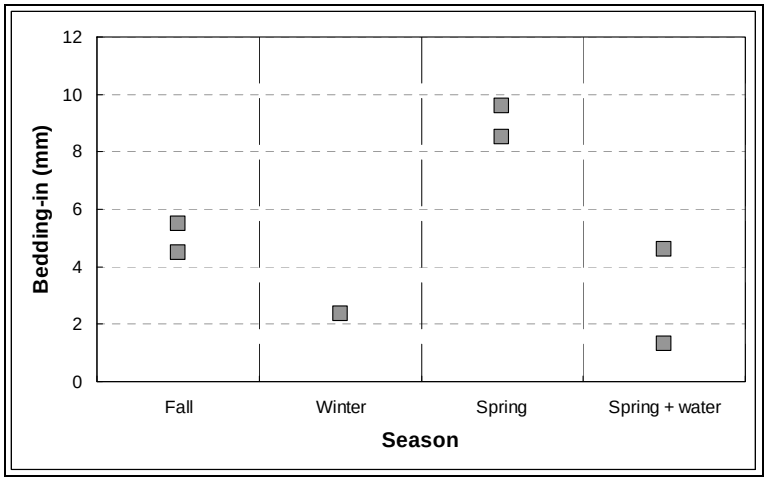

Figure 6.6: Seasonal effects on embedment.

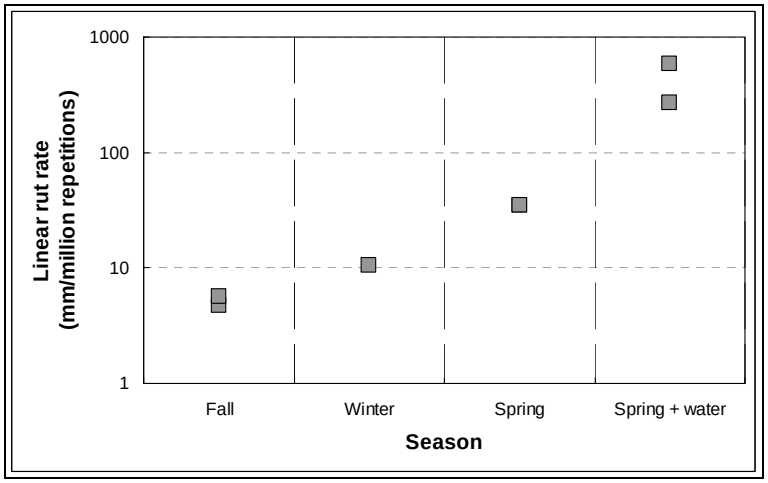

Figure 6.7: Seasonal effects on rut rate.

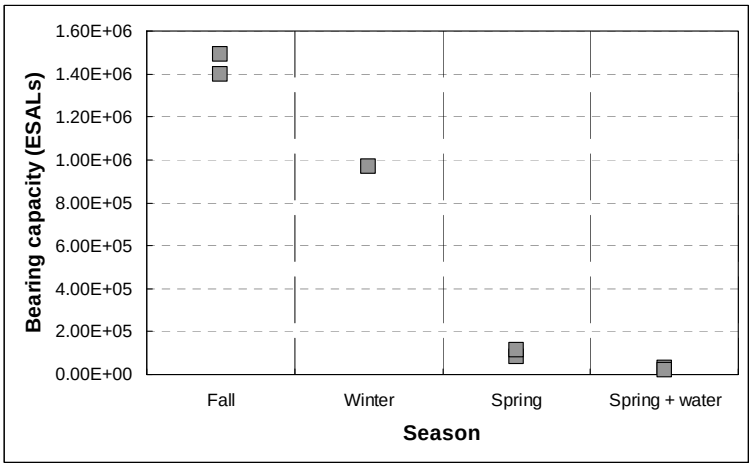

Figure 6.8: Seasonal effects on bearing capacity.

The following observations were made from the analysis of the rut data:

- The bearing capacity of the pavement only exceeded the design value under favorable conditions in the fall and early winter. The pavement structure of the HVS test lane was, however, not representative of the mainline pavement structure specifically, or of full-depth reclaimed, foamed asphalt treated pavements in general;
- The bearing capacity of the pavement was subject to seasonal effects and could not be estimated from a single HVS test result. A seasonal simulation should be carried out using the results from the HVS tests in each season and seasonal traffic data;
- The embedment parameter was the highest during spring and it is recommended that pavements of similar construction in similar climatic environments should not be opened to traffic during this period;
- The linear rut rate increased exponentially from fall to spring and even further with the addition of surface water. This seasonal sensitivity is believed to be caused by high moisture contents in the pavement. The most critical period is therefore in the spring if rainfall occurs and the surfacing layer is cracked.

7. CONCLUSIONS

Results from field surveys prior to, during, and after HVS testing show that the pavement structure of the HVS test sections on State Route 89 was not representative of the mainline and foamed bitumen treated, reclaimed asphalt concrete in general. The base layer thickness on the HVS test sections varied between 74 mm and 100 mm. The base layer was supported by a weak clay-like layer and decomposed granite subgrade. A very weak support layer was identified in the vicinity of Section 595FD and test-pit results show that the moisture content in the subgrade of Section 595FD exceeded 20 percent.

The mode of distress of the test sections differed between the favorable conditions in summer and fall and unfavorable conditions in winter and spring. The mode of distress before the onset of winter consisted of gradual deformation of the pavement resulting in a terminal surface rut with limited fatigue cracking. In the spring, the mode changed to a more rapid rate of rutting, with shear failure of the base layer occurring in certain locations on Sections 595FD and 596FD, which were tested during this period. These sections also showed extensive fatigue cracking, but this was probably caused by the weak soft base layer (low resilient modulus) with large plastic strains generating high tensile strains in the asphalt surfacing layer.

The pavement structure of the HVS test section on State Route 89 showed sensitivity to high moisture contents in terms of elastic and plastic response. The resilient modulus of the base layer decreased during the winter and spring and the rut rate increased. Although not to the same extent, a reduction in base layer resilient modulus on the mainline was also observed from FWD results. It is recommended that FWD surveys be carried out in each of the four seasons of the year to track changes in pavement condition. If the reduction in base layer resilient modulus is permanent, it may lead to early fatigue of the asphalt surfacing layer.

The pavement bearing capacity only exceeded the design value under favorable conditions in the fall and early winter. The pavement structure of the HVS test sections was, however, not representative of the mainline pavement structure and therefore not representative of the bearing capacity of foamed bitumen treated, reclaimed asphalt pavements. The bearing capacity of the pavement was subject to seasonal effects and could not be estimated from a single HVS test result. It is recommended that a seasonal simulation be undertaken in a second level analysis using seasonal traffic data and the results from the HVS tests in each season. Embedment (initial rutting in each HVS test) was the highest during spring and it is recommended that pavements of similar construction in freeze-thaw or very wet area should not be opened to traffic during this period.

8. REFERENCES

1. THEYSE, H. 2003. **1st Level Analysis Report: HVS testing of the foamed bitumen treated crushed stone base on the slow lane of the southbound carriageway on the N7 near Cape Town.** Pretoria, SA: CSIR Transportek. (CR-2003/23).
2. LONG, F. and Brink, A. 2004. **2nd Level Analysis of the HVS Data for the Southbound Carriageway of the N7 (TR11/1).** Pretoria, SA: CSIR Transportek. (CR-2004/12).
3. PETERSON, J. 2004. **Personal communication.** Sacramento, CA: California Department of Transportation.
4. ***CALBACK* back-calculation software.** 2004. Davis and Berkeley, CA: University of California Pavement Research Center.